Fraunhofer IRB Verlag Suttgart 1995 (ISBN 3-8167-4103-7)

Simultaneous Heat and Moisture Transport in Building Components

One- and two-dimensional calculation using simple parameters.

Hartwig M. Künzel

Fraunhofer Institute of Building Physics
(Director: Prof. Dr.-Ing. habil. Dr. h.c. Dr. E.h.mult. Karl Gertis)

The present report is based on my PhD-thesis which was written in the course of my activity as a scientific researcher at the Fraunhofer Institute for Building Physics in Holzkirchen. It was supported with funds from the German Federal Ministry für Research as part of a joint project for the protection of heritage buildings. Scientific exchange among 14 countries during the IEA-Annex 24 project provided valuable input to this study.

I wish to express special thanks to Professor Gertis for being my thesis supervisor, and particularly for his critical suggestions which have been a considerable contribution to my work. I thank Professor Reinhardt for being my assistant thesis supervisor. I also wish to thank Dr. Kießl and Mr. Krus, and many other colleagues who have contributed considerably to the success of this study through suggestions and assistance. My special thanks are due to Mrs. Westner for her patience in writing and re-writing the manuscript. I also thank my wife Sylvie for her understanding and support. Last but not least I thank Mr. Kumaran and the NRC in Canada for the English translation of this report.

Contents

Nomenclature

Roman-letter notations

A	[kg/m^{2}s^{0,5}]	Water absorption coefficient
a_r	[-]	Precipitation absorptivity
a_s	[-]	Short-wave absorptivity
B	[m/s^{0,5}]	Water penetration coefficient
b	[%/M.-%]	Moisture-related thermal conductivity supplement
c_e	[J/kgK]	Specific heat capacity of ice
c_s	[J/kgK]	Specific heat capacity of dry building material
c_w	[J/kgK]	Specific heat capacity of water
D_L	[m^2/s]	Solution diffusion coefficient
D_p	[kg/msPa]	Capillary pressure-related transport coefficient
D_w	[m^2/s]	Liquid transport coefficient
D_{ws}	[m^2/s]	Liquid transfer coefficient for suction
D_{ww}	[m^2/s]	Liquid transport coefficient for capillary redistribution
D_T	[kg/msK]	Thermodiffusion coefficient
D_φ	[kg/ms]	Liquid conduction coefficient
g_v	[kg/m^{2}s]	Vapour diffusion flux density
g_w	[kg/m^{2}s]	Liquid flux density
H	[J/m^3]	Total enthalpy
H_s	[J/m^3]	Enthalpy of dry building material
H_w	[J/m^3]	Enthalpy of moisture in the building material
h_e	[J/kg]	Melting heat of water
h_v	[J/kg]	Evaporation heat of water
L	[kg/m^{3}Pa]	Solubility
P_k	[Pa]	Capillary suction stress (capillary pressure)
P_L	[Pa]	Ambient atmospheric pressure
p	[Pa]	Partial pressure of water vapour
p_{sat}	[Pa]	Saturation vapour pressure
q	[W/m^2]	Heat flux density
R	[kg/m^{2}s]	Precipitation
R_D	[J/kgK]	Gas constant for water vapour
R_N	[kg/m^{2}s]	Normal rain
R_S	[kg/m^{2}s]	Driving rain
r	[m]	Pore radius
r_s	[s/m]	Site-specific driving rain coefficient
S_h	[W/m^3]	Heat source or heat sink
S_w	[kg/m^{3}s]	Moisture source or moisture sink
s	[m]	Depth of water penetration
T	[K]	Absolute temperature
t	[s]	Time
v	[m/s]	Wind velocity
w	[kg/m^3]	Water content
w_e	[kg/m^3]	Content of frozen water
w_f	[kg/m^3]	Free water saturation (capillary saturation)
W_{max}	[kg/m^3]	Maximum water saturation (vacuum saturation)
x	[m]	Spacial coordinate
y	[m]	Spacial coordinate

Greek-letter notations

α	[W/m^{2}K]	Total heat transfer coefficient
α_k	[W/m^{2}K]	Convective heat transfer coefficient
α_s	[W/m^{2}K]	Radiation-related heat transfer coefficient
β_p	[kg/m^{2}sPa]	Water vapour transfer coefficient
δ	[kg/msPa]	Water vapour permeability of stagnant air
δ_p	[kg/msPa]	Water vapour permeability of a building material
η	[kg/ms]	Dynamic viscosity of water
θ	[grd]	Contact angle
ϑ	[°C]	Temperature
λ	[W/mK] moist	Thermal conductivity of a building material
λ_o	[W/mK]	Thermal conductivity of a dry building material
μ	[-]	Water vapour diffusion resistance factor of a dry building material
μ^*	[-]	Ficticious water vapour diffusion resistance factor of a moist building material
ρ_s	[kg/m^3]	Bulk density of a dry building material
ρ_w	[kg/m^3]	Density of water
σ	[N/m]	Surface tension of water
φ	[-]	Relative humidity

Mathematical symbols

d	Operator for total differential
∂	Operator for partial differential
Δ	Difference operator
∇	Nabla operator

1. Objectives in terms of building physics

Every year, damage to buildings as a direct or indirect result of water runs into billions in Germany alone. This is particularly obvious in the case of historical buildings which have been exposed to the effect of water for a long time [56]. Modern buildings are not spared either, as is shown for example by the concrete slab buildings in the new federal states [27]. But water causes not only structural damage. The thermal insulation value of building components can also be considerably reduced by moisture. It is demonstrated in [35] that this is an important subject again today in connection with the necessary reduction of carbon dioxide emissions in housing construction. There are also important hygienic reasons why excess moisture in building components must be avoided. If the surface moisture in residential quarters, for example in corners or on heat bridges, reaches an equilibrium moisture of 80% relative humidity, mould formation can be expected according to [49]. Considering the allergic effect of moulds and the toxins contained in some species, this presents not only a cosmetic problem, but it can also have a detrimental effect on the health of the occupants [107].

The goal should therefore be to keep water out of building components or at least to lower their water content to a point where its detrimental effect is minimized. To do this, we must first of all clarify how the water enters a component and under what conditions it can cause damage. Fig. 1 schematically shows the main mechanisms which contribute to moisture entering the building components. On the one hand, moisture can affect a building component in liquid form -as rain or rising damp -, on the other hand it can do so in the form of water vapour condensing on the surface or inside the component, in the case of components with several layers, this usually happens at the boundary of a layer. Increased water content can also be caused during the formation process of a component, for example by the mixing water for mortar and concrete, by the production moisture of bricks or blocks, or by the lack of rain protection in the construction phase. Until now, lengthy and expensive experimental studies were usually necessary to clarify to what moisture loads these effects could lead and how they might be prevented. However, by using suitable calculative methods, such studies could be reduced in extent, and in some cases they could be eliminated or considerably accelerated. As will be shown in section 2.6, a number of models already exist for calculating the simultaneous heat and moisture transport in building components, some of which, e.g. the model by Kießl [57], have proven to provide reliable results. Others can only be used to a limited extent or have not been rigorously experimentally assessed. However, even some of the reliable models use relatively complex transport and storage functions, the determination of which requires not only a high level of measuring technology, but also specific experience. For that reason, it is hardly

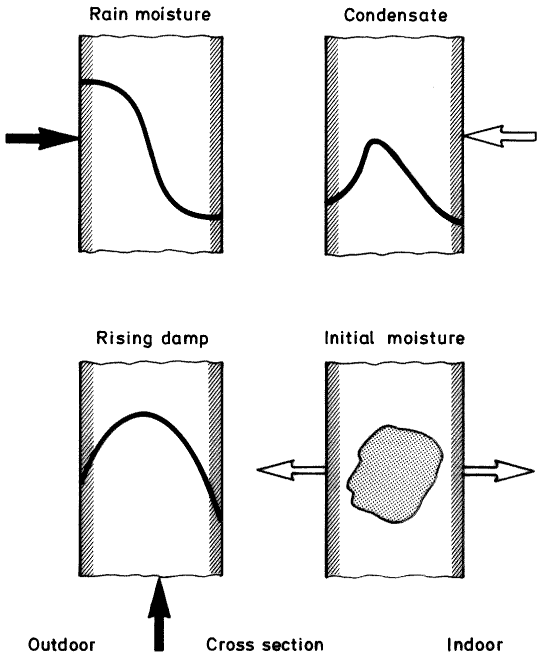

Fig. 1 Schematic diagrams showing the effect and distribution of moisture in an outside wall caused by irrigation, dew water on the inside and at the layer boundaries, rising ground moisture and initial moisture from construction

common practice yet for solving problems in building physics to make moisture transport calculations beyond the calculation of vapour diffusion, as with the Glaser method [38] in standard DIN 4108 [23]. It is therefore the objective of the present study to develop a process, based on the calculation model of Kießl [57] and on new results, to calculate the simultaneous heat and moisture transport in multi-layered components, which can work with relatively simple transport and storage functions, largely derived from standard material parameters. It must be suited for one and two-dimensional applications in practical building physics and must take into account natural climatic influences such as rain, frost and solar radiation. Table 1 lists the heat and moisture transport mechanisms in building components, which can possibly be encountered in practice. In calculating heat transport, we have taken into account thermal conduction and enthalpy flows through moisture movement with phase change, as well as short-wave solar radiation. Long-wave radiation interchange is included in the form of equivalent conductivities. Since air flows through joints and other leakage sites are difficult to quantify, the heat and moisture transport caused by air convection through a building component is not the object of this study. With that exception, we have analyzed all other transport mechanisms for vapour transport listed in Table 1. The liquid transport mechanisms taken into account are capillary conduction and surface diffusion. In practical building physics, seepage flow through gravitation plays a role only in isolated cases. Since it also cannot be taken into account with regard to one-dimensional moisture transport through a vertical building component, it is not dealt with in this paper. The same applies to liquid transport through hydraulic flow, electrokinesis and osmosis. These three transport mechanisms represent special cases for the building practice, and we are still in part lacking reliable transport models for their description [45].

Below we will examine in detail and at different moisture conditions the moisture transport mechanisms considered in this study, and their effect on heat transport. By presenting a summary of the present state of knowledge, supplemented by the most recent results obtained at the Fraunhofer Institute of Building Physics, the physical principles of simultaneous heat and moisture transport will be developed. Following a critical analysis of previously published moisture calculation methods, we will describe a new numerical solution method for the resulting transport equations. The calculative procedure we developed and the results obtained

Table 1 List of heat and moisture transport mechanisms occuring in practice, their causes and driving potentials.

Transport mechanism		Cause and potential of transport
heat transport	heat conduction	temperature
	heat radiation	tempeature in 4th power
	air flow	total pressure, density differentials
	enthalpy flows through moisture movement	vapour diffusion with phase change and liquid transport flows in temperature field
vapour transport	gas diffusion	vapour pressure (temperature, total pressure)
	Molecular transport (effusion)	vapoure pressure
	solution diffusion	vapour pressure
	convection	total pressure gradient
liquid transport	capillary conduction	capillary suction stess
	surface diffusion	relative humidity
	seepage flow	gravitation
	hydraulic flow	total pressue differentials
	electrokinesis	electrical fields
	osmosis	ion concentration

with this method will be validated for one and two-dimensional applications with the aid of experimental results. The study is rounded off by an assessment of the new calculative procedure and the resulting practical conclusions.

2. Critical assessment of the literature and new considerations on simultaneous heat and moisture transport

2.1 Basic hygric terms and formulas

A building material is called dry when it contains no water or only chemically bonded water. According to standard DIN 52620 [26], this state is reached by drying the material to constant weight. In contact with moist air, non- hygroscopic building materials remain dry, while hygroscopic materials pick up water molecules at the inner surfaces of their pore system until they reach a water content at equilibrium with the humidity of the ambient air.

If a building material in contact with water absorbs moisture by capillary suction, it is called capillary-active, if it does not, it is regarded as hydrophobic. A capillary-active material absorbs liquid water until it reaches a certain state of saturation called free water saturation or capillary saturation. Higher water contents of up to pore saturation or maximum water saturation can only be reached by applying pressure or by water vapour diffusion in a temperature gradient. This also applies to hydrophobic building materials. In the case of capillary-active building materials, we often speak of a critical moisture content. It represents the moisture condition below which no capillary conduction can be observed, i.e. by the limitted spreading of a drop of water on the surface of the building material [116].

The symbols used in this study correspond by and large to those recommended in international standards ISO 7345 [51] and ISO 9346 [52]. An exception is the heat transfer coefficient, which is represented by the Greek letter α because of its close association with the moisture transfer coefficient β, and to avoid mistaking it for enthalpy. All measures are given in SI units.

2.2 Moisture storage

Depending on environmental conditions, the moisture in a building material can be present in solid, liquid or vaporous form, and in the micropores it may also occur in not exactly definable physical states. Since it is often difficult to determine the different physical states separately by measuring, and since the ratio of individual states constantly changes under natural conditions, it is only useful to examine their sum total. In this paper we are calling this sum total water content w.

A building material can theoretically absorb moisture until all its pores are filled with water. But this fact provides no information about its real moisture storage capacity under natural conditions. It is therefore important to establish a connection between the water content of a building material and the ambient conditions. Prerequisite for the mathematical modelling of the moisture storage capacity of a building material is the existence of the clearest possible function of the water content in relation to the major climatic parameters. As will be shown later, the determining climatic parameter of moisture storage is the relative humidity. To derive such a function, we distinguish below the following three moisture regions which may occur in building materials due to increasingly intensive moisture conditions.

Region A

The sorption moisture or hygroscopic region. This region, which ranges from the dry state all the way to an equilibrium moisture of about 95% relative humidity, includes all water contents resulting from water vapour sorption up to a state of equilibrium.

Region B

The capillary water region, which follows the sorption moisture region and reaches up to free water saturation. This region, too, is characterized by states of equilibrium. Similarly to what was suggested in [57], this region is described by means

of moisture storage functions over pore radius distribution or suction stress.

Region C

The supersaturated region, which can no longer be reached by normal suction (or only after a very long time by dissolution of the encapsulated pore air in water). In practice, this region occurs through diffusion in the temperature gradient, and in the laboratory it occurs through suction under pressure. In this region, which lies above free water saturation and ranges to the filling of all cavities, there are no more states of equilibrium.

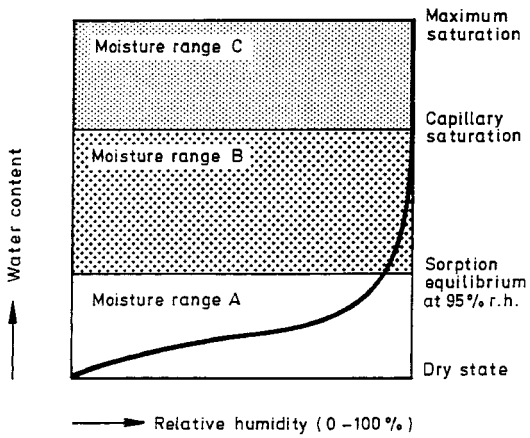

Fig. 2 Schematic diagram of the moisture storage function of a hygroscopic capillary-active building material

Region A: This region characterises the sorption moisture region up to a relative humidity of 95%. In building physics it is described by sorption isotherms
Region B: In this region, which is also called the super-hygroscopic region, increasingly larger pores of the building material are filled with water up to free water saturation (capillary saturation), the equilibrium moisture in contact with water.
Region C: This region, the supersaturated region, has no more equilibrium states. The relative humidity is always 100% regardless of the water content.

The three regions characterize the moisture storage behaviour of hygroscopic, capillary-active building materials such as building stones, mortar and wood products, as shown in Fig. 2 by means of a schematic moisture storage function for such materials. Only region C occurs in non-hygroscopic, non capillary-active materials such as most insulation materials. This means that moisture in liquid form can be found in these materials only under dew point conditions, i.e. at a relative humidity of 100%. In polymeric coatings or films on the other hand, only region A (the sorption moisture region) occurs, since they are initially without pore spaces able to absorb water. The absorbed water molecules must first find room in the polymer structure, which is usually connected with the micellar swelling of such substances. A direct transition from region A to region C is also possible, e.g. in mortar or building stones made hydrophobic by a water repellent agent. They are still hygroscopic, but no longer capillary-active. Below we will describe in greater detail the moisture storage phenomena in the three regions and the models based on these.

2.2.1 Sorption moisture region

When hygroscopic building materials are in contact with moist air, they become subject to equilibrium moisture which is determined by the ambient relative humidity. As far as building physics is concerned, the effect of the temperature can be disregarded according to measurements by Kast and Jokisch in the range of 20 to 70 °C [54] and by Künzel at 5 °C and 15 °C [74]. For that reason, the hygroscopic equilibrium moisture values of building materials are shown in the form of so-called sorption isotherms. As the measuring results in Fig. 3 show, the hysteresis between absorption and desorption isotherms is not very distinct in most building materials, and generally the absorption isotherm is enough to characterize the moisture storage of a building material. If hysteresis is somewhat more distinct, as in the case of expanded clay concrete (Fig. 3, bottom right), a sufficiently accurate calculation of the moisture behaviour of such materials is possible by averaging the absorption and desorption isotherms, according to studies by Rode [110] who compared the calculative results with and without taking hysteresis into account. It is therefore possible to clearly allocate the water content of a building material to a relative humidity with the aid of sorption measurements which are

feasible up to a relative humidity of about 95%. Since the relative humidity constitutes a continuous potential that does not depend on the material, and since in practice the actual moisture contents in building components are most of the time in the sorption region, the relative humidity should also be sought as the potential for the other moisture regions.

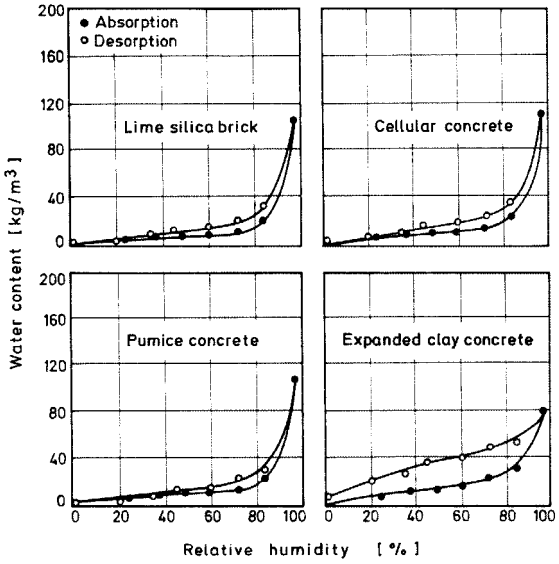

Fig. 3 Absorption and desorption isotherms of four commonly used building stones.

The samples were granulated and stored on average for 25 days at one relative humidity step [78]. Apart from expanded clay concrete, the difference between the absorption and desorption curves is minor.

2.2.2 Capillary water region

When a capillary-active building material comes in contact with liquid water, it absorbs water until it reaches free water saturation w_f. When it contacts another super-hygroscopic moist substance, there is also a moisture exchange until an equilibrium is reached. It is assumed in this case that the smaller capillaries have greater suction forces and therefore draw off water from the larger capillaries until all pores up to a certain diameter are filled with water in both materials. As a rule, in this state of equilibrium the water contents of the two building materials thus connected by capillary action are not equal. For the quantitative determination of the capillary suction forces it is customary to use a cylinder capillary model, as shown in Fig. 4. Then, the following relation results for the capillary pressure, which is also called suction stress:

$$P_k = 2\sigma \cos\theta / r \qquad (1)$$

where

P_k	[Pa]	suction stress
σ	[N/m]	surface tension of water
r	[m]	capillary radius
θ	[O]	contact angle

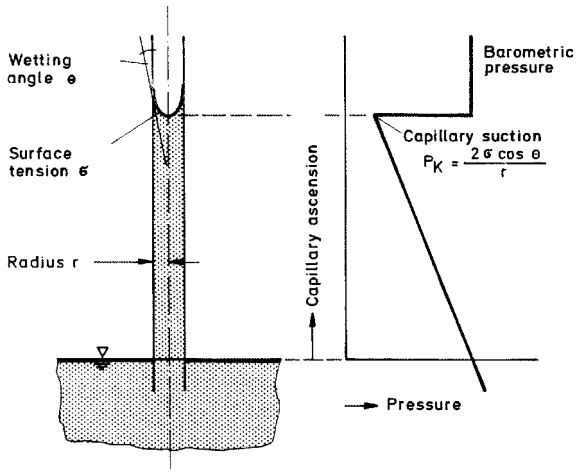

Fig. 4 Schematic view of the water column (left) and the pressure conditions (right) in a cylindrical capillary

There is air pressure over every water surface. Directly under the meniscus in the capillary the greatest capillary suction stress is reached, which can exceed the barometric pressure in the micro-capillaries, thus becoming tensile stress. Due to a higher order of the water molecules in the micro-capillaries, the water can take up these tensile stresses.

In porous construction materials, this suction stress can exceed the air pressure without the formation of vapour bubbles. Because of the strong order of water molecules in the small capillaries, the water there is also able to absorb tensile stresses [124]. This also explains why trees can transport water by capillary action to a height of more than 10m.

When we observe the pore system of a building material under the microscope, as seen in Fig. 5, a cylinder capillary model appears as a very coarse

approximation of the actual conditions. For that reason it is more practical to determine the suction stress directly and not via a capillary model from the

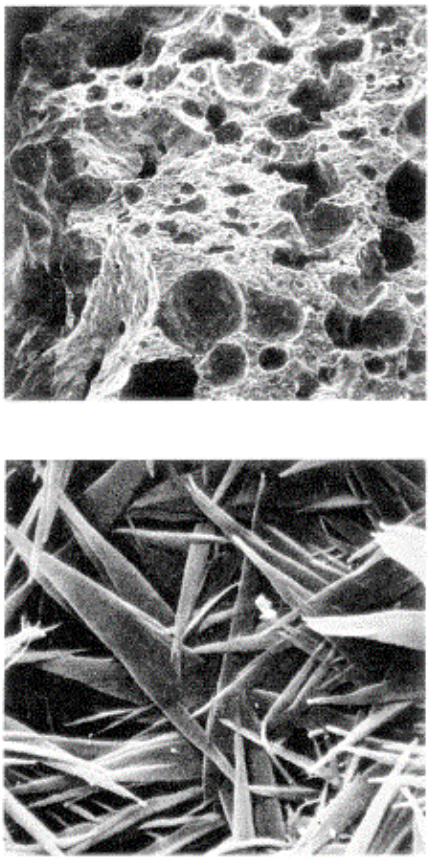

Fig. 5 Scanning electron micrograph of cellular concrete [37] with 22 x magnification (top) and 11 000 x magnification (bottom).

While the pores in the structure of the building material seem to be round at low magnification, the microstructure actually appears in the form of pointed needles at a higher magnification. A cylindrical capillary model therefore seems unsuitable to describe the pore structure in this case

pore sizes. With the help of thermodynamic equilibrium conditions, we can calculate, as derived in [57], the relation between the relative humidity φ over a concavely curved water surface and the developing capillary pressure, which is known as Kelvin's formula (see also Fig. 6):

$$\varphi = \exp\left(-\frac{P_K}{\rho_W R_D T}\right) \qquad (2)$$

where

P_k	[Pa]	suction stress
ρ_w	[kg/m^3]	density of water
R_D	[J/kgK]	gas constant for water vapour
T	[K]	absolute temperature

If it is possible to determine by measuring how the equilibrium water content of a building material depends on the suction stress in the just barely filled pores, equation (2) allows to derive a unique functional relation between water content and relative humidity, extended to the capillar water region.

As in case of the sorption isotherm, this function could also have a hysteresis between wetting and drying. Our own studies with samples of natural stone show that approximately the same super-hygroscopic moisture equilibria develop, regardless of whether they were reached by wetting or drying (Fig 7). This indicates that at least in mineral building materials, hysteresis in the capillary water region is no more pronounced than in the sorption moisture region. For that reason, a single storage function for drying and wetting seems adequate in this case as well. Suitable measuring methods for determining the storage function are centrifugal tests [117] and pressure plate tests [108]. In the case of building materials with a high proportion of micropores, a suitable method is the calometric examination of ice formation in the pore water [88]. These measuring methods work directly with water, which eliminates the detour via an idealized cylinder capillary model to determine the suction stress. Considerably simpler and quicker is to measure the pore radius distribution by means of mercury intrusion porosimetry. But since it covers all pores, while only some of the pores are filled with water during free water saturation, the results must be corrected accordingly. However, in the absence of salts, this method is often sufficiently accurate, as has been shown through comparative tests [69].

Results from [59], shown in Fig. 8, serve as examples for the seamless transition from the hygroscopic part determined by sorption measurements to the super-hygroscopic part determined by pressure plate measurements. Fig. 8

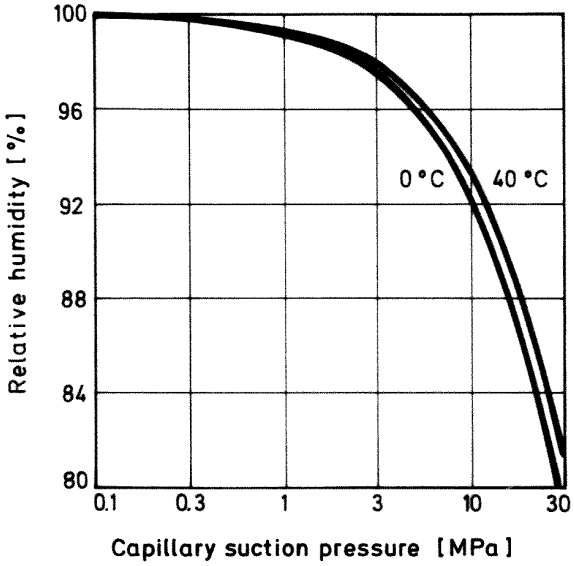

Fig. 6 Relative humidity over a water surface in dependence of the capillary suction stress in water. The curves were calculated with the help of Kelvin's formula in equation (2) for a water temperature of 0°C and 40°C.

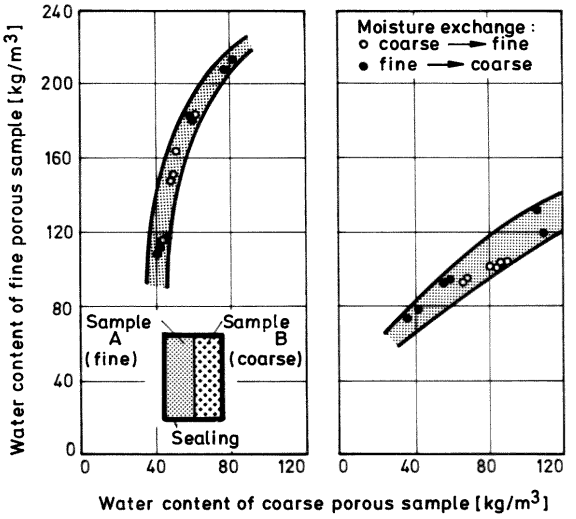

Fig. 7 Super-hygroscopic equilibrium moisture in two building materials with capillary connection across layer boundaries (sandstone with coarse and fine pores, with large (left) and small (right) differences in porosity)

The initial water contents of the samples were chosen in such a way that always half of the coarse pored reference samples reached equilibrium water content through moisture uptake, the other half through water release. The narrow regions (shaded curve areas) of the position of equilibrium states, regardless of the initial moisture situation, indicate an insignificant hysteresis of the capillary moisture exchange in natural sandstone

shows the water content of lime silica brick over the suction stress measured at a state of equilibrium or calculated according to equation (2). The same measured values, this time plotted over the relative humidity, are shown in Fig. 9 (top). It is demonstrated that for pore radii above 10^{-7} m - corresponding to a relative humidity of 99% -the moisture storage function rises steeply. This steep rise is caused by the non-linear relation between pore size and relative humidity. Table 2 shows the suction stress, the moisture potential of Kießl [57] and the relative humidity as a function of the pore radius. In comparison with the two potentials named first, the relative humidity for pore radii above 10^{-7} very quickly approaches its maximum value. Therefore, the rise of the storage function in the vicinity of free saturation is often several magnitudes higher than in the sorption region, which can lead to problems in the case of numerical calculation methods due to round-off errors. For that reason, Kießl [57] has introduced a new generalized

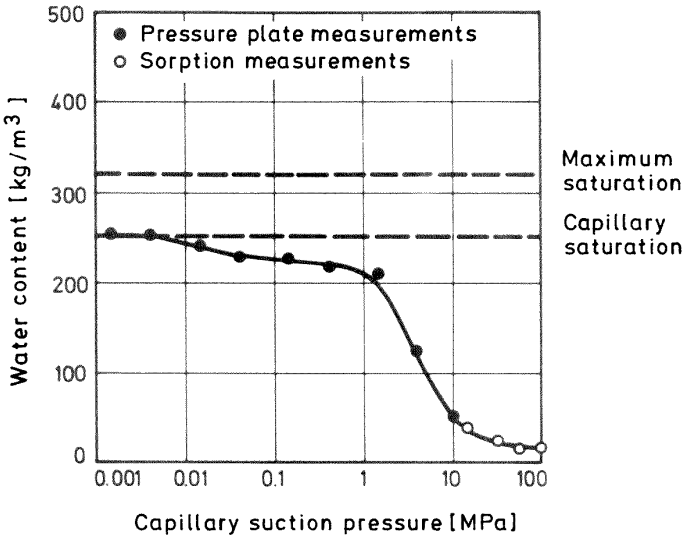

Fig. 8 Moisture storage of lime silica brick as a function of the capillary suction stress in pore water.

The equilibrium water contents in the super-hygroscopic region up to a capillary suction stress of 10 MPa are determined by pressure plate measurements, the others by sorption tests. The seamless transition of the results of both measuring methods shows the suitability of pressure plate measurements for determining the moisture storage function in the super-hygroscopic region

moisture potential Φ, which consists of the relative humidity and the pore radius distribution, as follows:

$$\varphi = 1{,}7 + 0{,}1 \log r \qquad \varphi > 0{,}9$$
$$\varphi = \varphi \qquad \varphi \leq 0{,}9 \qquad (3)$$

where

r	[m]	capillary radius
φ	[-]	relative humidity.

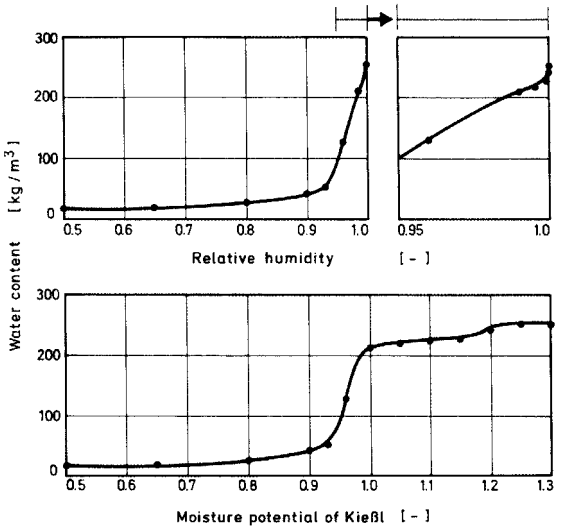

Fig. 9 Comparison of moisture storage in a building material as a function of the relative humidity (top) and the moisture potential according to Kießl [57], with lime silica brick as example

Kießl's potential allows a better resolution of the moisture storage function in the region of higher water contents. However, this does not necessarily lead to a higher computation accuracy, since at a 99% R.H. the majority of pores are already filled with water

The resulting moisture storage function is shown in Fig. 9 (bottom). The maximum value for φ is 1.3, which corresponds to a pore radius of 0.1 mm. This limit is practical, since larger pores are normally no longer filled with water by suction, considering that the maximum rise in a pore of r = 0.1 mm is less than 15 cm. For the water uptake of larger pores, gravitation and wind pressure play a more important role than the capillary suction forces which are examined in this study.

However, the above definition of the moisture potential leads to two problems. Firstly, a further differentiation $\partial\varphi/\partial\varphi$ has to be carried out and secondly the rise of the moisture storage function in the sorption region, in the following capillary water region (φ≥1) drops again in most capillary-active building materials. Since this, too, can lead to inaccuracies in the numerical calculation, we are not using the moisture potential suggested by Kießl. Instead, we use the relative humidity as the driving potential also in the capillary water region. The effect of numerical round-off errors can be minimized by an appropriate solution method [11].

2.2.3 Supersaturated region

In this region, the relative humidity is always 100 % or higher; this applies, for example, to dew water formation in hydrophobic insulation materials. Here, because of the initially very small radii of the dew water droplets due to the convex curving of the surface, relative humidity values of above 100%

Table 2 Relationship between the capillary suction stress in a capillary, the moisure potential according to Kießl [57], the relative humidity and the equivalent pore radius.Since in comparison with the first two potentials named, the relative humidity quickly goes toward ist maximum value in the case of pore radii over 10^{-7} m, the moisture storage function of coarsly porous building materials rises steeply in the region of free water saturaion

pore radius [m]	capillary suction stress [MPa]	moisture potential according to Kießl [-]	relative humidity [-]
10^{-8}	15	0,9	0,9
10^{-7}	1,5	1,0	0,99
10^{-6}	0,15	1,1	0,999
10^{-5}	0,015	1,2	0,9999
10^{-4}	0,0015	1,3	~1,0

may occur for short periods of time. In addition, this region is marked by transient processes, and steady-state moisture equilibria cannot occur under natural conditions. This region is best defined in hydrophobic insulation materials. As soon as vapour diffusion causes condensation to occur in the temperature gradient, the supersaturated region is reached. Regardless of the water content, the relative humidity is always 100 % in this case. But a supersaturated region can even be defined for capillary-active building materials. In this case, at water contents above free water saturation, pores are also filled which would not be filled through suction forces under natural conditions and which do not contribute to the capillary transport. Water contents in the supersaturated region can occur in most building materials due to vapour diffusion, and we must be able to calculate these as well. However, as stated in [13], since there is no clear connection between moisture potential and water content in this region - from a mathematical point of view, the moisture storage function between free water saturation w_f and maximum saturation w_{max} has an infinitely large rise -, it can only be described by a moisture storage capacity $\Delta w_ü$, which is independent of the potential and is given by the difference between maximum and free water saturation:

$$\Delta w_ü = w_{max} - w_f \qquad (4)$$

where

w_f	[kg/m^3]	free water saturation
w_{max}	[kg/m^3]	maximum water saturation.

In the case of non hygroscopic insulation materials, free water saturation corresponds to the saturation vapour concentration in the pore space, while maximum water saturation means that all pores are filled with water.

2.2.4 Determining moisture storage functions

Sorption isotherms of up to about 90% relative humidity are known for many building materials. A rather comprehensive catalogue can be found in [42]. However, in some materials the variation range is relatively wide, and separate measurements are often preferable. In such cases it is usually sufficient to measure the water content at 80 % relative humidity, which is required under standard DIN 52620 [26] to establish the design value of thermal conductivity, and to use it as the basis for determining the moisture storage function.

It is considerably more difficult to find in the literature suction stress curves or pore radius distributions for building materials. However, the accurate determination of the moisture storage function is necessary only in case of building component layers with a direct capillary connection, in which the liquid transport from layer to layer plays an important role (e.g. plaster or stucco over masonry). In such cases, the progress of moisture storage functions of the adjacent materials is of crucial importance for the liquid transport beyond the boundary layer, as is shown in [71]. In the case of other constructions with capillary-breaking separating layers, the accurate determination of the storage function is not necessary. It is also unnecessary when elevated water contents are expected in a building component layer only for a short time if at all. In such cases, an approximation of the moisture storage function is sufficient on the basis of parameters that are simple to determine. The literature does not lack formulations for describing sorption isotherms. The following approximation is used in [47] an [109] for the sorption of porous building materials:

$$w = w_0 - \frac{\ln(1-\varphi)}{d} \qquad (5)$$

where

w	[kg/m^3]	equilibrium water content
w_0	[kg/m^3]	water content at zero R.H.
d	[m^3/kg]	approximation coefficient
φ	[-]	relative humidity

In this case, the water content for $\varphi = 0$ corresponds to the equilibrium water content at 30% relative humidity. The approximation coeff. d is determined

by inserting another base point of the measured sorption curves. In contrast to this purely empirical formula a simple relation for porous materials was derived by [61] from the BET theory [14], so named after the first letters of its three authors:

$$w = w_m \cdot \frac{1}{1-\varphi} \qquad (6)$$

where

w	[kg/m3]	equilibrium water content
φ	[-]	relative humidity.

The water content in case of a monomolecular layer on the inner surface w_m must be determined by means of sorption tests. The two expressions (5) and (6) have one serious disadvantage. At a relative humidity of 100%, the calculative equilibrium water content goes toward infinity, while in practice it is limited by free water saturation. For that reason we suggest the following approximation for the moisture storage function, which is similar to equation (6):

$$w = w_f \cdot \frac{(b-1)\varphi}{b-\varphi} \qquad (7)$$

where

w	[kg/m^3]	equilibrium water content
w_f	[kg/m^3]	free water saturation
b	[-]	approximation factor
φ	[-]	relative humidity.

The approximation factor b must always be greater than one. It can be determined from the equilibrium water content at 80% relative humidity by substituting the corresponding numerical values in equation (7). Fig. 10 shows moisture storage functions approximated in this manner for lime silica brick, cellular concrete, clay brick, and gypsum board, in comparison with other measured values. However, the fact that the approximation compares well with the measured values in these four building materials does not prove in general that this approximation is suitable for all building materials. It is therefore recommended only for estimating purposes.

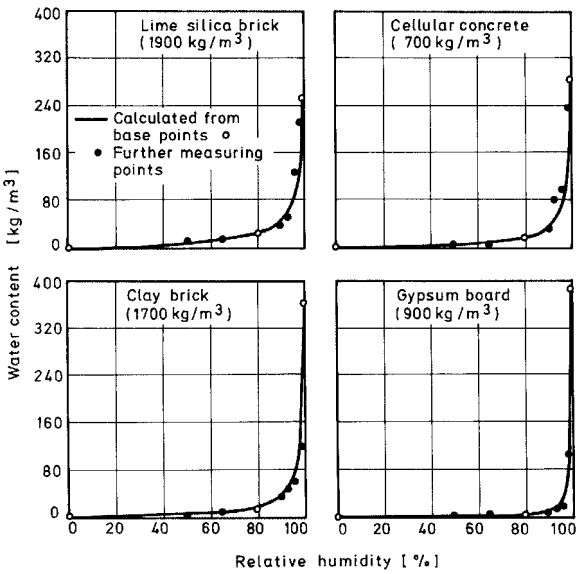

Fig. 10 Comparison of the moisture functions of lime silica brick, cellular concrete, clay brick and gypsum board, approximated according to equation (7), with the measured values determined by means of sorption and suction stress experiments [65]. Base points for the approximation are the equilibrium moisture at 80% relative humidity and the free water content.

2.3 Moisture transport mechanisms

As already explained in section 1, it is not part of this study to examine convection effects in building components based on total pressure differences, either for liquid transport or for vapour transport. The same applies to the effect of gravitation, electrical fields and ion concentration gradients on moisture transport. The moisture transport mechanisms relevant to calculations in building physics are water vapour diffusion and liquid transport through capillary forces.

The interaction of water vapour diffusion and liquid transport in building components can best be explained graphically in Fig. 11. Looking at a capillary in the component, we find that under winter conditions the temperature on the inside of the building, and thus also the vapour pressure, is higher than on the outside. Because the humidity is often higher on the outside (80% relative humidity is the annual mean in Germany), the gradient of relative humidity or water content runs in the opposite direction. If the building component is dry,

vapour diffusion in the capillary takes place only from the inside to the outside. The water absorbed in the walls remains immovable because of high adhesive forces. When the total moisture rises, the pore walls are covered with a sorbate film which is thicker on the outside than on the inside because the relative humidity outdoors is higher than indoors.

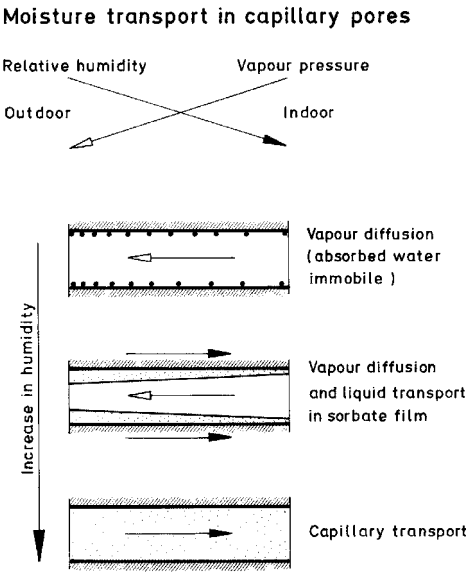

Fig. 11 Schematic diagram showing the moisture transport in a porous hygroscopic building material with the gradients of vapour pressure and relative humidity running in opposite directions (winter conditions)

The higher the moisture of the building component, the higher the liquid transport in terms of vapour diffusion until there is a reversal in transport direction

But the thicker the film, the more mobile the water molecules become, moving from the thicker film sections to the thinner sections. This process is called surface diffusion. Its driving gradient is the suction stress or the relative humidity. Surface diffusion (as well as capillary conduction) is therefore part of liquid transport and not part of vapour diffusion, as is frequently assumed. In the capillary in question, surface diffusion, which runs opposite to vapour diffusion, reduces moisture transport from the inside to the outside, and when the total humidity increases this moisture transport is even reversed through the onset of capillary conduction. It is confirmed in [67] that this hypothesis based on a model capillary is indeed valid. However, a prerequisite for this is the assumption on which the capillary model is based, namely that vapour and liquid transport do not influence each other. This assumption applies in the sorption moisture region of most building materials, since vapour diffusion takes place mainly in the larger pores, while liquid transport - independent of vapour diffusion - takes place via the micropores and on the pore walls. The introduction of a moisture-related diffusion resistance for water vapour diffusion calculations, as several authors, such as [41],[93],[109], have suggested, does not take the actual physical process into account and leads to wrong estimates.

2.3.1 Water vapour diffusion

The kinetic gas theory describes the diffusion of molecules in multi-component gas mixtures by means of equations which basically contain three diffusion potentials, the mass fraction, the temperature and the total pressure [9]. When we apply this to the diffusion of water vapour in air for the purpose of building physics, assuming negligible total pressure gradients, we obtain the following simplified relation:

$$g_V = (D_m \nabla m + D_T \nabla T) \qquad (8)$$

where

g_v	[kg/m^{2}s]	vapour diffusion flux density
m	[-]	mass fraction of water vapour related to the total mass of the vapour and air mixture
D_m	[kg/ms]	mass-related diffusion coefficient
D_T	[kg/msK]	thermodiffusion coefficient.

The diffusion caused by differences in the mass fraction is often called Fick's diffusion. By comparison, the thermodiffusion based on temperature gradients - also called the Soret effect - is negligible in building components [4]. Since in ideal gases there is a proportional relationship between the mass fraction of a component and its portion of the total pressure [8], water vapour diffusion in air can be described for practical purposes by the following equation:

$$g_v = -\delta \nabla p \qquad (9)$$

where

g_v	[kg/m^{2}s]	water vapour diffusion flux density
δ	[kg/msPa]	water vapour diffusion coefficient in air
p	[Pa]	water vapour partial pressure

According to standard DIN 52615 [24], the water vapour diffusion coefficient in air can be determined as a factor of the absolute temperature and the air pressure:

$$\delta = 2{,}0 \cdot 10^{-7} T^{0{,}81} / P_L \qquad (10)$$

where

T	[K]	ambient temperature
P_L	[Pa]	ambient air pressure.

Instead of the water vapour partial pressure, the vapour concentration is often used to calculate diffusion. In the case of non-isothermal conditions, this is basically not permissible. However, the errors caused by this in calculating diffusion are minor under practical conditions [36].

Only in large pores can vapour diffusion in porous building materials be compared with the diffusion of water vapour in air. When the pores are so small that collisions between molecules and pore walls are more frequent than collisions between molecules, we speak of effusion or Knudsen transport. With ambient pressure, pure effusion predominates in pores with a radius of < 5.10^{-9}m, and Fick's diffusion in pores larger than 10^{-6}m [34]. In pore sizes between these, we may speak of a mixed transport. In the case of effusion as well as with Fick's diffusion, the vapour pressure is the driving gradient. The temperature dependence of the two diffusion coefficients differs [58] as well as the dependence of the total pressure (effusion is independent of the pressure). Nevertheless, as far as building physics is concerned, the effects of the micro structure and the interaction of effusion and Fick's diffusion on the water vapour transport through porous media can be allowed for by simply introducing a water vapour diffusion resistance factor [64] which is characteristic for each building material.

$$g_v = -\frac{\delta}{\mu} \nabla p \qquad (11)$$

where

g_v	[kg/m^{2}s]	water vapour diffusion flux density
p	[Pa]	water vapour partial pressure
δ	[kg/msPa]	water vapour diffusion coefficient in air
μ		water vapour diffusion resistance factor

A condition for the validity of this equation is, however, that the vapour pressure does not exceed about 10% of the total pressure; otherwise convection phenomena occur, especially in porous building materials, which can be better described with Stefan's equation [64]. At temperatures below 40 °C, this condition is always met [61], and at low relative humidities, higher temperatures are permissible, too.

The water vapour diffusion resistance factor, which represents the ratio of the diffusion coefficients of water vapour in air and in the building material, is independent of the temperature according to measurements in [93] and [119]. Its dependence on the water content will be only briefly discussed here. As already mentioned, the diffusion resistance of most building materials in the sorption moisture region can be regarded as constant. Since in that moisture region, vapour and liquid transport take place largely independently of each other, this is also physically plausible. In the capillary water region, we can no longer assume with certainty that this independence is maintained. Since here, even larger pores are filled with water, the diffusion transport can be obstructed or -as is often assumed -accelerated through water islets. Theoretical considerations, the consequences of which have been compared with measured results [80], indicate

that the answer to the question whether water islets in the building material pores obstruct or accelerate vapour diffusion depends on local temperature and moisture conditions in the building component. In regions with high temperature but low moisture gradients, vapour diffusion is accelerated by the water islets in the pore structure, while at high moisture gradients, for example in the drying zone, the opposite effect must be expected. So far, these effects could not be quantified. Since this is furthermore a phenomenon that occurs only at higher water contents when capillary conduction dominates over vapour diffusion, it seems reasonable to remain with the concept that the vapour diffusion resistance does not depend on moisture.

2.3.2 Surface diffusion

As mentioned earlier, surface diffusion is defined as moisture transport in the water molecule layers adsorbed at the pore walls of hygroscopic materials and in micro-capillaries. In contrast to capillary conduction, which normally is observed only at water contents above the critical moisture described in [116], surface diffusion in paper products [112] begins to be noticed already at 30% relative humidity and in sandstone [65] at about 60% relative humidity. Fig. 12 shows the example of a paper membrane to demonstrate the extent which surface diffusion can reach in contrast to vapour diffusion. The top diagram shows the diffusion flow through the membrane related to the partial pressure difference. Below 20% relative humidity this is a case of pure vapour diffusion, while at about 30% relative humidity the onset of the rise of the diffusion flow with moisture can be attributed solely to surface diffusion. It can also be explained by means of Fig. 12 that the surface diffusion is a liquid transport whose driving potential is the relative humidity. The considerably greater increase of the diffusion flow related to the partial pressure at lower temperatures in spite of the fact that the vapour diffusion coefficient rises with the temperature (equation 10), shows that the partial pressure cannot be the driving potential. However, when the pure surface diffusion flow is related to the relative humidity instead of the partial pressure (Fig. 12, bottom), a higher diffusion flow results when the temperatures are higher, which is to be expected due to the temperature dependence of the surface diffusion coefficient; according to [97] it is inversely proportional to the viscosity of water. At the same time, this example shows that even under isothermal conditions, when the driving potentials are the same for vapour and liquid transport, the inclusion of surface diffusion in the vapour diffusion equation by means of a moisture-dependent diffusion resistance value leads to errors in the calculation when there are differences between the temperature for the coefficient determination and the calculation temperature. It is therefore advisable to take into account the surface diffusion together with the capillary conduction through a calculation technique that is independent of vapour diffusion.

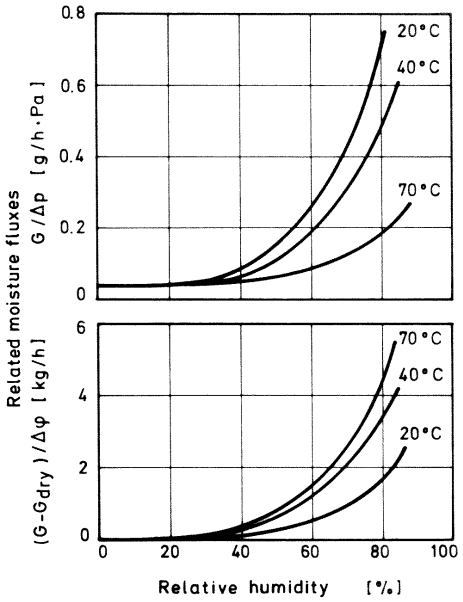

Fig. 12 Dependence of the measured moisture fluxes G through a paper membrane [112] on the mean relative humidity φ and on the ambient temperature

When we relate the moisture flux to the vapour pressure difference Δp (top), it decreases with the rising temperature, in contrast to the gas diffusion laws. When we relate the moisture-related increase of the moisture flux (moisture flux G minus moisture flux under dry conditions G_{dry}) to the relative humidity (bottom), the temperature dependence corresponds to the laws of physics.

2.3.3 Capillary conduction

Although, as mentioned above, we only speak of capillary conduction at water contents above the critical moisture, this form of liquid transport already occurs considerably below this in micro-capillaries. Similarly to vapour transport, which, depending on pore size, occurs in the form of effusion or Fick's diffusion, capillary conduction and surface diffusion also occur simultaneously in liquid transport. For that reason they can only be determined together by experimental means. At first, the question arises whether liquid transport can be practically described at all, as suggested in [64] and [57], by means of a diffusion equation. A diffusion equation requires that the moisture flow is proportional at every site to the water retention gradient which occurs at that site. While this applies to surface diffusion, the requirement is not met as far as suction in a capillary is concerned that is examined in isolation. There, the concentration gradient is zero everywhere - except for the site where the meniscus is located with the theoretically "infinite" moisture gradient. The position of the meniscus, which changes in time during suction in contact with water, can be calculated for a cylindrical capillary by means of the Hagen-Poiseuille law by equation (11):

$$s = \sqrt{\frac{\sigma r \cos\Theta}{2\eta} t} \qquad (12)$$

where

s	[m]	water penetration depth
r	[m]	capillary radius
σ	[N/m]	surface tension of the water
Θ	[°]	contact angle
η	[kg/ms]	viscosity of the water
t	[s]	suction time

Although capillary suction is clearly a "flow", the diffusion equation used by many authors,

$$g_w = -D_w(w)\nabla w \qquad (13)$$

where

g_w	[kg/m^{2}s]	liquid flux density
w	[kg/m^3]	water content
D_w	[m^2 /s]	capillary transport coefficient

with the capillary transport coefficient D_w strongly dependent on the water content, can lead to a good approximation of the suction process under certain conditions. The reason is this: according to Crank [18], a diffusion equation, even with concentration-dependent diffusion coefficients, shows the same root-time dependence of mass increase as the capillary suction process (equation 12). As the comparison of measurements and calculations in Fig. 13 shows, water content profiles can be produced through the exponential variation of the liquid transport coefficient, which are very similar to those of the suction process.

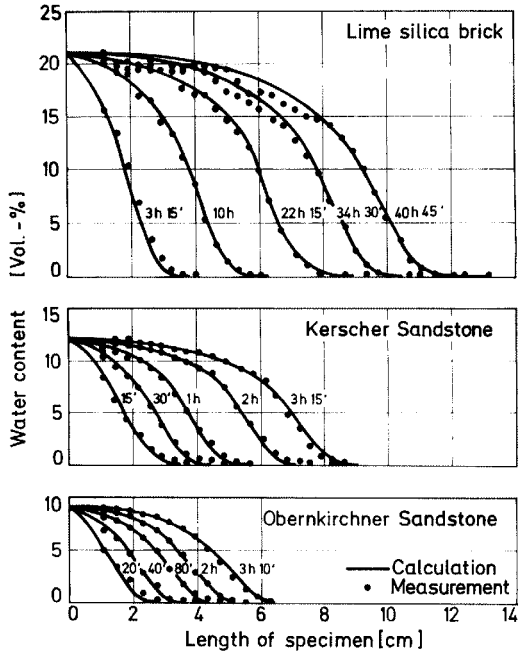

Fig. 13 Moisture profiles – measured and calculated according to equation (13) – of stone prisms at various times during the capillary suction process [68].

The good agreement between calculated and measured results was achieved by adapting the capillary transport coefficients which rise exponentially with the water content. In the three types of stone, they rise through a region of about three decimal powers.

The temperature dependence of D_w is based on the temperature dependence of surface tension σ and viscosity η of the water [57], and as Fig. 14 shows

the variation of σ is negligible compared to that of η. As has been confirmed experimentally in [19], the following relationship can thus be stated for the temperature dependence of D_w:

$$D_w(\vartheta) = \frac{\eta_{ref}}{\eta(\vartheta)} \cdot D_{w,ref.} \qquad (14)$$

where

η [kg/ms] viscosity of the water.

It is practical to select 20 °C as the reference temperature, since the liquid transport coefficient is usually determined in the laboratory at room temperature.

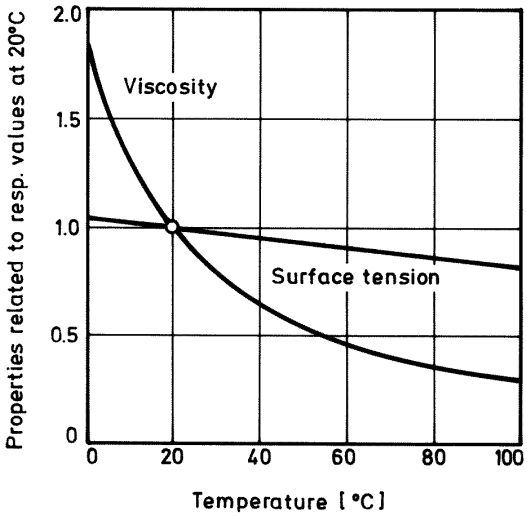

Fig. 14 Change in viscosity and surface tension of a water as a function of temperature, related to the values at 20°C, according to [21].

While the viscosity in the region of importance in building physics to 40°C, drops to almost one third, the surface tension changes less than 10%.

Although the measured and calculated values shown in Fig. 13 compare well, the calculation technique according to equation (13) is problematic. Krischer [64] had already pointed out that the capillary transport coefficient D_W also depends on the boundary conditions, a fact that has been confirmed by experiments [106]. This problem becomes especially clear with an interruption of the suction process, which is determined by the larger capillaries due to their greater suction velocity. As

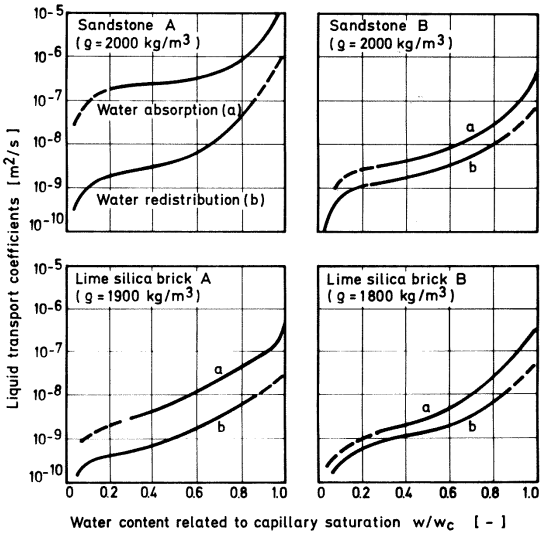

Fig. 15 Moisture transport coefficient of our different building stones as a function of the standardized water content [65]. The difference between the coefficients for capillary suction in contact with water (a) and redistribution after interruption of the water supply (b) is considerably greater in natural stone A (coarse pores) than in natural stone B (fine pores). In the case of lime silica brick, too, there are differences in transport coefficients which are based on density or production, but these differences are less pronounced.

soon as the water is removed from the suction surface, the menisci there are curved until the suction forces of these menisci and those in the water front region cancel each other out. Now, moisture can only be redistributed through capillary action as the small pores are filled at the expense of the larger pores, a process that is relatively slow. Measuring results in [40] and [59] with various building materials show that the capillary transport coefficients determined during this redistribution can be smaller by more than one decimal power in comparison with the suction process. This is illustrated in Fig. 15 by means of the moisture-dependent capillary transport coefficients of four different building materials. The liquid transport coefficients for redistribution are of similar magnitude, and the difference between these and the coefficients for capillary suction for finely porous natural stone B and lime silica brick B is approximately a factor of 3 to 5. In the case of lime silica brick A, the difference can be one decimal power, and in case of natural stone A it may even

reach two decimal powers. It is therefore necessary to characterize the capillary liquid transport in porous materials by means of two different transport coefficients for suction and redistribution. The process of redistribution, which cannot take place in a capillary observed in isolation, but which can only be understood through the interaction of pores of different sizes, corresponds macroscopically to the conditions of a diffusion model.

More plausible in physical terms is the description of the liquid transport in porous building materials by means of a flow model. Based on the Darcy formula customary in hydraulic engineering [9] for laminar flows in water- saturated porous materials, the following relation can be given for liquid transport:

$$g_w = K_1 \nabla P_k \qquad (15)$$

where

g_w	[kg/m^{2}s]	liquid flux density
K_1	[kg/msPa]	permeability coefficient
P_k	[Pa]	capillary suction stress

Contrary to the flow through water-saturated materials, which is based on an approximately constant permeability coefficient K_1, this coefficient is very dependent on moisture below the free water saturation, since the flow resistance of capillaries with a diminishing radius rises quadratically. By substituting the capillary suction stress in equation (15) with Kelvin's relation in equation (2) and by multiplying the constant terms to K_1, we obtain the following for the capillary transport:

$$g_w = -K_2 \nabla (T \ln \varphi) \qquad (16)$$

where

K_2	[kg/msK]	capillary coefficient
T	[K]	absolute temperature
φ		relative humidity.

Performing the differentiation in equation (16) we obtain:

$$g_w = -K_2 \frac{T}{\varphi} \nabla \varphi - K_2 \ln \varphi \nabla T \qquad (17)$$

where

g_w	[kg/m^{2}s]	liquid flux density
K_2	[kg/msK]	capillary conduction coefficient
T	[K]	absolute temperature
φ	[-]	relative humidity.

Under practical conditions, the second element of this equation, which describes the capillary transport based on a temperature gradient, is small in comparison with the first element; at a relative humidity of one it even becomes zero. It is therefore disregarded in the following. When we combine in the first term the elements before the gradient into one coefficient, which we will call here the liquid conduction coefficient D_φ, the liquid transport in porous building materials can be described by means of the following simplified relation:

$$g_w = -D_\varphi \nabla \varphi \qquad (18)$$

where

g_w	[kg/m^{2}s]	liquid flux density
D_φ	[kg/ms]	liquid conduction coefficient
φ	[-]	relative humidity.

In contrast to equation (13), equation (18) contains a material-independent moisture transport potential that is continuous also at the boundaries of layers. However, by comparing these two equations, the following connection between their transport coefficients can be established:

$$D_\varphi = D_w \cdot dw / d\varphi \qquad (19)$$

where

D_φ	[kg/ms]	liquid conduction coefficient
D_W	[m^2/s]	capillary transport coefficient
dw/dφ	[kg/m^3]	derivative of moisture storage function.

This relation allows us, at water contents in the capillary water region (> 95% relative humidity) in which the relative humidity can no longer be determined exactly by means of measuring, to derive the liquid conduction coefficient $D\varphi$ from the moisture storage function and the capillary transport coefficient D_W. To be consistent, we would also have to differentiate for D_φ between the capillary suction process and the redistribution, although there is no physical reason to do so, since the formula for equation (18) is based on a flow model. This is only a provisional model for which we can disregard the hysteresis effects in the moisture storage function which are difficult to determine. In reality, D_φ does not change during the transition from suction to redistribution. However, due to the curving of the menisci on the wetted side after the water supply is interrupted, the capillary suction stress there quickly increases, and the relative humidity drops accordingly, which leads to the already described delay in reaching moisture equilibrium. Since this hardly changes the local water content, it is a type of "transient hysteresis" of the moisture storage function.

2.3.4 Moisture transport in the supersaturated region

As described in section 2.3.3, the relative humidity in the supersaturated region, i.e. at water contents higher than free water saturation, is 100% everywhere. But this also means that the capillary suction stress is practically zero, i.e. in principle there can be no liquid transport by means of capillary conduction. This was confirmed by our own research [70]. In our measuring series, we connected pairs of cellular concrete and lime silica brick samples by means of a thin kaolin layer, bringing them in capillary contact; one sample was always at free saturation, the other at vacuum-saturation. We then sealed the sample pairs and stored them up to 40 days. In spite of the differences in water content, there was practically no moisture exchange between the connected samples, as shown in Fig. 16 by results from the teste cellular concrete and lime silica brick samples. The moisture difference of the connected sample pairs remained almost constant for 40 days , which shows how little moisture exchange there is in the over-saturated region.

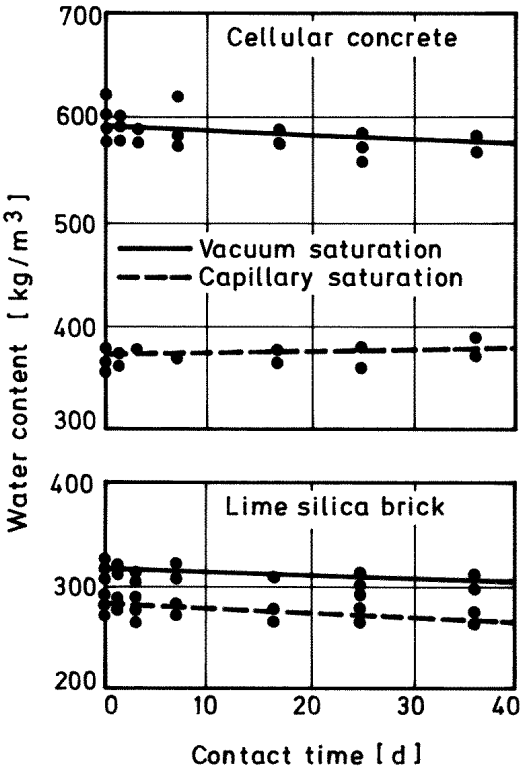

Fig. 16 Moisture state of sample pairs connected by Kaolin, with one vacuum-saturated and one freely saturated (capillary saturation) sample disk each of cellular concrete (top) and lime silica brick (bottom) as a factor of the contact period.

The moisture profile measurements by Nielsen [99] can serve as another example of the very low capillary transport in the supersaturated region. Fig. 17 shows the moisture profiles (at various points in time) of a cellular concrete sample at maximum water saturation drying out on one side under laboratory conditions. In the beginning, the moisture profiles drop steeply toward the drying surface, but when free water saturation is reached (at about 320 kg/m^3), a balanced moisture field is established, which shows a stronger drop on the drying side only when the value falls below the critical water content (about 180 kg/m^3).

This phenomenon is attributed to the fact that hardly any capillary transport processes take place in the

supersaturated region, since the transport potential, the capillary suction stress or relative humidity, remains unchanged across the profile. Only when the value falls below free water saturation does a defined relationship develop between moisture potential and water content, with a slight potential gradient at high capillary conductivity leading to a moisture field that is almost balanced across the sample. Distinct water content profiles return only when capillary conduction is further reduced and the value falls below the critical moisture.

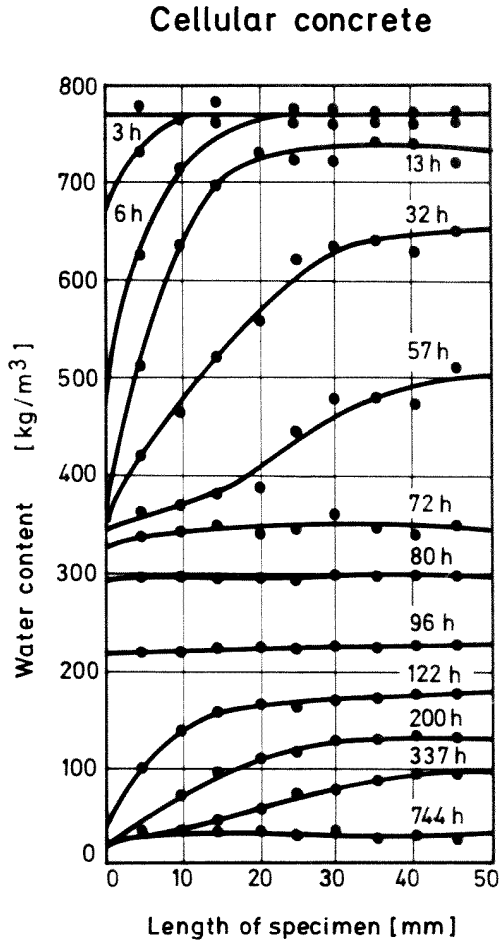

Fig. 17 Measured moisture profiles in a cellular concrete sample, 50 mm long, completely water-saturated, drying out on one side, at various time points after onset of drying

The measurements were carried out by means of gamma rays under ambient conditions of 21.5°C and 52% relative humidity at an air velocity of 1.5 m/s [99].

Even though capillary conduction plays no role in the supersaturated region, some moisture migration may be observed. Especially in the case of building materials with coarse pores, this is due to the effect of gravitation. Under the influence of temperature gradients, vapour diffusion may also play a major role, depending on the degree in which the pores are filled. Differences in vapour pressure, which become differences in total pressure when the gas exchange is obstructed, can also move the pore water.

Moisture transport in the supersaturated region of capillary-active building materials is difficult to cover by means of a model. Since these states usually occur only temporarily, it is usually sufficient to calculate with the existing capillary transport equations, but the transport coefficients must be determined separately for each case.

2.3.5 Solution diffusion

Solution diffusion is the term for moisture transport in organic polymers which are used in buildings, for example for seals and coatings in the form of vapour barriers and underlays. In contrast to mineral building materials and most insulation materials, which have a largely rigid pore system in which moisture is transported in liquid or vaporous form, water creates its own pore spaces in polymers by attaching itself to the macromolecules, thus causing the plastic to swell. Since the movement of the incorporated water molecules is coupled to the movement of the polymer molecules, it must be examined first whether solution diffusion can be described with any of the calculation techniques introduced so far. According to a paper by Buchner [15], the solution diffusion of gases and vapours in organic polymers can be calculated with the following equation:

$$g = -D_L \cdot L \nabla p \qquad (20)$$

where

g	[kg/m^{2}s]	diffusion flux density
D_L	[m^2/s]	solution diffusion coefficient
L	[kg/m^{3}Pa]	solubility
p	[Pa]	partial pressure.

The solubility of the polymer for water vapour depends on whether the macromolecule chains and the plasticizer are polar or non-polar. It decreases exponentially with the temperature. The solution diffusion coefficient depends on the structure and the degree of cross-linking of the polymer. It increases greatly with the temperature.

As far as the already described moisture transport equations are concerned, the solution diffusion can best be compared with the vapour diffusion equation (11), and we obtain the following diffusion resistance factor μ:

$$\mu = \frac{\delta}{D_L \cdot L} \qquad (21)$$

where

δ	[kg/msPa]	vapour permeability of air.

In contrast to other building materials, the diffusion resistance factor μ thus defined for polymeric films or membranes depends on the temperature and moisture. Depending on the type of plastic, it may decrease, but also increase as the temperature or moisture rises.

Especially pronounced is the decrease in the diffusion resistance of hydrophilic polymers as the moisture increases [61]. Since there can be up to one decimal power between the value in dry condition and that at almost 100% relative humidity, as Fig. 18 shows, the moisture dependence should always be taken into account by means of a variable diffusion resistance factor, while the temperature dependence can generally be disregarded as a matter of simplification.

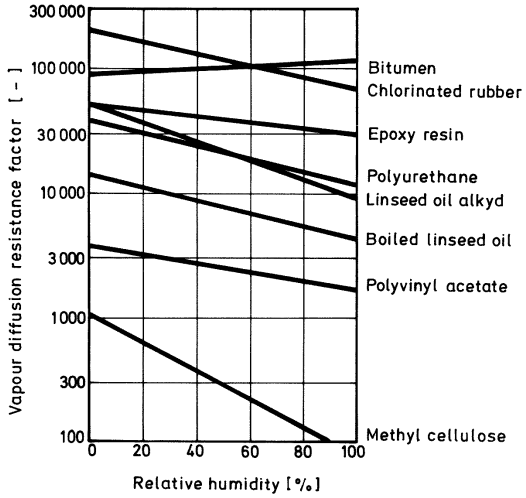

Fig. 18 Moisture dependence of the water vapour diffusion resistance factor of different organic building materials and coatings, according to [61]

The difference between the diffusion resistance in dry and wet state can be up to one decimal power in some synthetic materials.

2.3.6 Moisture transport below the freezing point

In contrast to vapour diffusion resistance above the freezing point, which - as proven in section 2.3.1 - can be formulated as moisture-independent, ice formation at high moisture levels in building materials can cause a block against vapour diffusion. As studies with porous media have shown [4], the diffusion resistance changes little through frost formation until about 60% of the pores are filled. This is explained by the dominance of the diffusion flow in large pores with few branches, which are filled only when the water content is high. For that reason, the influence of ice formation on vapour diffusion can be disregarded in most cases.

Frost affects the liquid transport more than the vapour transport. Below 0 °C there is no capillary suction any more. But the water in the micropores freezes only at lower temperatures, so that even below zero degrees, liquid transport can occur with relatively little interference from ice formation in the large pores [97]. Fig. 19 shows the freezing temperature of the pore water as a function of the pore radius. The relative humidity over the menisci of the pore water just above freezing, calculated

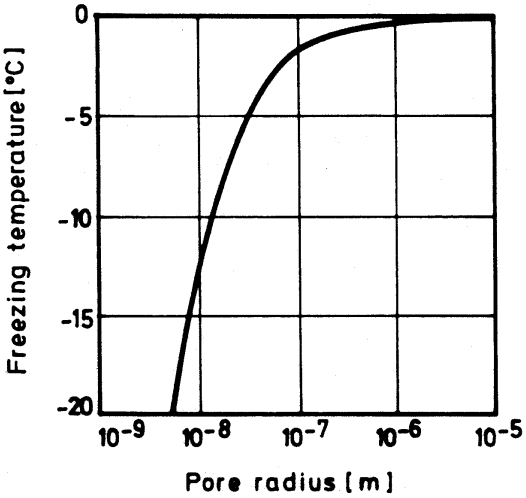

Fig. 19 Dependence of the freezing temperature of pore water in cylindrical capillaries on the pore radius, according to [97]

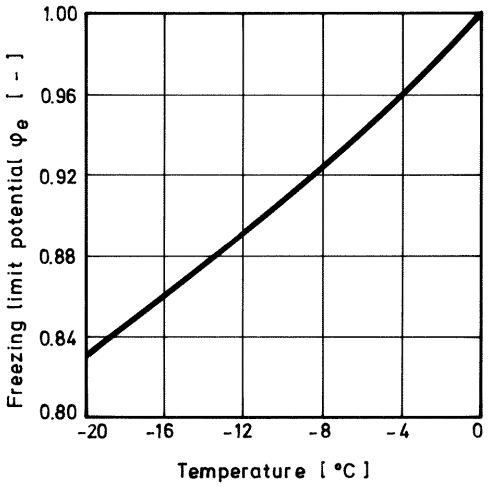

Fig. 20 Relationship between temperature and freezing limit potential which corresponds to the relative humidity over the pore water in the largest still unfrozen pores of capillary-active building materials.

from the pore radius with the aid of the Kelvin equation (2) and equation (1) is called the freezing limit potential. Its dependence on the temperature is shown in Fig. 20. From this limit potential, with the aid of the moisture storage function, we derive the maximum content of still liquid and thus movable water at the corresponding building component temperature. From this we obtain for the liquid conduction coefficient below 0 °C:

$$D_\varphi(\varphi) \le D_\varphi(\varphi_e) \qquad (22)$$

where

D_φ	[kg/ms]	liquid conduction coefficient
φ	[-]	relative humidity
φ_e	[-]	freezing limit potential.

2.3.7 Determining the moisture transport coefficients

German Standard DIN 4108, part 4 [23] provides tables for the diffusion resistance factors μ of building materials. For the accurate determination of the vapour diffusion resistance of a building material, steady-state diffusion measurements as described in standard DIN 52 615 [24], or in the case of homogeneous materials, transient diffusion measurements [85] can be carried out. It was already discussed that in selecting the moisture region for measuring, it should be taken care that surface diffusion effects are negligibly small. This is generally the case for the dry region defined in standard DIN 52 615 [24] of 3 to 50% relative humidity.

In comparison, it is more difficult to determine the moisture conduction coefficient D_φ. In the sorption region, D_φ, can be calculated by determining a fictitious*) vapour diffusion resistance factor μ*, according to standard DIN 52 615 [24], but in higher moisture regions, from the following equation:

$$D_\varphi = p_{sat}\delta\left(\frac{1}{\mu^*(\varphi)} - \frac{1}{\mu}\right) \qquad (23)$$

where

D_φ	[kg/ms]	liquid conduction coefficient
p_{sat}	[Pa]	saturation vapour pressure
δ	[kg/msPa]	vapour permeability of stagnant air
μ	[-]	vapour diffusion resistance factor (in dry condition)
μ*	[-]	fictitious diffusion resistance factor (measured at higher humidity).

*) In this study, parameters are called fictitious when they are allocated to a certain transport equation (in this case diffusion equation) but which due to their experimental determination also include other transport components (in this case liquid transport).

Table 3 Vapour diffusion resistance factors of various building materials according to standard DIN 52615 [24] from dry-cup and wet-cup test

The difference between the measured results of the cup tests which are attributable to liquid transport effects (surface diffusion) can be used to determine the liquid conduction coefficient.

building material	bulk density [kg/m^3]	vapour diffusion resistance factor	
		dry-cup (3 % - 50 % r.F.)	wet-cup (50 % - 93 % r.F.)
cellular concrete	500	7,7	7,1
lime silica brick	1700	27	18
solid clay brick	1600	9,5	8,0
gypsum board	900	8,3	7,3
concrete	2250	260	210
cement-lime mortar	1900	19	18
lime mortar	1400	7,3	6,4
Saaler sandstone	2300	60	28
Wüstenzeller sandstone	2300	62	38
Worzeldorfer sandstone	2250	38	22

As an example, Table 3 lists the vapour diffusion resistance factors for dry-cup and wet-cup conditions of various capillary-active building materials. While in some materials, the diffusion resistance factor μ* (wet-cup value) is hardly smaller than the diffusion resistance factor μ (dry-cup value), the wet-cup diffusion resistance is cut in half in case of the three natural stones shown at the end of Table 3. The liquid conduction coefficients calculated from these results with the aid of equation (23) for the various building materials in the selected moisture region are also correspondingly different.

In the capillary water region, D_φ is calculated as a product of the derivative of the moisture storage function and the capillary transport coefficient D_w. D_w can be determined by measuring transient moisture profiles in building material samples, as described in [59]. Since a major technical effort is required to measure the moisture transport coefficients, we will introduce below a simplified method of determination, which is sufficiently accurate in many cases.

The standard parameter for describing the capillary suction characteristics of a building material in contact with water is the water absorption coefficient A. Between this water absorption coefficient A and the capillary transport coefficient at contact with water D_{ws} there is a relationship, which, however, is not unique because D_{ws} is moisture depending. That is why further input is required which describes this moisture dependence. As Kießl [57] shows, the increase of D_{ws} with the moisture content can be approximated in many cases with an exponential function, which in the case of most mineral building materials extends over about three decimal powers. Under these presumptions, the capillary transport coefficient for the suction process can be estimated as follows:

$$D_{ws}(w) = 3{,}8 \cdot (A / w_f)^2 \cdot 1000^{w / w_f - 1} \qquad (24)$$

where

D_{ws}	[m²/s]	capillary transport coefficient for the suction process
A	[kg/m²s^{0,5}]	water absorption coefficient
W	[kg/m³]	water content
W_f	[kg/m³]	free water saturation.

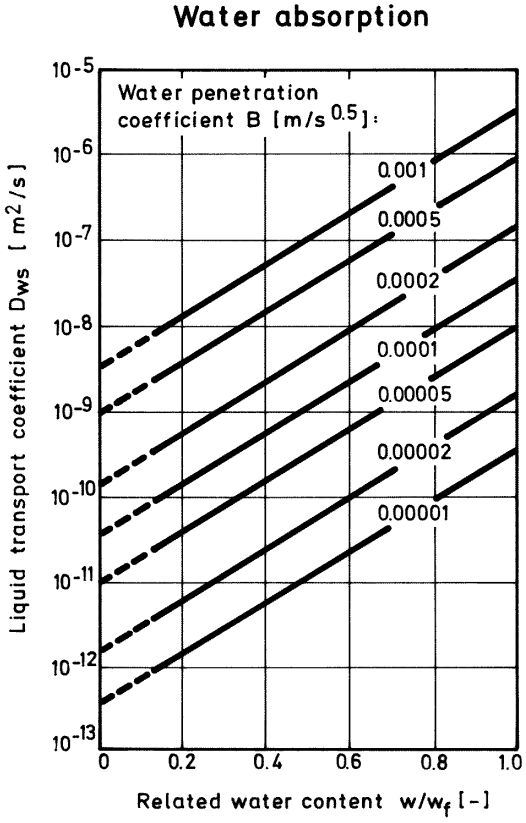

Fig. 21 Dependence of the capillary transport coefficient for the suction process on the water content and the water penetration coefficient of the building material, determined by means of the approximation relation in equation (24).

The ratio of A and w_f is also called the water penetration coefficient B. Equation (24) is not valid for water contents above free water saturation, since in that region there is no clear connection between the capillary transport and the water content. Fig. 21 shows the resulting dependence of the capillary transport coefficient of building materials on the water content. This approximation is adequate for calculating the moisture behaviour of building components which are in contact with water only for short periods at a time, e.g. when it rains. So far there is no determination method for the liquid transport coefficient of redistribution. Even pore models, such as those described in [33] and [94], do not help in this case, since they have only been designed and tested for the approximation of water absorption. But because the liquid transport coefficient of redistribution D_{ww} is important for calculating the moisture behaviour of building components, we will try here to provide at least a rough estimate for this coefficient.

When we base redistribution, too, on an approximately exponential dependence of the liquid transport coefficient on the water content, we require only two values to describe this function. As was shown already, the first value in the hygroscopic moisture region can be determined by means of equations (19) and (23) from the water vapour diffusion resistance factors obtained by dry-cup and wet-cup tests. According to research done so far [65], the second value in the free water saturated region lies about one decimal power below the value of the transport coefficient for suction D_{ws}. However, the coefficients determined in this manner can only be used for estimating or calculating building components in which liquid transport processes do not play a dominant role.

2.4 Hygric effect on heat storage and transport

The principles of calculating the thermal behaviour of building components in dry condition are known in building physics. Since this study is concerned primarily with moisture transport and its effect on heat transport, we will not deal with the pure temperature dependence of thermal quantities such as heat capacity, thermal conduction, specific heat of melting and evaporation. The hygric effects on these quantities are however so important that they have to be dealt with.

2.4.1 Heat storage in moist building materials

The heat content of a material under isobaric conditions is called the enthalpy. In the temperature

range which is of concern in building physics, there is an approximately linear relationship between the enthalpy of a material and its temperature. The enthalpy of a dry building material, related to the enthalpy at 0 °C, is therefore described by means of the following equation:

$$H_s=\rho_s c_s \vartheta \qquad (25)$$

where

H_s	[J/m^3]	enthalpy of the dry building material
ρ_s	[kg/m^3]	bulk density of the building material
c_s	[J/kgK]	specific heat capacity of the building material
ϑ	[°C]	temperature

In the case of moist building materials, we must add to this enthalpy the enthalpy of the water contained in the material. However, the enthalpy of the water depends on the existing physical states, which, as mentioned above, are difficult to define exactly in the micropores.

Fig. 22 shows the development of the volume-related enthalpy of ice, liquid water and saturated vapour as a function of temperature. At temperatures below 0 °C, the enthalpy of water lies in the shaded area. The exact determination of the enthalpy of a phase mixture is possible only when the pore radius distribution or the moisture storage function of the building material is known. The broken line describes the enthalpy of water vapour in the free pore space under saturated conditions, taking into account latent heat effects during the phase change to maintain the state of saturation. However, this excludes any transport of this water vapour. The change in saturation vapour enthalpy with the temperature, which constitutes a measure

Table 4 Moisture supplement (in percent) in terms of the thermal conductivity of various building materials, related to the water content in mass percent, according to [16]

building material	bulk density [kg/m^3]	thermal conductivity [W/mK]	moisture supplement [%/M.-%]
cellular concrete	400 – 800	0,09 – 0,19	4
lime silica brick	1800	0,7	8
pumice concrete, expanded clay concrete	1400 – 1800	0,5 – 1,0	4
light-weight concrete with EPS supplement	300 – 900	0,07 – 0,28	3
normal concrete	2300	1,3 – 1,5	8
wood	400 – 700	0,08 – 0,15	1,5
expanded polystyrene foam (EPM)	15 - 30	0,04	0,05 *)
extruded polystyrene foam (XPS)	28 - 40	0,03	0,1 *)
polyurethane foam (PUR)	40 - 80	0,03	0,4 *)

*) Values are valid only up to a water content of about 100 mass-%. In case of organic foam insulation, there is no linear relationship between thermal conductivity and water content

for the heat capacity of pore moisture, is minor in comparison with the corresponding change in the enthalpy of liquid water and ice in the temperature range shown, and it is therefore disregarded.

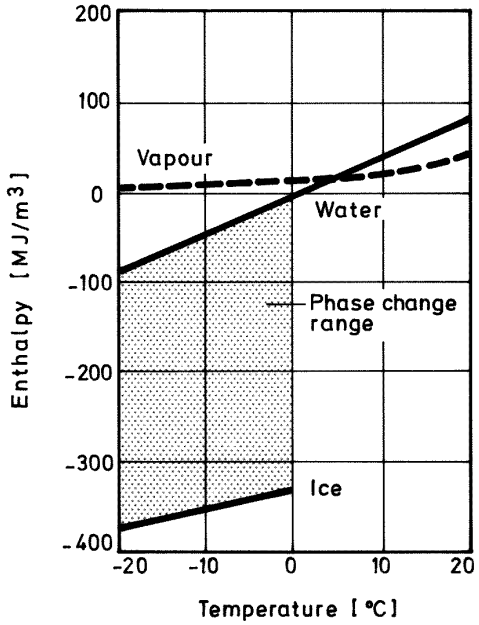

Fig. 22 Volume-related enthalpy of the various physical states of water at normal pressure as a function of temperature (reference enthalpy is the enthalpy of water at 0°C)

While the temperature-related enthalpy change of saturated water vapour is negligible due to its low density, it plays a major role in the phase change of water to ice (shaded area).

Thus the following equation can be used to determine the enthalpy of water in the building material:

$$H_w = \left[(w - w_e)c_w + w_e c_e - h_e \frac{dw_e}{d\vartheta} \right] \cdot \vartheta \qquad (26)$$

where

H_w	[J/m³]	enthalpy of moisture in the building material
c_w	[J/kgK]	specific heat capacity of liquid water
c_e	[J/kgK]	specific heat capacity of ice
h_e	[J/kg]	specific melting enthalpy (melting heat)
w	[kg/m³]	total water content
w_e	[kg/m³]	content of frozen water
ϑ	[°C]	temperature

The ice content in the building material w_e is determined with the help of the moisture storage function and the relationship between the freezing limit potential φ_e and the temperature in Fig. 20.

2.4.2 Thermal conduction in moist building materials

We are using the term "thermal conduction in moist building materials" only to describe the effect of localized water on heat transport. While the evaporation and condensation of transported moisture also contributes to heat transport, it cannot be described in practical terms by means of the thermal conduction equation. Information about the dependence of thermal conductivity on the water content can be found in [16] for various building materials. Since standard measurements also include the effect of water vapour diffusion, the results of measurements in the guarded hot plate apparatus for diffusible materials, such as mineral wool, can only be used with caution. According to [72], the following relation can be used to calculate the moisture-dependent thermal conductivity λ(w) of mineral building materials:

$$\lambda(w) = \lambda_0(1+b \cdot w/\rho_s) \qquad (27)$$

where

$\lambda(w)$	[W/mK]	thermal conductivity of moist building material
λ_0	[W/mK]	thermal conductivity of dry building material
ρ_s	[kg/m³]	bulk density of dry building material
b	[%/M.-%]	thermal conductivity supplement

Supplement b indicates by how many percent the thermal conductivity increases per mass percent of moisture. Its value is determined by the type of building material, but in the case of hygroscopic materials, it is largely independent of their bulk density. Table 4 lists a number of these supplements for various building materials.

Although ice has four times the thermal conductivity of water, it is usually not possible to differentiate between thermal conductivity above and below the freezing point, since no corresponding measuring values exist for most building materials. As examinations in [64] at different water contents show, the differences in thermal conductivity above and below 0°C are smaller than expected considering the difference in conductivity between ice and water.

2.4.3 Heat transport through enthalpy flows with phase change

In contrast to heat flows based on temperature gradients, the enthalpy flows considered now are always connected with a flowing medium. As already mentioned, convection effects through differences in total pressure are disregarded here, and the only medium to be considered is either diffused water vapour or liquid water moved through capillary pressure. An example is to estimate how important the resulting enthalpy flows are in comparison with thermal conduction. The greatest influence of moisture movements can be expected in a building component that is exposed to high moisture loads while in the presence of temperature gradients. This is the case, for example, in a cavity wall at western exposure, with visible masonry, during the winter months heating period (September - March). The following values were obtained under conditions which are average during the winter months in the foothills of the Alps, with a high incidence of driving rain:

outside air temperature	2.0°C
radiation at western exposure	40 W/m^2
total driving rain	200 kg/m^2
room air temperature	20°C

At a short-wave radiation absorption value of 0.7 and a U-value for the wall of 0.5 W/m^{2}K, the structure shown in Fig. 23 indicates the following heat balance, as an average for the winter months. Without taking into account the effects of moisture, the heat transferred from the inside to the outside surface is 8.5 W/m^2, and that transferred by radiation is 28 W/m^2 (see Fig. 23). This results in a surface temperature for the wall of about 4°C and an average temperature across the rain screen of 5°C. during the winter months,

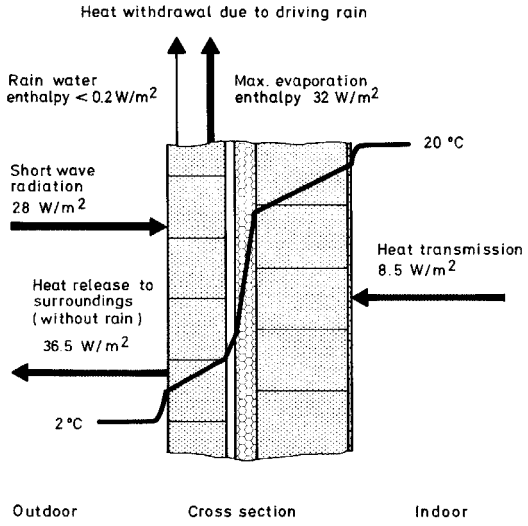

Fig. 23 Schematic view of steady-state heat balance in a two-layered exterior wall during the winter semester, under Munich climate conditions.

In comparison with the radiation and transmission heat, the mean heat withdrawal due to rain water penetration of the weather shell is negligibly small. However, heat withdrawal due to the subsequent evaporation of rain water is not negligible.

Assuming that the driving rain hits the wall at the outside temperature, is completely absorbed and evenly distributed over the rain screen, we obtain a heat transfer rate of less than 0.2 W/m^2 through liquid transport. However, if we assume that the moisture introduced by the rain dries out again evaporative cooling results in a heat loss for the rain screen of 32 W/m^2, which in this relatively extreme example is of the same magnitude as the gain from solar radiation. This example shows that in practice, enthalpy flows as the result of liquid transport play a negligible role in comparison with other thermal flows, while vapour diffusion flows connected with phase changes, such as drying processes, can be of great importance in terms of the heat balance.

An experimental example for the strong influence of these latent heat effects at high vapour diffusion

flows is demonstrated by studies in [1], the results of which are shown in Fig. 24.

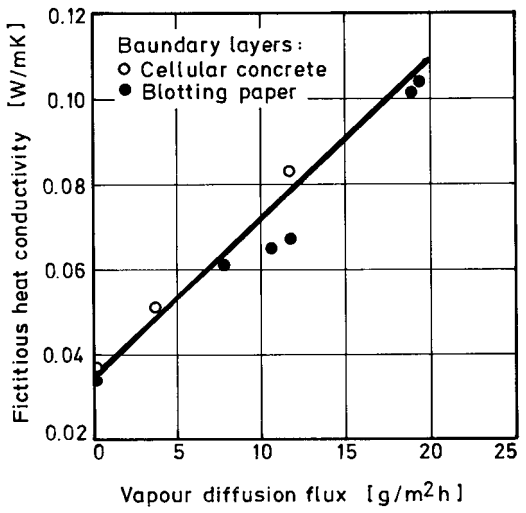

Fig. 24 Relationship between the fictitious thermal conductivity of a mineral fibre slab and the water vapour diffusion flux density through the insulation material, measured with a modified guarded hot plate apparatus with cellular concrete and with blotting paper, each as a moisture-releasing and moisture-uptaking medium surrounding the mineral fibre slab.

The linear relationship between the fictitious thermal conductivity and the diffusion flux indicates that the change in thermal conductivity is attributable solely to latent heat effects through phase change and has effects through phase change and ahs nothing to do with the actual heat conduction.

They show the fictitious thermal conductivity of dry mineral fibre slabs between moistened blotting paper or cellular concrete plates in dependence of the vapour diffusion flux density. Considering that at a diffusion flux density flow of 12 g/m^{2}h, which corresponds to about one tenth of the water evaporated from a wet building facade under avarage outside air conditions, the heat flow already doubles as a result of vapour diffusion through the insulation layer, it becomes clear that these enthalpy flows must be taken into account by a separate equation. Adding a corresponding moisture supplement to the thermal conductivity does not represent the real situation, since it is not the moisture in the insulation layer, but the water content in the layers adjacent to it, and the diffusion resistance of the insulation, which affect the moisture-related heat transport.

The interaction of vapour diffusion and phase change is therefore taken into account in the form of a source or sink term in the heat balance equation:

$$S_h = h_v \nabla \cdot g_v \qquad (28)$$

where

S_h	[J/m^{3}s]	heat source or heat sink due to condensation/evaporation
h_v	[J/kg]	latent heat of phase change
g_v	[kg/m^{2}s]	water vapour diffusion flux density.

The latent heat of phase change consists of the specific evaporation enthalpy of pure water (h_v=2500 kJ/kg) and the material-dependent sorption enthalpy. However, according to findings in [34], this sorption enthalpy can be disregarded (in contrast to the evaporation enthalpy) in the moisture range above 50% relative humidity, which is the important range in terms of building physics, for most building materials.

2.5 Heat and moisture transfer at building component boundaries

The heat and moisture exchange between a building component and its surroundings can be described by means of boundary conditions of the first, second and third kind. Boundary conditions of the first kind, where surface conditions are the same as the ambient conditions, occur in terms of heat and vapour transport only when the building component is in contact with water or the earth. In the case of liquid transport, this boundary condition applies when the component surface is completely wetted from rain or ground water. Boundary conditions of the second kind, which require on the surface a constant heat or mass flow, characterize the influence of solar radiation on heat transport and the uptake of rain water when the surface is not completely wetted. Symmetry conditions and adiabatic or water and vapour-tight conditions are covered by zero flows at the component boundaries.

Boundary conditions of the third kind, which require a transitional resistance between the component surface and its surroundings, constitute the most frequent kind of heat and moisture exchange.

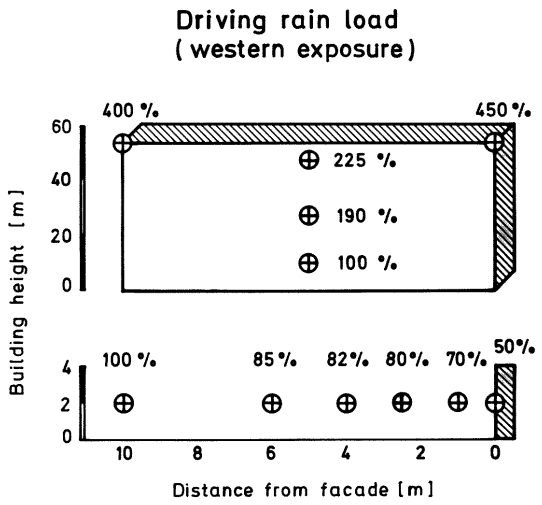

Fig. 25 Distribution of driving-rain volume on the weather side of a higher rise building (top); the driving-rain volume at a height of 10 m equals 100 % [115]. Approaching the facade the driving-rain load diminishes as measurements at various distances in front of a 4 m high test hall have shown (bottom); the reference point (driving-rain volume = 100 %) is located 10 m from the wall at a height of 2 m [79].

When two different kinds of boundary conditions occur simultaneously, as in case of solar radiation and convection at building facades, this can be covered in the solution by using appropriate source terms.

Heat exchange on a surface based on convection and long-wave radiation is calculated in building physics by means of the following equation [39];[91]:

$$q=\alpha(\vartheta_a-\vartheta_s) \qquad (29)$$

with $\alpha=\alpha_c+\alpha_r$

where

q	[W/m^2]	heat flux density
α_c	[W/m^2]	convective heat transfer coeff.
α_r	[W/m^2]	radiative heat transfer coeff.
ϑ_s	[°C]	surface temperature
ϑ_a	[°C]	ambient temperature

The dependence of the heat transfer coefficient α on the local air flow conditions, the temperature and the geometry of the building component is relatively complex; to simplify calculations in building physics, it is assumed to be constant. The following values of a are prescribed for the calculation of the thermal transmittance of building components (the U-value) in standard DIN 4108 [23]:

outside	α=25 W/m^{2}K
inside	α=8 W/m^{2}K.

While the value of the heat transfer coefficient for the component surface on the inside is confirmed by measuring results in [29] for an undisturbed wall at homogeneous room air temperature, the value of the outside transfer coefficient is too high for German climatic conditions. Based on a mean wind velocity of 3.6 m/s in Germany, [113] suggests a value of 17 W/m^{2}K, with the convective portion at about 10 W/m^{2}K. This average value does not apply to greatly exposed building components or building surfaces at great height, where correspondingly higher heat transfer coefficients must be substituted. The inside heat transfer coefficient in the region of corners or edges is generally below the normal value of 8 W/m^{2}K. Should there be a stratification of temperature in a room, this must not be covered in moisture transport calculations by a transfer coefficient based on the mean temperature, as described in [29], since this leads to errors in evaluating the moisture conditions on component surfaces on the inside. If the distribution of room temperature values must be taken into account in the calculation, this can only be done by specifying the boundary conditions as a function of height.

The water vapour transfer can be described in a manner similar to the heat transfer:

$$g_v=\beta_p(p_a-p_s) \qquad (30)$$

where

g_v	[kg/m^{2}s]	water vapour flux density

β_p [kg/m^{2}sPa] water vapour transfer coefficient
p_s [Pa] water vapour pressure on the building component surface
p_a [Pa] ambient water vapour pressure

where β_p, can be derived from the convective heat transfer coefficient through analogous relations [48], as confirmed by experimental results in [114]:

$$\beta_p = 7 \cdot 10\text{-}9\ \alpha_c \qquad (31)$$

where

α_c [W/m^{2}K] convective heat transfer coefficient.

The resulting values for the water vapour transfer of outside and inside building component surfaces, together with the coefficients for heat transfer, are shown in Table 5.

The effect of solar radiation and rain can be taken into account by means of boundary conditions of the second kind or by a source term. The heat flow from solar radiation to the surface can be calculated as follows:

$$q = a_s \cdot I \qquad (32)$$

where

Table 5 Mean surface transfer coefficient for calculating the heat and moisture exchange between outdoor and indoor building component surfaces and the surroundings.

building component surface	transfer coefficients	
	heat transfer α [W/m^{2}K]	water vapour transfer β_p [kg/m^{2}sPa]
outdoors	17	$75 \cdot 10^{-9}$
indoors	8	$25 \cdot 10^{-9}$

q [W/m^2] heat flow from short-wave solar radiation
a_s [-] short-wave absorptivity
I [W/m^2] solar radiation vertical to the building component surface

Table 6 Short-wave absorptivity and brightness reference value of various building material surfaces [89].

In red building materials and in wood, light absorption, expressed by the brightness reference value, is greater than energy absorption in the total short-wave spectral range.

building material	short-wave absorptivity [-]	brightness reference value [%]
roof tile red brown	0,6 0,8	20 10
bituminous roof covering	0,9	10
plaster, white (aged)	0,4	60
klinker brick dark red	0,7	15
lime silica brick dry wet	 0,45 0,6	 55 40
Schilf sandstone dry wet	 0,7 0,85	 30 15
red Main sandstone	0,75	19
Sandstone with patina	0,9	10
wood (spruce) untreated weathered (silver-gray) painted brown	 0,4 0,7 0,8	 50 20 10

The solar radiation vertical to the building component surface can be calculated depending on the incline and the orientation of the surface, from direct (or global) and diffuse solar radiation to a horizontal surface, with the help of the approximation relations in [120]. However, any shade cast on the surface must be taken into account as well. According to [6], the absorption value can be determined from the brightness reference value and a colour-specific parameter. Table 6 lists short-wave absorptivities and brightness reference values for various building material surfaces.

More difficult than the determination of solar radiation is the calculation of rain or the driving-rain load for a building component surface, unless it was measured throughout the calculation period directly on the surface of the component to be tested. In the case of approximately horizontal surfaces, the normal rain data from nearby weather stations can be used. This does not apply to surfaces with extreme circulatory flow conditions, such as the walls or roofs of highrise buildings. In such cases, local measurements must be used if the amount of rain is to be quantified accurately. When rain data from German test reference years [12] are used, caution is advisable as well. As shown in [84], these artificially produced sets of weather data are realistic in terms of the total amounts of precipitation, but not in terms of average rain periods. The number of hours with precipitation events is too high by at least a factor of two. In the case of building components with only moderately absorbent surfaces, this can lead to considerably wrong estimates. Since the excess rain water runs off, the duration of surface wetting is more significant in these cases than the precipitation intensity at a given time.

It is best when the driving-rain load of vertical surfaces of building components is measured on site. As the measurements of driving rain in [79] and [115] have already shown (illustrated in Fig. 25), driving-rain intensities of a building can vary by almost one decimal power, depending on the height of the building and the position of the wall section in question. However, since it is often impossible to measure driving rain over the long term, we will provide here one possibility for estimating the driving-rain load based on the weather data for normal rain, wind velocity and wind direction. As shown in Fig. 26, there exists - due to the frequently repeating circulatory flow pattern of buildings - a reasonably linear relationship between the vectorial wind velocity, multiplied by normal rain, measured at a site not influenced by buildings, and the driving-rain load of a wall section:

$$R_s = r_s \cdot v \cdot R_N \qquad (33)$$

where

R_s	[kg/m^{2}s]	driving-rain load of the wall section
R_N	[kg/m^{2}s]	normal rain
r_s	[s/m]	site-specific driving-rain coefficient
v	[m/s]	wind velocity vertical to the wall

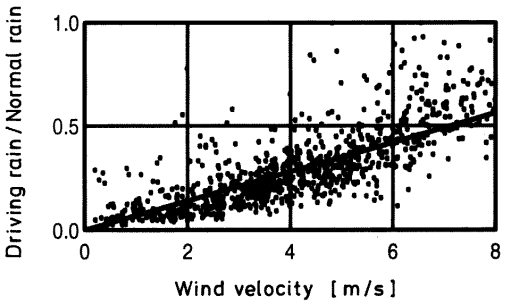

Fig. 26 Correlation between the ratio of driving rain, hitting the middle of the facade of a 4 m high test wall, and normal rain, and the wind velocity perpendicular to the facade measured at the standard height of 10 m. The measuring points represent hourly values continuously recorded during a period of 4 years. The straight line was determined by linear regression

The site-specific driving-rain coefficient for a free-standing surface (undisturbed flow conditions) about 2 meters above the ground is about 0.2 [87]. With the aid of Fig. 25, this can be used to estimate coefficient r_s for a wall section. However, it is better to determine r_s experimentally as has been explained in Fig. 26 by measuring the driving rain for a short period at the wall site in question.

If the rain or driving-rain load of a building component surface is known, the moisture state of the surface (as long as the surface is not completely

wetted) can be calculated with an equation similar to that of solar radiation:

$$g_w = a_r \cdot R \qquad (34)$$

where

g_w	[kg/m^{2}s]	surface liquid flux density
R	[kg/m^{2}s]	precipitation load vertical to building component surface
a_r	[-]	precipitation absorptivity.

Using the precipitation absorptivity enables us to take into account that a part of the rain water impacting on vertical surfaces splashes off again. The value of a_r depends on the roughness of the surface and the type of precipitation. In the case of hail or snow, a_r is approximately zero. Since no systematic studies exist so far in this connection, the precipitation absorptivity must be estimated or determined by comparing measurements and calculations. In the case of horizontal building components, a_r is generally 1, since the splashing rain water drops back onto the surface again.

As soon as the surface is completely wetted with water (i.e. when there is more rain than the component can take up), we must "switch" from a boundary condition of the second kind to one of the first kind by substituting the relative humidity on the surface as 1. When the conditions change again, e.g. through a decrease in precipitation intensity, we can "switch back" again to a boundary condition of the second kind. The question as to which of the two boundary conditions occurs more frequently depends on the given precipitation load and on the absorbency of the building component surface. Since in most building component surfaces, with the exception of exposed masonry and natural stone walls, the ability for capillary water takeup is only moderate, the boundary condition of the first kind predominates. This also means that in such cases it is not as crucial to have an accurate knowledge of the quantitative rain load, and that the precipitation absorptivity as well as the site-specific driving-rain coefficient may be estimated.

2.6 Calculation methods used until now

A comprehensive list of studies and calculation methods to quantify the moisture transport in building materials was already compiled by Kießl and Gertis [57], [58]. We examined these as well as more recent studies and classified them in conjunction with the fundamental publications in the field of moisture transport calculations, according to their transport equations and potentials. At the same time we tried to show the advantages and problems of the different models from today's perspective.

In contrast to heat transport in building components, where the driving potential without a doubt is the temperature, there is no unanimity about the choice of driving potentials for the moisture transport. In spite of the theoretical possibility of converting one potential into another, the choice of these potentials is of great importance for the general applicability and accuracy of mathematical models and the computer programs developed from them. Since in porous materials moisture can move in vaporous or liquid form, with different driving forces, most publications assume two or more potentials for moisture transport.

But as before, calculation methods are still being developed today, which - as the standard method based on Glaser [38] in standard DIN 4108 [23] - consider only the vapour transport in building components. As examples we cite studies by Husseini [47] and Ricken [109] as well as the method by Keresteciogl u and Gu [55] based on a calculation technique by Crank [18]. In contrast to the above-mentioned standard method, these methods use simplified calculation techniques to determine moisture storage through sorption and moisture dependence of vapour diffusion resistance. Ricken's calculation model also considers capillary conduction by means of a special algorithm, which upon reaching the critical moisture content in a numerical grid distributes the excess water to the adjacent elements through "calculative shovelling". Since in these models liquid transport effects are not or not properly taken into account, they are of limited use and we will not discuss them any further.

One of the first to study thoroughly the moisture movements in porous materials under the influence of temperature gradients was Krischer [64]. By analyzing the water content of sand wetted and dried in temperature gradients, he discovered that there are two transport mechanisms for material moisture, which may also act against each other. One is vapour diffusion, which at room air temperature can be described with equation (11). Krischer called the other transport mechanism "capillary water movement", and he attributed it to the capillary suction stress which develops as the result of curved water surfaces in the pore system of moist building materials. For capillary-active building materials with a broad pore size spectrum he derived a material-specific connection between water content and capillary pressure, so that the moisture transport in the liquid region, as in equation (13), can be described with the water content as the driving potential. For the temperature range that is of interest in building practice, Stefan's diffusion equation chosen by Krischer can be substituted by Fick's diffusion equation, which results in the following transient differential equation for calculating the moisture transport in porous building materials:

$$\frac{\partial w}{\partial t} = \nabla \cdot \left(D_w \nabla w + \delta_p \nabla p \right) \qquad (35)$$

where

w	[kg/m^3]	water content
D_w	[m^2/s]	capillary transport coefficient
p	[Pa]	water vapour partial pressure
δ_p	[kg/msPa]	water vapour permeability.

Based on a calculation technique as in equation (35), Gagarin [32], Bagda [5], Greubel [41] and Andersson [2] have developed computer programs for calculating transient heat and moisture flows in building components. Gagarin [32], who assumed in his model a steady-state temperature field, calculated the moisture behaviour of insulated stables built with light-weight concrete slabs with and without vapour barrier, and compared these results with measurements. Bagda's computer program was designed more for calculating the moisture behaviour of homogeneous building components. To calculate multi-layered components, it is necessary to determine the so-called coupling constants. It is used primarily to estimate the effect of coatings on the water uptake or drying behaviour of building components. Greubel [41] calculated and measured experimentally the behaviour of wooden building materials subjected to vapour diffusion in a temperature gradient. Andersson's calculation example [2] concerned the drying behaviour of a basement wall made of light-weight concrete. But no experimental comparison was provided for evaluating the computing technique.

A disadvantage of the models based on equation (35) is the discontinuity of the water content in multi-layered building components. Distinct jumps in the water content, as they occur for example at the layer boundaries between plaster and masonry, make it necessary to calculate the moisture transport through complex transitional functions at the material boundaries. Furthermore, as shown in section 2.3.5, there is no direct connection in the supersaturated region between the water content and the driving force for the liquid transport - the capillary suction stress. That is why in this region, the use of water content as the moisture potential can lead to wrong estimates.

In this connection, relating the water content of a building material to the water content of a reference material, as suggested by Fischer et al [31] does not make for an improvement. While the thus standardized water content is continuous at the layer boundaries, the condition on which the assumption in [31] is based, namely that all moisture storage functions must resemble that of the reference material, is met only in exceptional cases. The same applies to the supersaturated region.

Instead of selecting the water content of a reference material, which can be subject to fluctuating properties, as the driving potential for the capillary transport, it is therefore more practical from a

physical point of view to use the already mentioned suction stress. Even without special pore models, a direct relationship between the water content and the equilibrium suction stress can be determined in the higher moisture range for hygroscopic capillary-active materials by pressure plate measurements as mentioned in section 2.2.2. In the sorption moisture region, the capillary suction stress can be calculated from the relative humidity by means of Kelvin's relation, i.e. equation (2). For materials that are not capillary-active, such as most insulation materials, the capillary suction stress cannot be defined, but they also do not have any liquid transport. If we substitute the water content in equation (35) by the capillary suction stress P_k, we obtain the following equation, taking into account a transport coefficient D_p related to the capillary pressure:

$$\frac{\partial w}{\partial t} = \nabla \cdot \left(\delta_p \nabla p - D_p \nabla P_k \right) \qquad (36)$$

where

w	[kg/m^3]	water content
p	[Pa]	water vapour partial pressure
δ_p	[kg/msPa]	water vapour permeability.

On this equation the models of Rode [110] and Nicolas [98] are based. Rode divides equation (36) into separate transport equations for vapour and liquid, which are solved by iterative adaptation in connection with the heat conduction equation. In addition to the moisture potentials given in this equation, the two-dimensional model of Nicolas takes into account the effect of the pore air. However, his calculations are limited to homogeneous sample elements made of sand or cement mortar.

Another more mathematical method of calculation, based on Luikov [90] or Phillip and de Vries [104], deals with porous materials as a kind of "black box" in which moisture is transported because of temperature and water content gradients. This calculation technique, which can be derived from methods used in the thermodynamics of irreversible processes, leads to the following description of moisture transport:

$$\frac{\partial w}{\partial t} = \nabla \cdot \left(k_w \nabla w + k_\vartheta \nabla \vartheta \right) \qquad (37)$$

where

w	[kg/m^3]	water content
k_w	[m^2/s]	moisture and temperature dependent transport coefficient for the water content gradients
ϑ	[°C]	temperature
k_ϑ	[kg/msK]	moisture and temperature dependent transport coefficient for the temperature gradient.

In this formulation, which can be found in many publications - for example in Crausse[19], Häupl et al [43], Kari et al [53], Kohonen [62], van der Kooi [63], and Mizuhata et al [95] - each of the two transport coefficients k_w and k_δ is dependent on both potentials. It is virtually impossible to determine this double dependence exactly, even with a major experimental effort, as has been proven in [20]. For that reason and because of the problem of the already described discontinuity of the water content, this calculating technique was used by Crausse [19], Kari et al [53] and van der Kooi [63] only for homogeneous building materials or sand, and not for multi-layered components. An exception is the two-dimensional moisture transport program by Kohonen [62]. Here, supported by extensive measurements of transport coefficients, the calculation of multi-layered components including convection effects is possible, too. But according to the author, the fairly complex transitional conditions at the border between two building materials can lead to numerical problems.

The initial advantage of the models based on equation (37), to be able to describe moisture transport without an exact knowledge of the physical background, is lost because of the great experimental effort required in determining the transport coefficients. By using Krischer's model [64], in which vapour and capillary water transport do not influence each other, the coefficients k_w and k_ϑ in equation (37) can be represented as follows:

$$k_w = D_w + \delta_p p_{sat} \frac{d\varphi}{dw} \qquad (38)$$

$$k_\vartheta = \delta_p \varphi \frac{dp_{sat}}{d\vartheta} \qquad (39)$$

where

D_w	[m^2/s]	capillary transport coefficients
δ_p	[kg/msPa]	water vapour permeability
p_{sat}	[Pa]	water vapour saturation pressure
w	[kg/m^3]	water content
φ	[-]	relative humidity
ϑ	[°C]	temperature.

This conversion of coefficients, which was used, for example, by Häupl et al [43] leads to a lessened experimental effort to determine these coefficients. But this model is mathematically identical with Krischer's model [64]. i.e. a possible influence of the vapour transport by capillary water in the pores can no longer be considered. If the transport coefficients in equation (37) are specified with the relations (38) and (39), the moisture transport formulas (35) and (37) are mathematically identical. But this means that in this case, the already described inadequacies of the water content as moisture potential apply to equation (37) as well. In addition, the numerical solution of equation (37) leads to problems due to the splitting-up of vapour diffusion into a temperature and a moisture-dependent portion, which are avoided when equation (35) is used. This will be explained by means of Fig. 27. Using as an example a heated room without moisture production (same absolute humidity inside as outside), the profiles of temperature, water content and vapour pressure are plotted schematically over the cross section of the outside wall. Disregarding the liquid transport phenomenon, in a steady-state case with opposite gradients of temperature and water content, the result is a constant vapour pressure in the cross section of the building component, and thus no vapour transport either.

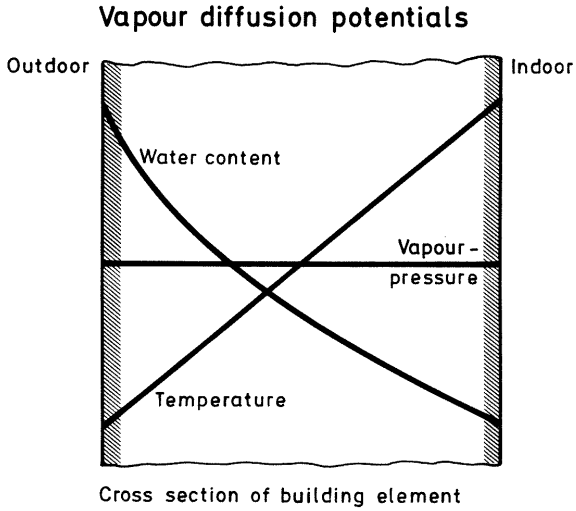

Fig. 27 Schematic diagram showing the steady-state water content, temperature and vapour pressure gradients in the exterior wall of a heated room without moisture production (same absolute humidity inside and outside).

Through the vapour transport potentials “temperature” and “water content” in equation (37) we obtain the fictitious diffusion flows based on the opposite gradients, which in this example must add up to zero across the entire cross section. (Due to minor inaccuracies in the numerical calculation this can never be achieved exactly.)

The calculative diffusion flows resulting from the moisture transport potentials "temperature" and "water content" in equation (37) must add up to zero across the entire cross section. But because of the exponential dependence of the vapour pressure on the temperature and because of inaccuracies in determining the local rise in sorption isotherms, small errors occur in the numerical calculation which can lead to local vapour diffusion flows of different magnitude. Since in most building constructions vapour diffusion constitutes the determining

moisture transport mechanism, this calculating technique is problematic in principle.

In a similar manner, Kießl [57] split up vapour diffusion into a temperature and a moisture-related portion. But for the capillary transport he introduced a new material-independent moisture potential which is continuous in multi-layered building components and which he calls generalized potential φ. This potential, which was already described under section 2.2.2, is identical in the hygroscopic region with the relative humidity, and it then becomes a function calculated from the pore radius distribution. The capillary moisture transport across material boundaries and the equilibrium states in the hygroscopic region can be calculated with this model without supplementary functions. With the moisture transport coefficients chosen by the author [57] - FDP and FDT for vapour diffusion and FKU for capillary conduction - the resulting moisture transport equation looks as follows:

$$\frac{\partial w}{\partial t} = \nabla \cdot \left(FKU \frac{dw}{d\phi} \nabla\phi + \rho_w \left(FDP \nabla\varphi + FDT \nabla\vartheta \right) \right) \quad (40)$$

where

w	[kg/m^3]	water content
ρ_w	[kg/m^3]	water density
φ	[-]	generalized potential
φ	[-]	relative humidity
ϑ	[°C]	temperature.

This equation serves as the basis for a computer program with which the non-isothermal moisture behaviour of various roof and wall constructions has been calculated. The mathematical results were validated by using an example of a flat roof built of cellular concrete; the drying-out behaviour of the roof was experimentally examined in [77].

Kießl's model was also adopted by Garrecht [33] and applied to two-dimensional but only isothermal conditions. With the aid of a finite element program system he calculated the moisture behavior of masonry moistened in the foundation section. Since in many buildings, temperature gradients in masonry play an important role, this approach is only of limited use. Not isothermal, but applicable only to steady-state conditions is the two-dimensional extension of Kießl's model by Eisner and Winter [28] for the calculation of the moisture effect on the heat transport in vertically perforated bricks.

Based on the diffusion model of Keresteciogl u [55] and supplemented by Kießl's capillary conduction formulas, Kupke and Pfrommer [86] have developed a calculating method that works with "temperature" and "water vapour concentration" as moisture potentials. However, the required mathematical conversion lead to transport coefficients which are no longer physically plausible. For example, the capillary transport is split up into concentration and temperature-related portions, with the temperature-related moisture flow running against the temperature gradient, i.e. from the cold to the warm side.

Although Kießl's model - equation (40) - has proven its suitability for calculating the moisture transport in buildings, its disadvantages and those of the calculating methods based on it lie in the great experimental effort required to determine the moisture transport coefficients FDP and FDT, and in the somewhat abstract definition of the generalized moisture potential. Moisture potentials similar to those of Kießl were used by Neiß [97] and Matsumoto and Sato [92] in their moisture transport models. The two-dimensional method by Neiß is designed for calculating the heat and moisture transport and ice formation in the soil. It is based on temperature and suction stress as moisture potentials. Instead of suction stress, Matsumoto and Sato chose the chemical potential of water to calculate condensation in building components.

In summary it can be stated that for calculating the non-isothermal moisture transport, two independent driving potentials are necessary. Most frequently used as moisture transport potentials are temperature, water content, vapour pressure and suction stress. Looking at the physical background

of vapour and liquid transport, we find that temperature and water content are only indirect moisture potentials. The transport coefficients resulting from a combination of these two potentials are generally difficult to determine, and they lead to relatively complex functions. Simpler and physically more plausible transport coefficients result from the selection of the real moisture driving forces "vapour pressure" and "capillary suction stress". However, capillary suction stress has the disadvantage that it cannot be defined in materials that are dry or not capillary-active. It also cannot be measured directly in moist material. But as section 2.2.2 has shown, it can be substituted by the relative humidity. Thus, vapour pressure and relative humidity constitute two physically plausible moisture transport potentials which are generally known and simple to measure. This is a great advantage especially in the formulation of boundary conditions. In spite of these advantages, these two potentials have so far not been used in combination for moisture calculation techniques.

3. Numerical calculation of the simultaneous heat and moisture transport

From the described physical principles of heat and moisture transport a closed differential equation system can be developed with which the moisture behaviour of multi-layered building components can be calculated under natural climatic boundary conditions. Since it is a non-linear equation system whose coefficients are greatly dependent on the potentials, an analytical solution is not possible. Described in detail below is the derivation of the coupled equation system and the numerical solution technique which forms the basis for the newly developed computer program called **WUFI** or WUFIZ [Wärme- und Feuchtetransport instationär zweidimensional = transient one or two-dimensional heat and moisture transport]. This will be followed by instructions on how to select the numerical grid and the time increments. Also described are the convergence criteria and controls to ensure the accuracy of the numerical calculation.

3.1 Derivation of transport equations

The law of continuity applies to heat as well as to moisture, i.e. the change in enthalpy or moisture in a volume element is determined by the divergence of heat or moisture flows through the surface of the element and the heat or moisture sources or sinks in the element. As far as heat is concerned, this results in the following balance equation:

$$\frac{\partial H}{\partial t} = -\nabla \cdot q + S_h \qquad (41)$$

where

H	[J/m^3]	total enthalpy
q	[W/m^2]	heat flux density
S_h	[W/m^3]	heat source or heat sink.

The total enthalpy of a building component layer consists of the enthalpy of the dry building material in equation (25) and the enthalpy of the water contained therein, in equation (26):

$$H=Hs+Hw \qquad (42)$$

where

H_s	[J/m^3]	enthalpy of the dry building material
H_w	[J/m^3]	enthalpy of building material moisture.

The heat flux density is proportional to the thermal conductivity of the moist building material in equation (27) and the temperature gradient:

$$q=-\lambda\nabla\vartheta \qquad (43)$$

where

q	[W/m^2]	heat flux density
λ	[W/mK]	thermal conductivity of the moist building material
ϑ	[°C]	temperature

The enthalpy flows through moisture movement and phase transition can be taken into account in the form of source terms in the heat balance equation. Since, as explained in section 2.4.3, only vapour diffusion with simultaneous phase transition is of practical importance, the following relation results for the source term:

$$S_h = -h_v \nabla \cdot g_v \qquad (44)$$

where

S_h	[J/m^{3}s]	heat source/heat sink through condensation / evaporation
h_v	[J/kg]	latent heat of phase change
g_v	[kg/m^{2}s]	vapour diffusion flux density.

The latent heat of phase transition consists of the specific evaporation enthalpy of pure water (h_v = 2500 kJ/kg) and the sorption enthalpy depending on the building material. However, as already mentioned, the sorption enthalpy in the humidity range of interest in building physics (over 50% relative humidity), is negligible in most building materials when compared with the evaporation enthalpy. The vapour diffusion flux density g_v is calculated with the moisture balance equation, which in analogy to the heat balance equation can be expressed as follows:

$$\frac{\partial w}{\partial t} = -\nabla \cdot \left(g_w + g_v\right) + S_w \qquad (45)$$

where

w	[kg/m^3]	water content of the building material layer
g_w	[kg/m^{2}s]	liquid transport flux density
g_v	[kg/m^{2}s]	vapour diffusion flux density
S_w	[kg/m^{3}s]	moisture source or moisture sink.

The liquid transport flux density g_w depends on the gradient of the relative humidity as has been shown in section 2.3:

$$g_w = -D\varphi \nabla \varphi \qquad (46)$$

where

D_φ	[kg/ms]	liquid conduction coefficient
φ	[-]	relative humidity.

The vapour diffusion flux density g_v can be determined as follows according to section 2.3:

$$g_v = -\delta_p \nabla p \qquad (47)$$

where

δ_p	[kg/msPa]	water vapour permeability of building material
p	[Pa]	water vapour partial pressure.

The water vapour permeability of the building material is the quotient from the water vapour permeability of stagnant air and the vapour diffusion resistance factor μ of the building material, as can be seen by a comparison with equation (11). It is very rare for moisture sources to occur in building components (e.g. in case of a ruptured water pipe); they are not taken into consideration here. Moisture sinks are of greater practical importance, since they can be used to characterize the curing behaviour of concrete and mortar. But since these are chemical processes, which are not subject of this paper, moisture sinks are disregarded here.

The equations for the heat balance (41) and the moisture balance (45) are closely coupled to each other through the moisture dependence of the total enthalpy, the thermal conductivity and the source term in equation (41) and through the temperature dependence of the moisture flows in equation (45). They can be solved together only when the total number of variables in both equations is limited to two. These two variables, from which all others can be derived through simple relationships, are the temperature and the relative humidity. Thus we obtain the following for the simultaneous heat and moisture transport:

$$\frac{dH}{d\vartheta} \cdot \frac{\partial \vartheta}{\partial t} = \nabla \cdot \left(\lambda \nabla \vartheta\right) + h_v \nabla \cdot \left(\delta_p \nabla \left(\varphi p_{sat}\right)\right) \qquad (48)$$

$$\frac{dw}{d\varphi} \cdot \frac{\partial \varphi}{\partial t} = \nabla \cdot \left(D_\varphi \nabla \varphi + \delta_p \nabla \left(\varphi p_{sat}\right)\right) \qquad (49)$$

where

$dH/d\vartheta$	[J/m³K]	heat storage capacity of the moist building material
$dw/d\varphi$	[kg/m³]	moisture storage capacity of the building material
λ	[W/mK]	thermal conductivity of the moist building material
D_φ	[kg/ms]	liquid conduction coefficient of the building material
δ_p	[kg/msPa]	water vapour permeability of the building material
h_v	[J/kg]	evaporation enthalpy of the water
p_{sat}	[Pa]	water vapour saturation pressure
ϑ	[°C]	temperature
φ	[-]	relative humidity

The water vapour saturation pressure can be calculated by means of an empirical relationship [22] as a function of temperature:

$$p_{sat} = 611 \cdot \exp\left(\frac{a \cdot \vartheta}{\vartheta_0 + \vartheta}\right) \qquad (50)$$

with

$a = 22{,}44$ $\quad \vartheta_0 = 272{,}44$ °C $\quad \vartheta < 0$ °C

$a = 17{,}08$ $\quad \vartheta_0 = 234{,}18$ °C $\quad \vartheta \geq 0$ °C

For two-dimensional conditions and cartesian coordinates we obtain the following transport equations for heat and moisture from equations (48) and (49), taking into consideration the anisotropic properties of some building components:

$$\frac{dH}{d\vartheta}\cdot\frac{\partial\vartheta}{\partial t} = \frac{\partial}{\partial x}\left(\lambda_x\frac{\partial\vartheta}{\partial x}\right) + \frac{\partial}{\partial y}\left(\lambda_y\frac{\partial\vartheta}{\partial y}\right) + \\ + h_v\frac{\partial}{\partial x}\left(\delta_{px}\frac{\partial\varphi p_{sat}}{\partial x}\right) + h_v\frac{\partial}{\partial y}\left(\delta_{py}\frac{\partial\varphi p_{sat}}{\partial y}\right) \qquad (51)$$

$$\frac{dw}{d\varphi}\cdot\frac{\partial\varphi}{\partial t} = \frac{\partial}{\partial x}\left(D_{\varphi x}\frac{\partial\varphi}{\partial x} + \delta_{px}\frac{\partial\varphi p_{sat}}{\partial x}\right) + \\ + \frac{\partial}{\partial y}\left(D_{\varphi y}\frac{\partial\varphi}{\partial y} + \delta_{py}\frac{\partial\varphi p_{sat}}{\partial y}\right) \qquad (52)$$

where

λ_x , $\lambda_{,y}$	[W/mK]	thermal conductivity in x or y direction
$D_{\varphi x}$, $D_{\varphi y}$	[kg/ms]	liquid conduction coefficient in x or y direction
δ_{pX} , δ_{py}	[kg/msPa]	vapour permeability in x or y direction.

Since axisymmetric building components such as columns, chimneys, etc. can also be calculated with the WUFIZ computer program, we also provide the transport equations with cylindrical coordinates:

$$\frac{dH}{d\vartheta}\cdot\frac{\partial\vartheta}{\partial t} = \frac{1}{r}\frac{\partial}{\partial r}\left(r\lambda_r\frac{\partial\vartheta}{\partial r}\right) + \frac{\partial}{\partial z}\left(\lambda_z\frac{\partial\vartheta}{\partial z}\right) + \\ + \frac{h_v}{r}\frac{\partial}{\partial r}\left(r\delta_{pr}\frac{\partial\varphi p_{sat}}{\partial r}\right) + h_v\frac{\partial}{\partial z}\left(\delta_z\frac{\partial\varphi p_{sat}}{\partial z}\right) \qquad (53)$$

$$\frac{dw}{d\varphi}\cdot\frac{\partial\varphi}{\partial t} = \frac{1}{r}\frac{\partial}{\partial r}\left(rD_{\varphi r}\frac{\partial\varphi}{\partial r} + r\delta_{pr}\frac{\partial\varphi p_{sat}}{\partial r}\right) + \\ + \frac{\partial}{\partial z}\left(D_{\varphi z}\frac{\partial\varphi}{\partial z} + \partial_{pz}\frac{\partial\varphi p_{sat}}{\partial z}\right) \qquad (54)$$

where

λ_r , λ_z	[W/mK]	thermal conductivity in radial or axial direction
$D_{\varphi r}$, $D_{\varphi z}$	[kg/ms]	liquid conduction coefficient in radial or axial direction
δ_{pr} , δ_{pz}	[kg/msPa]	vapour permeability in radial or axial direction.

The liquid conduction coefficients and the water vapour permeability can differ more or less in x and y direction or in r and z direction, depending on the building material. The directional dependence of the transport coefficients is especially pronounced in the case of wood and wood products [60]. But also mineral building materials such as some natural stone [73] can possess anisotropic properties due to sedimentation effects. The coupled equation systems are only numerically soluble, and the coupling of heat and moisture transport equations must be done iteratively by solving the individual equations repeatedly and successively. The numerical discretization and the solution technique will be described in greater detail below.

3.2 Discretization of the differential equations

For the spatial discretization of the partial differential equations, a finite volume technique [101] is preferred to the finite element technique [46]. In comparison with the finite volume technique, the discretization through finite elements is more complex and has not yet been satisfactorily developed so far in terms of the simultaneous heat and moisture transport. On the other hand, the advantages of the finite elements, which allow the better approximation of complex geometries, play only a secondary role in building physics, since most of the building components to be examined for moisture are either rectangular or cylindrical. Discretization in time can be done with an explicit or implicit formulation [17];[50]. In case of explicit formulation, the variables at the new point in time are determined exclusively from the values already known at this point in time. However, the stability of such a formulation depends on certain conditions, which in case of fine local grid spacing lead to very short time increments [55]. Generally, the computing effort as the result of the required short time increments exceeds by far the effort needed when the somewhat more complex implicit formulation is used. The implicit formulation leads to a matrix equation, since all variables must be solved for simultaneously at the new point in time. However, it is stable for all time increment choices. The same applies to a combination of explicit and implicit formulation, named the Crank-Nicolson formulation after its authors [18]. The Crank-Nicolson formulation is of a higher order and thus theoretically more accurate. It is therefore used more often than the fully implicit formulation. However, when it is used for transport calculations, it is subject to numerically induced oscillations due to the non-linear transport coefficients, as studies by [102] and [111] have shown. But also for fundamental reasons explained in [101], the fully implicit formulation, especially at longer time increments, is a better approximation of the physical situation than the Crank-Nicolson formulation. For that reason, we are using the implicit formulation for the discretization in time of the transport equations.

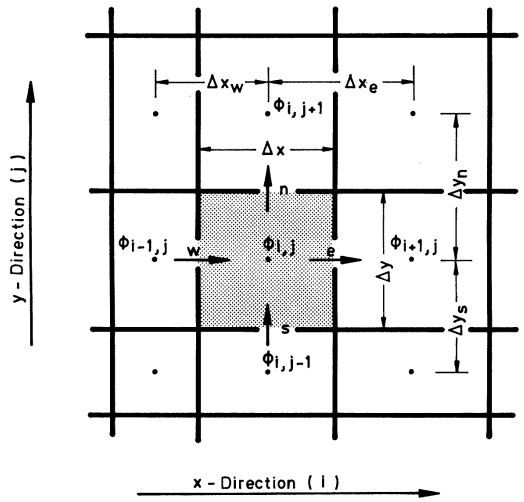

Fig. 28 Schematic diagram showing the finite volume discretization by means of a control volume with lateral lengths of Δx and Δy (shaded) and its adjacent elements. The variables in west (w) and east (e) direction and in north (n) and south (s) direction via the transport flows marked by arrows.

Below we will explain by means of the two-dimensional transport equations (51) and (52) for cartesian coordinates the discretization technique which can also be done in analogous form for axisymmetric transport equations. First we integrate the equations over a discrete volume, extending from the west (w) side to the east (e) side in x direction and from the south (s) to the north (n) side in y direction, as shown in Fig. 28. This discretization process assumes that everywhere in the volume in question the same conditions prevail and that the heat and moisture fluxes across the respective volume boundaries (with dimensions Δx and Δy) are constant along the length of the boundary. A linear interpolation of the transport coefficients, using the designations in Fig. 28, yields the following difference equation for a scalar quantity φ (such as temperature or relative humidity) at the new point in time (n+1) in the volume element in question:

$$
\begin{aligned}
&c\left(\phi_{i,j}^{n+1}-\phi_{i,j}^{n}\right)\frac{\Delta x\Delta y}{\Delta t}= \\
&\Gamma_{xe}\left(\phi_{i+1,j}^{n+1}-\phi_{i,j}^{n+1}\right)\frac{\Delta y}{\Delta x_e}-\Gamma_{xw}\left(\phi_{i,j}^{n+1}-\phi_{i-1,j}^{n+1}\right)\frac{\Delta y}{\Delta x_w}+ \\
&+\Gamma_{yn}\left(\phi_{i,j+1}^{n+1}-\phi_{i,j}^{n+1}\right)\frac{\Delta x}{\Delta y_n}-\Gamma_{ys}\left(\phi_{i,j}^{n+1}-\phi_{i,j-1}^{n+1}\right)\frac{\Delta x}{\Delta y_s}+S\Delta x\Delta y
\end{aligned}
\qquad (55)
$$

where

ϕ	scalar quantity (temperature or relative humidity)
c	storage capacity of the volume element at position i, j
Γ_{xe}, Γ_{xw}, Γ_{yn}, Γ_{ys}	transport coefficient at the east, west, north or south boundary of the volume element i, j
S	source or sink in the volume element i, j
Δt	length of time increment
Δx , Δy	dimension of volume element i, j in x or y direction
Δx_e, Δx_w, Δy_n, Δy_s	distances between the center of the volume element i, j and the mid points of the adjacent elements in east, west, north or south direction
i	indexing of volume elements in x direction
j	indexing of volume elements in y direction
n	indexing of the time increments

By solving this equation for the unknown scalar ϕ, we obtain the following matrix equation, taking into consideration all volume elements:

$$a_p\phi_{i,j}^{n+1} + a_e\phi_{i+1,j}^{n+1} + a_w\phi_{i-1,j}^{n+1} + a_n\phi_{i,j+1}^{n+1} + a_s\phi_{i,j-1}^{n+1} = b \quad (56)$$

where

a_p	matrix coefficient to volume element at position i, j
a_e	matrix coefficient to adjacent element to the east
a_w	matrix coefficient to adjacent element to the west
a_n	matrix coefficient to adjacent element to the north
a_s	matrix coefficient to adjacent element to the south
b	component of the determination vector.

The matrix coefficients characterize the coupling of the individual volume elements. Together they form five diagonals in the quadratic coefficient matrix. The components of the determination vector contain the boundary and initial conditions as well as possible source terms. Expressions for these matrix coefficients and vector components are obtained by substituting the temperature ϑ or the relative humidity φ for the quantitiy φ in equation (56). The results are shown in Table 7. In this manner, the differential equations (51) and (52) were developed into a coupled matrix equation system, the solution of which will be explained below.

3.3 Solution of the matrix equation system

The matrix equations for the heat and moisture transport are solved by means of a very efficient combination of a direct solution method, the tridiagonal algorithm, and an iterative solution method similar to the so-called Gauss-Seidl algorithm [105]. Applied to equation (56), this means that first the pentadiagonal matrix must be converted into a matrix with only three occupied diagonals, for example by including the terms for the north and south direction in the determination vector b:

$$a_p\phi_{i,j} + a_e\phi_{i+1,j} + a_w\phi_{i-1,j} = b_1 \quad (57)$$

where

a_e, a_p, a_w	matrix coefficients in east-west direction
$\varphi_{i+1,j}$, $\varphi_{i,j}$, $\varphi_{i-1,j}$	in east-west direction
b_1	new determination vector with north-south coupling terms.

Subsequently, equation (57) is solved by means of a tridiagonal algorithm, a direct elimination algorithm. However, since the couplings in north-south direction in the determination vector were only estimated values, the solution vector we thus obtained is not yet the exact solution. For that reason, we now convert equation (56) in such a way

Table 7 Matrix coefficients and determination vectors of the discretized heat and moisture transport equations. The indexes refer to the spatial directions shown in Fig. 28

matrix coefficients	discretized differential equations	
	heat transport	moisture transport
a_p	$-\lambda_{xe}\Delta y/\Delta x_e$ $-\lambda_{xw}\Delta y/\Delta x_e$ $-\lambda_{yn}\Delta x/\Delta y_n$ $-\lambda_{ys}\Delta x/\Delta y_s$ $-dH/d\vartheta\cdot\Delta x\Delta y/\Delta t$	$-D_{\varphi xe}\Delta y/\Delta x_e - p_{sati,j}\delta_{pxe}\Delta y/\Delta x_e$ $-D_{\varphi xw}\Delta y/\Delta x_w - p_{sati,j}\delta_{pxw}\Delta y/\Delta x_w$ $-D_{\varphi yn}\Delta x/\Delta y_n - p_{sati,j}\delta_{pyn}\Delta x/\Delta y_n$ $-D_{\varphi ys}\Delta x/\Delta ys_n - p_{sati,j}\delta_{pys}\Delta x/\Delta y_s$ $-dw/d\varphi\cdot\Delta x\Delta y/\Delta t$
a_e	$\lambda_{xe}\Delta y/\Delta x_e$	$D_{\varphi xe}\Delta y/\Delta x_e - p_{sati+1,j}\delta_{pxe}\Delta y/\Delta x_e$
a_w	$\lambda_{xw}\Delta y/\Delta x_e$	$D_{\varphi xw}\Delta y/\Delta x_w - p_{sati-1,j}\delta_{pxw}\Delta y/\Delta x_w$
a_n	$\lambda_{yn}\Delta x/\Delta y_n$	$D_{\varphi yn}\Delta x/\Delta y_n - p_{sati,j+1}\delta_{pyn}\Delta x/\Delta y_n$
a_s	$\lambda_{ys}\Delta x/\Delta y_s$	$D_{\varphi ys}\Delta x/\Delta y_s - p_{sati,j-1}\delta_{pys}\Delta x/\Delta y_s$
b	$-\vartheta^n_{i,j}dH/d\vartheta\cdot\Delta x\Delta y/\Delta t$ $+S_h\Delta x\Delta y/\Delta t$	$-\varphi^n_{i,j}dw/d\varphi\cdot\Delta x\Delta y/\Delta t$

that the east-west coupling terms are added to the determination vector:

$$a_p\phi_{i,j} + a_n\phi_{i,j+1} + a_s\phi_{i,j-1} = b_2 \qquad (58)$$

where

a_n, a_p, a_s	matrix coefficients in north-south direction
$\varphi_{i,j+1}$, $\varphi_{i,j}$, $\varphi_{i,j-1}$	variables in north-south direction
b_2	new determination vector with east-west coupling terms

Now equation (58) can also be solved with the tridiagonal algorithm. The two equations (57) and (58) are solved in alternation - constantly updating the variables (i.e. always substituting them with the values calculated last) - until the appropriate convergence criterion is reached. This solution method is called the ADI (alternating direction implicit) method [103], since the variable field is calculated alternately in x and y direction.

The coupling of the heat and moisture transport equations is done by solving the two equations repeatedly in succession with the aid of the ADI method, up-dating the storage and transport coefficients before each solution step to the new temperature and moisture fields. The final variable fields for each time increment are reached when the maximum changes of temperature and moisture in a building component fall below predetermined limit values from one iteration step to the next. Since the moisture transport coefficients are generally very strongly dependent on the water content, it is usually an advantage to calculate the current moisture field by averaging the present values and the values of the previous iteration step. This method has no implications at all for the accuracy of the calculation; its only purpose is to accelerate convergence.

3.4 Schematic diagram of the numerical calculation method

To explain the important steps in solving the coupled heat and moisture transport equations, we will describe by means of the flow chart in Fig. 29 the calculation method on which the WUFIZ (WUFI-2D) computer program is based. To calculate the heat and moisture behaviour of building components, it is first of all necessary to provide the following sets of data:

- The design of the building component to be calculated and the numerical grid whose mesh sizes must be adapted to the layer structure and the expected local climatic effects, as shown for example in section 4 (Fig. 41).

- The thermal and hygric material parameters and material functions of the building materials forming part of the design, i.e. the bulk density, the porosity, the specific heat capacity, the moisture-dependent and perhaps direction-dependent thermal conductivity, the moisture-dependent (only in case of polymeric plastics) and perhaps direction-dependent water vapour diffusion resistance, and in the case of hygroscopic capillary-active materials also the moisture storage function and the perhaps direction-dependent liquid conduction coefficients for the suction process and the redistribution. Examples for the compilation of these data are given in section 4.

- The climatic boundary conditions inside and outside or on four different sides in a two-dimensional case, and the setting of time increments which depends on the climate data and the required calculation accuracy. The temperature and the relative humidity serve as climatic parameters. As is explained in section 4.1 through the example of a natural-stone wall, the effect of short-wave radiation, long-wave irradiance and precipitation on the building component surface can also be taken into account.

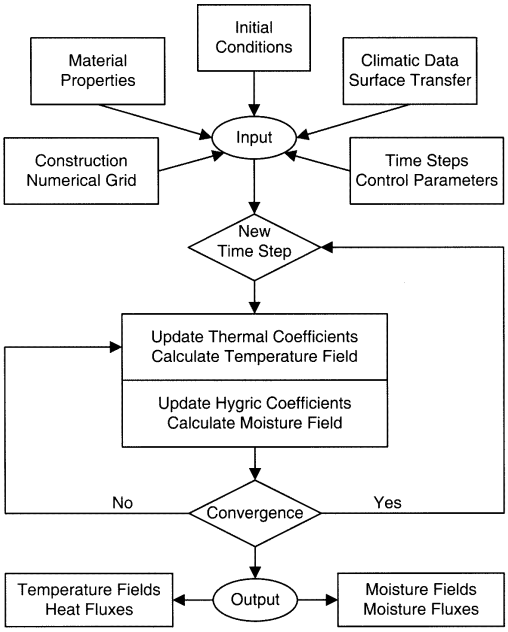

Fig. 29 Flow chart of the calculation technique on which the WUFI or WUFIZ computer program is based.

- The transitional or symmetrical conditions at the building component boundaries, and the control parameters. The transitional conditions include the heat and moisture transfer coefficient, the short wave absorptivity, and the rain absorptivity, all of which become zero in case of a symmetry condition at the corresponding position. The control parameters are used to adjust the calculation accuracy (see section 3.5), the type of initial conditions and other calculation-specific parameters.

Following the input of these sets of data, the steady-state initial distributions of moisture and temperature are calculated, or any initial states, such as distributions from measurements or other calculations are entered. Now begins the transient calculation of the temperature and moisture fields. For every new time increment the coupled heat and moisture transport equations are solved in alternation until the predetermined termination criterion is reached. Before every iterative solution of the heat transfer equation, all moisture and temperature-dependent thermal storage and transport coefficients are updated. The same

applies to the calculation of the hygric coefficients before the solution of the moisture transport equation. At the end of the predetermined calculation period begins the output of the required temperature and moisture fields or heat and moisture flows, and the evolution in time of these variables. The moisture and temperature fields in turn can serve as the initial conditions for further calculations.

3.5 Accuracy of the numerical solution

The accuracy of the numerical solution technique depends on the choice of termination criteria, the length of time increments and the mesh sizes of the numerical grid. To establish termination criteria for the numerical iteration, in most cases it is sufficient when the maximum change of variables in the calculation area during two successive iteration steps falls below one thousandth of one percent in relative humidity and one thousandth of one degree centigrade in temperature. When a building component has a high water content for a long period of time, the termination criterion for moisture should again be reduced by a factor of ten, since minor changes in relative humidity can lead to relatively major changes in water content.

The length of the time increments depends on the time structure of the boundary conditions and on the expected temperature and moisture transients in the building component. When hourly climatic boundary conditions are used, time increments of one hour are adequate. For calculating moisture transport in building physics, time increments between 10 minutes and about 24 hours are practical. In the case of shorter time increments, the calculation time becomes very long, and in the case of longer intervals, the calculation can become inaccurate. To optimize the calculation, the length of the time increments at constant boundary conditions should continuously be adapted to the temperature and moisture changes in the building component.

The mesh sizes of the numerical grid depend on the expected moisture and temperature fields in the building component. In the range of high moisture and temperature gradients and perhaps also at layer boundaries, mesh sizes of only a few millimeters are required, while the grid distances in the range of low gradients can be several centimeters and in exceptional cases even decimeters without having to fear a loss in accuracy. To save storage capacity and computing time without losing accuracy, it is therefore necessary to produce a numerical grid with variable mesh sizes. The grid elements should be adapted in a spatially continuous manner without jumping to the expected gradients in the building component. An example of such an adapted grid is shown in section 4.3 (0). The continuous change of mesh sizes in a grid is achieved best by means of expansion or contraction factors:

$$\Delta x_{i+1} = \varepsilon \cdot \Delta x_i \qquad (59)$$

where

Δx_j, Δx_{j+1}	mesh size of adjacent grid elements
ε	expansion or contraction factor

If the factor ε is larger than one, the grid expands, for values smaller than one it contracts. The factor need not be constant throughout the entire domain. It can vary from one layer of the building component to the other.

To check the correct choice of termination criteria, the size of time increments and the numerical grid, the following tests must be carried out in addition to a plausibility control:

a) Repeat the entire calculation with termination criteria reduced by a factor of ten and with time increments and mesh sizes of the numerical grid reduced by a factor of two, compare the results with those of the first calculation.

b) Compare the accumulated moisture flows across the building component boundaries with the difference in water content in the building component at the end and the beginning of the calculation.

If the differences between the results of tests a) and b) are negligible in terms of the objectives, it can be assumed that the solution is sufficiently accurate. If this is not the case according to test a), the parameters in question must be reset, and the test must be repeated. If the discrepancies in test b) are too high, this may be caused by round-off errors in the computer arithmetic [100]. In that case, the use of a higher precision arithmetic is necessary. However, an accurate numerical solution says nothing about the quality of the transport model on which it is based or the reliability of the material parameters. For that, a comparison with experimental findings is necessary, which follows under section 4.

4. Assessing the results through comparing measurements by means of examples

Before a new calculation method can be generally applied, it must be assessed by means of practical examples, in which the heat and moisture behaviour of building components has been examined experimentally. It must be taken into account that the calculated results depend to a large degree not only on the mathematical model on which they are based, but also on material parameters and climatic data. For that reason, only test examples are suitable in which the initial and boundary conditions as well as the design of the building component are well documented, and for which representative material parameters are available. If that is not the case, there is a danger that lacking data are substituted by "cooked" assumptions, which can help to achieve the desired calculative results, but could also hide any model errors which may exist. Unfortunately, the literature contains few experimental studies which meet the above criteria. For that reason, the examples discussed here rely in part also on experimental studies not yet published.

4.1 Test example I (one-dimensional): Natural stone wall with natural weathering

The first test example, the examination of the moisture behaviour of a natural stone wall section with western exposure [66], meets all the above-named conditions. The material properties of the natural stone as well as the climatic boundary conditions during the experiment are well documented. The standard material parameters of the natural stone, a "Schilf" **) sandstone, are shown in Table 8. The moisture storage function for this material, determined with the aid of sorption and pressure plate measurements, is shown in Fig. 30.

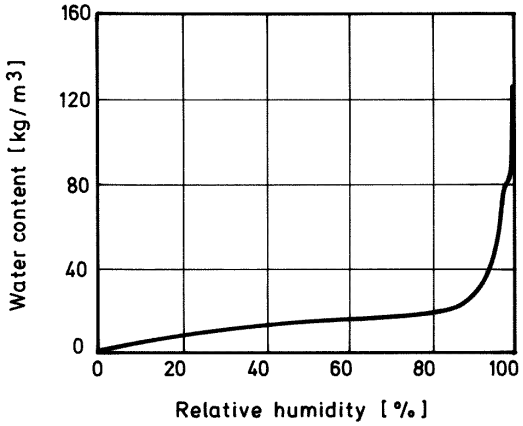

Fig. 30 Moisture storage function of “Sander Schilf” sandstone determined by means of sorption and pressure plate tests [65].

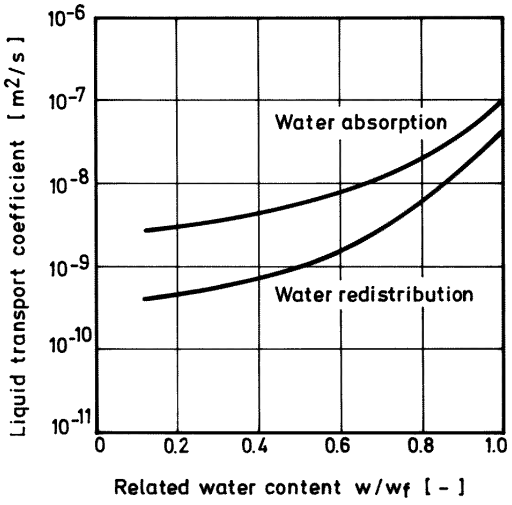

Fig. 31 Liquid transport coefficients for the suction process and the capillary redistribution of “Sander Schilf” sandstone, determined from NMR moisture profile measurements

**) This sandstone is common in southern Germany. "Schilf" means "reed". The stone's fossil impressions were once thought to be caused by reeds

Table 8 Standard material paameters of the building materials used for the calculation example in section 4.

	Building material	Schilf sand-stone	cellular con-crete	Lime silica brick
basic parameters	bulk density [kg/m^3]	2100	600	1800
	pososity [-]	0,16	0,72	0,35
thermal parameters	heat capacity [J/kgK]	850	850	850
	thermal conductivity[W/mK]	1,6	0,14	0,9
	moisture supplement [%/M.-%]	8	3	8
hygric parameters	sorption moisture at 80 % rel.humidity [kg/m^3]	19	27	38
	free water saturation [kg/m^3]	128	340	275
	water vapour diffusion resistance factor [-]	32	8	28
	water absorption coefficient [kg/m2s0,5]	0,02	0,10	0,05

The following figure (Fig. 31) shows the liquid transport coefficients (determined with the aid of NMR moisture profile measurements) for the suction process and capillary redistribution. According to measurements [89], the short-wave absorption value of the sandstone surface lies between 0.7 in dry condition and 0.85 in wet condition (see Table 6). Thus all material parameters required for the calculation are available in measured form.

We carried out the experiment with flank-sealed stone prisms, 25 cm in length, having a cross section of 5 x 5 cm^2. We installed these prisms in dry condition into the west wall of an unheated experimental hall. The inside surface of the prisms was sealed against dew water, while the outside surface was exposed to natural weathering. From the time of .installation, we continuously measured the outside air temperature and humidity as well as solar radiation (western exposure) and the driving rain (which was measured at the same level as the prisms by means of a drop counter integrated into the wall). These climatic data are shown in Fig. 32 (top) in the form of daily means or totals, for an observation period of 80 days. During the same period, the room air temperature dropped relatively evenly from 21 °C to 10°C. Since the prisms were sealed on the inside, the inside relative humidity was irrelevant. The moisture uptake and moisture release behaviour of the natural stone prisms under the described boundary conditions were determined by weighing the prisms regularly. At certain time intervals we also recorded the moisture profiles in the prisms by means of NMR measurements.

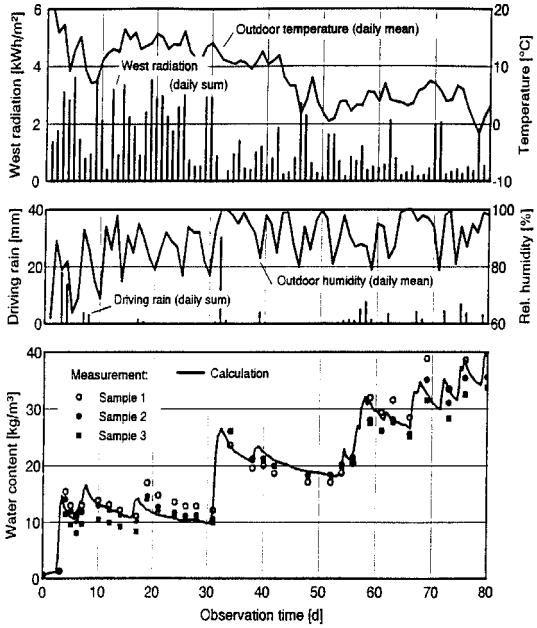

Fig. 32 Calculated time curves of water content of a natural stone masonry wall western exposure, 25 cm thick, in comparison with measurements of 3 natural stone wall samples according to [66], including the meteorological boundary conditions prevailing during the observation period.

Top: Measured curve of radiation intensity and outdoor air temperature

Middle: Measure curve of driving rain and relative outdoor humidity.

Bottom: Water content curve (calculated and measured).

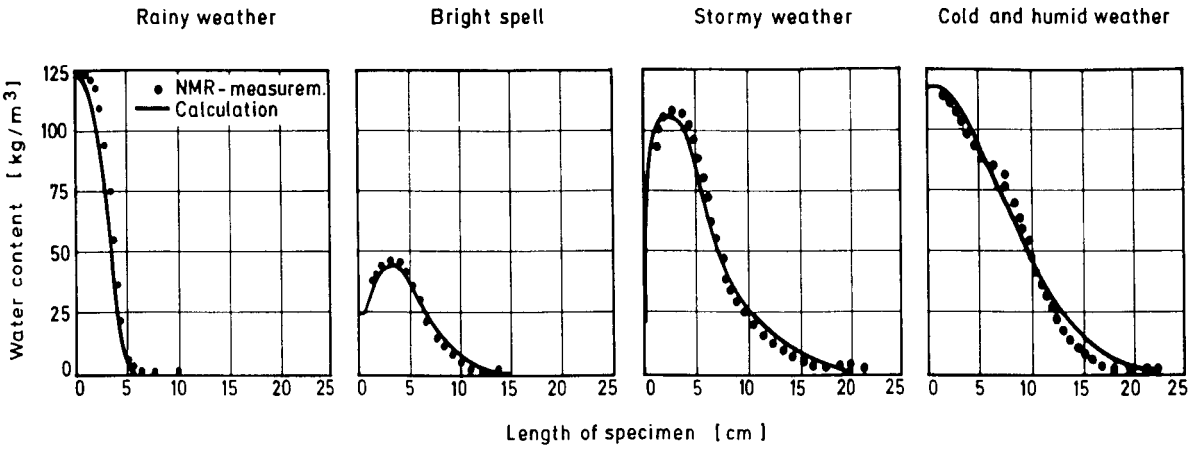

Fig. 33 Comparison between moisture profiles calculated and measured on sample 2 in Fig. 32 [66] at four significant time points.

Time point 1: After the first major rainfall at the beginning of the experiments.
Time point 2: After a one-week period of fair weather.
Time point 3: During stormy, dry weather following rain.
Time point 4: During a long period of wet and cold weather at the end of the observation period

To calculate the moisture behaviour of a natural stone wall under the described conditions, we used hourly mean values for the recorded climatic parameters. As transfer coefficients for heat and moisture we used the values shown in Table 5. Since there are no empirical data about realistic rain absorption values which quantify the relationship between impacting rain water and rain water remaining on the surface, we varied the driving rain absorptivity for the calculation between 0.5 and 1.0.

Fig. 32 (bottom) shows the calculated change in water content of the natural stone wall, averaged across the total thickness of 25 cm, in comparison with the measured moisture change in three natural stone prisms during an observation period of 80 days after the onset of weathering. Good correlation of the calculated and measured moisture behaviour as shown in Fig. 32, was achieved with a driving rain absorptivity of 0.7. However, the influence of that absorptivity in the example examined here is not very great. When we repeated the calculation with a value of 1.0, the water content after 80 days was only 2 kg/m^3 higher, which corresponds to a difference of less than 5%. Both the measured and the calculated results clearly show a moisture increase in the building component (interrupted only by brief dry periods) as the result of driving rain (Fig. 32), which continued even after 80 days.

The moisture profiles of the wall prisms during the same period are shown in Fig. 33 for four distinctive points in time. The profile at point 1 shows the moisture of the stone following the first rain period. Similar to a suction experiment in the laboratory, a narrowly defined moisture front can be recognized. At time point 2 - following a long period of fair weather - this moisture front has already flattened out toward the middle of the prisms through drying-out and redistribution. At point 3 the moisture profile is shown during stormy weather at low outside humidity (known in the foothills of the Alps as a foehn storm). Here the steep moisture content gradient can be recognized clearly in the surface zone; it results from the high drying rate under such climatic conditions. The moisture profile at the end of the 80-day observation period (time point 4) shows a relatively even moisture gradient in the wall, with nearly free water saturation on the outside surface and a still very low water content on the inside surface.

At all four points in time, the measured and calculated results agreed almost perfectly. This confirms that the WUFI computer model furnishes reliable results when the material parameters and climatic boundary conditions are known exactly.

4.2 Test example II (one-dimensional):

Drying-out of a flat cellular concrete roof

In contrast to the previous test example, we are looking now at an example in which the moisture storage and transport functions and the climatic conditions are not exactly known, as is unfortunately often the case in practice. The drying-out behaviour of a moist cellular concrete roof cannot be explained only by considering vapour diffusion. For that reason, several building physicists (e.g. Künzel [77] and Vos [122]) have studied and measured this process thoroughly. Kießl's calculations [57] for a flat roof of cellular concrete with a thickness of 15 cm under the weather conditions found in Holzkirchen have shown good agreement between his calculated results and the measured results in [77]. The same example is to serve as a test for the WUFI computer model, in which we base the determination of moisture storage and liquid transport functions exclusively on the thermal and hygric standard parameters of the building material. These material parameters of cellular concrete, which consist of the mean values of the measured results from [76], are listed in Table 8.

The moisture storage function is calculated with the help of equation (7) from the sorption moisture of the building material at 80 % relative humidity and free water saturation; it corresponds to the storage function of cellular concrete in Fig. 10 (top right). The capillary transport coefficient dependent on the water content is determined with equation (24) from the water absorption coefficient. It has been plotted in Fig. 34 as a factor of the water content. The same figure also shows the liquid transport coefficient for redistribution, whose top and bottom corner points were estimated as described below. As already discussed in section 2.3.7, the liquid transport coefficient for redistribution at free water saturation of the material lies below the one for the suction process by about one decimal power. The lower corner point of the transport coefficient for redistribution can be determined with equation (23) from the water vapour diffusion resistance factors (μ factor) from a dry-cup test and a wet-cup test according to standard DIN 52 615 [24]. The corresponding μ factors for cellular concrete are listed in Table 3. The transport coefficient thus obtained will be allocated to the water content, which results from the mean of the equilibrium water contents at 50 % and 93 % relative humidity. Thus we have determined the lower corner value of the transport coefficient for redistribution. It is shown in Fig. 34 together with the upper corner value. The intermediate values for other water contents are determined by logarithmic interpolation (linear interpolation on a logarithmic scale). The capillary transport coefficient FKU for the calculation of the drying-out behaviour of a flat cellular concrete roof, used by Kießl [57], is indicated in the same figure by a broken line. It coincides largely with the approximated transport coefficient for redistribution. The coefficient for the suction process is not needed in this example, since cellular concrete no longer comes in contact with water after the roof covering is installed. The bituminous roof covering is assumed to be water and vapour proof. The short-wave radiation absorption value of the roof surface is 0.9 according to Table 6, which corresponds to a very dark roof surface.

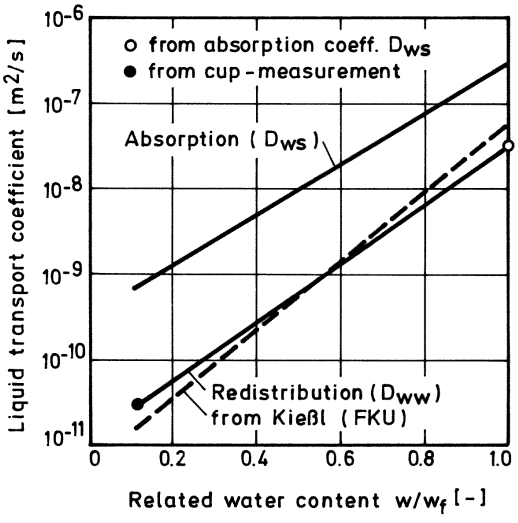

Fig. 34 Liquid transport coefficients of cellular concrete as a function of the related water content.

The transport coefficient for the suction process was determined by means of equation (24) from the water penetration coefficient. From this and from diffusion measurements we determined the coeff. for redistribution required for the calculation.

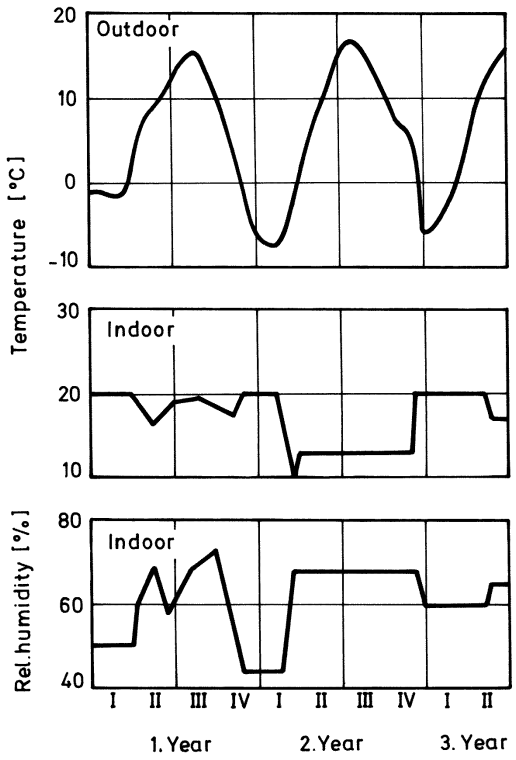

Fig. 35 Curves showing monthly means of outdoor and indoor temperatures and humidity during drying-out of a flat roof made of cellular concrete, after [77]

The climatic boundary conditions recorded during the study period [77] are shown in Fig. 35. The room air temperature (Fig. 35, middle) and indoor humidity (Fig. 35, bottom) were continuously recorded almost throughout the entire test period. Of the meteorological data, only the outside air temperatures (Fig. 35, top) are available in the form of monthly mean values. No data are available for the test period with regard to global radiation, which plays a major role in the calculation of flat roofs. For that reason, when we chose the meteorological boundary conditions, we used sets of recent climatic data which contain all significant parameters in the form of hourly mean values. To check whether this action is permissible, we first examined the effect of meteorological boundary conditions on the calculated results by examining the moisture changes on the roof during the first year.

To pre-select the sets of climatic data, we compared in Table 9 the mean outside air temperatures in the summer and winter semesters during the first two years of the study period with the corresponding values from recent local meteorological data and the

Table 9 Comparison between semi-annual means of the outside temperature during various years in Holzkirchen, and the TRY for Munich [12].

climate data	temperature mean [°C]	
	summer	winter
measuring period, year 1	11,8	-0,5
measuring period, year 2	12,7	-1,8
Holzkirchen, year A	12,4	0,2
Holzkirchen, year B	12,7	1,7
Holzkirchen, year C	12,8	3,2
Holzkirchen, year D	14,1	1,6
Munich, test reference year	14,1	1,9

test reference year for Munich [12], which is located about 30 km north of Holzkirchen. In relation to these seasonal temperature data, the measuring period is best represented by year A, followed by year B. Less suitable in comparison seem to be year C because of the warmer winter and year D because of the warmer summer. The same applies to the test reference year for Munich, which corresponds roughly to year D in Holzkirchen.

The effect of the outdoor climate on the calculation results when using the hourly data sets for the years A and B and the Munich test reference year (TRY) is shown in Fig. 36 (left). Shown beside it in Fig. 36 (right) are the corresponding developments calculated with the data for year A, for which the daily and monthly means were used as well. While the different weather conditions in individual years hardly affect the calculation results, the results seem to be influenced slightly when a mean value of the boundary conditions is formed, especially during the summer. This becomes apparent in Fig. 37, looking at the moisture profiles in the roof cross section at the end of the summer. Here, too, the influence of different sets of climatic data (left) is less than that from the averaging of data (right).

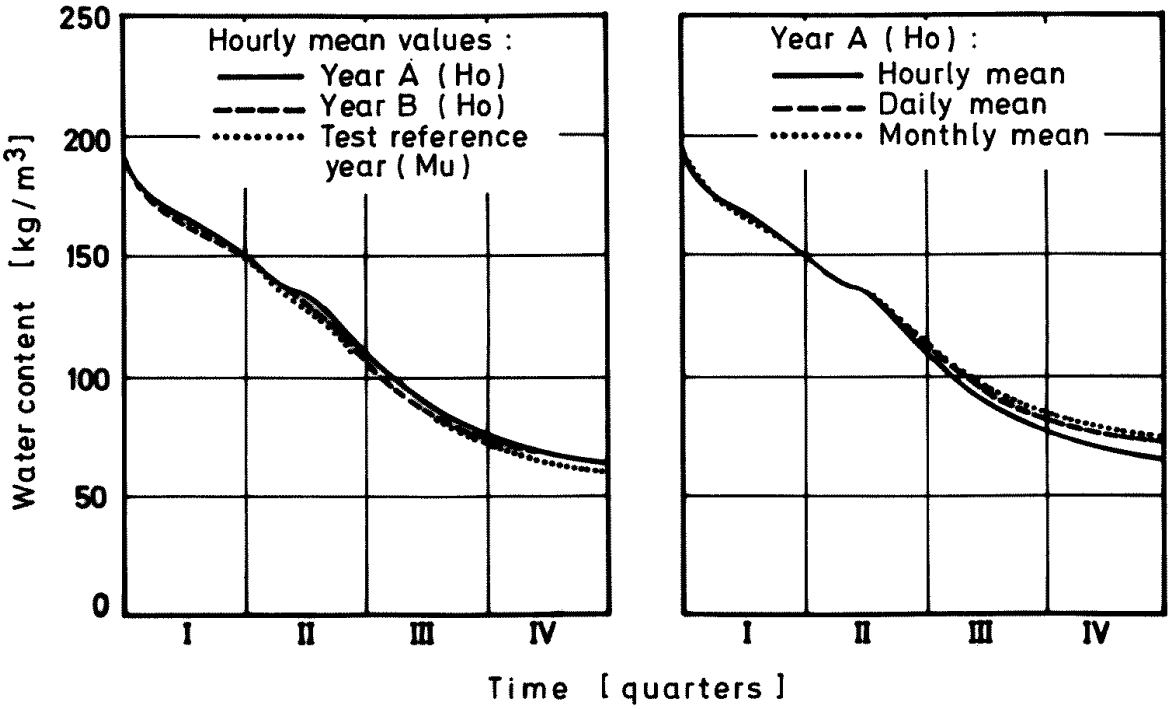

Fig. 36 Calculated curves of the water content averages over the cross section in the cellular concrete roof during the first year after completion, using hourly climate data from various years (left) and various

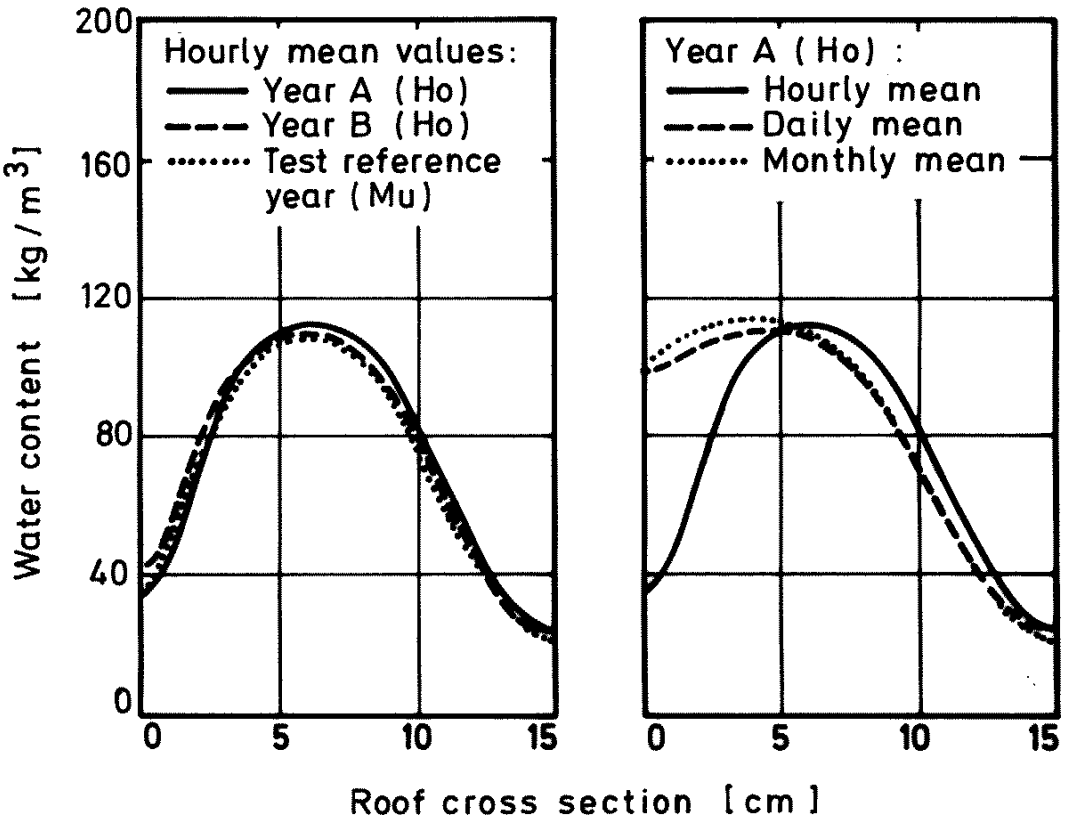

mean values from the climate parameters of one year (right)

Fig. 37 Calculated moisture distribution over the cross section of the cellular concrete roof at the end of the first summer after the onset of experiments, using the same boundary conditions as in Fig. 36.

While the effect of the hourly climate data from different years is negligibly small (left), there is a clear difference between using daily and monthly mean values and calculating with hourly values (right).

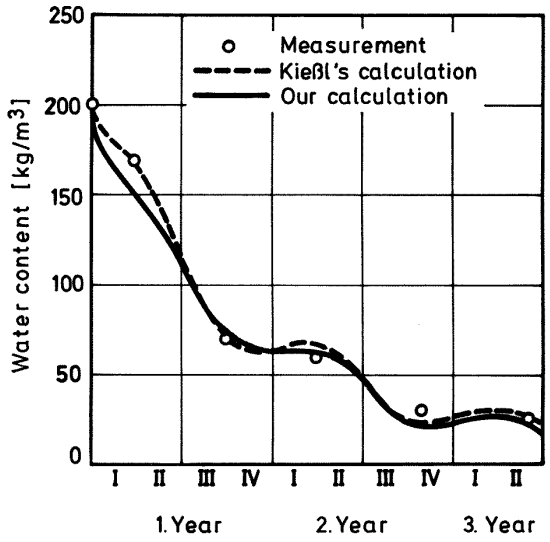

Fig. 38 Diagram showing the mean water contents measured over a period of two and a half years after the onset of the experiments in a cellular-concrete roof [77] in comparison with the calculated moisture curves according to Kießl [57] and according to our own method.

It seems to be relatively unimportant whether daily or monthly means are used. The results deviate to about the same degree from those based on hourly means. This can be attributed mainly to the effective damping of temperature peaks on the roof surface when global radiation is averaged over a period of 24 hours. Due to the exponential dependence of the saturation vapour pressure on the temperature, it is precisely these temperature peaks which are of great importance in terms of vapour diffusion. Instead of using the monthly means of the measuring period, it is therefore more useful to substitute them for the calculation with hourly climatic data for the same locality from another year.

The following calculation results are based on the meteorological data of year A in Table 9, with short wave absorptivity in the winter months of January to March set at zero because a more or less permanent snow cover can be assumed. Fig. 38 shows the calculated development of mean moisture in the flat roof for a period of two and a half years after the roof was completed, in comparison with the measured results of Künzel [77] and the calculated results by Kießl [57]. It is found that the initially wet roof dried out to a state of hygroscopic equilibrium moisture within two and a half years in spite of sometimes high inside humidity (Fig. 35).

It is found that the calculated and experimental results compared well in the case of both calculation methods. The same applies to the calculation of the moisture distribution in the roof crosssection, shown in **Fehler! Verweisquelle konnte nicht gefunden werden.** for three significant time points compared with the measured profiles. At the first time point, about three months after the onset of drying-out, a relatively steep water content gradient occurred in the lower third of the cellular concrete ceiling. At the end of the first summer (time point 2), this inside gradient was somewhat flatter, but it was still approximately in the same location. Almost symmetrically to this, a moisture gradient was formed close to the outside surface of the roof. This can be attributed to the high surface temperatures of the roof covering due to radiation. Through vapour diffusion - the liquid transport at a water content of 100 kg/m^3 is already clearly reduced - a "moisture hill" is thus produced in the middle of the roof cross section. At the end of the second winter, about 15 months after the onset of drying-out (time point 3), this "moisture hill" had shifted again toward the roof surface.

Both calculation methods realistically reflect the complex moisture behaviour of a cellular concrete roof. However, in contrast to Kießl's calculation [57], we used only simple, easily measurable material parameters without any negative effect on the quality of the calculation results.

4.3 Test example III (two-dimensional): Moistening and drying a masonry stone model

The first two test examples showed that the calculation results with the WUFI computer program compare well with experimental results in one-dimensional cases. Since there is no fundamental difference between a two-dimensional and a one-dimensional calculation, it must be assumed that the one-dimensional validation of the calculation model

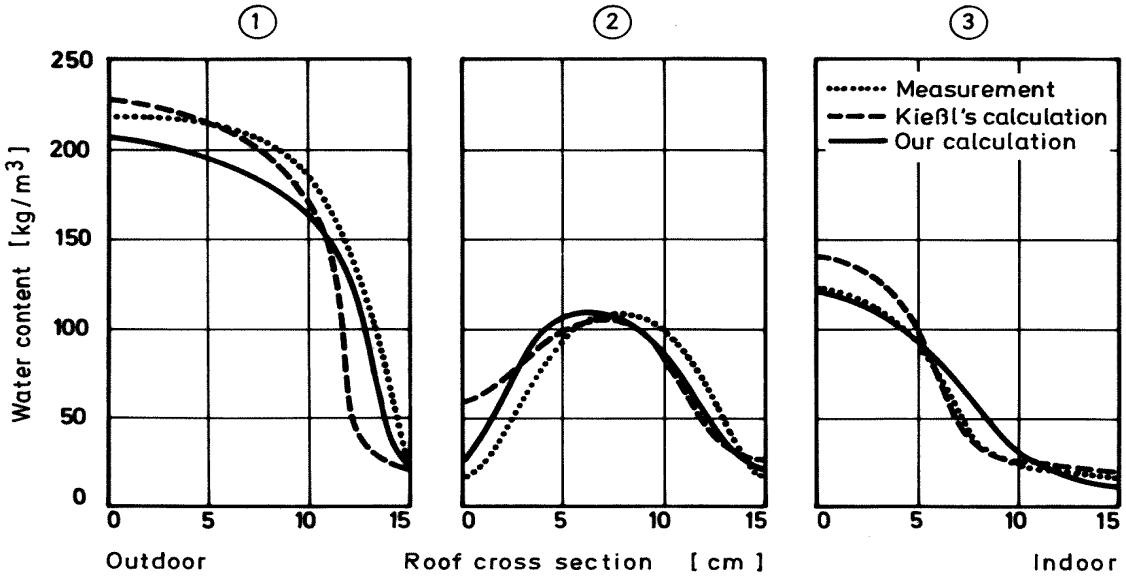

Fig. 39 Comparison between moisture distribution values measured [77] and calculated according to Kießl's [57] and our own method, in a flat roof at three significant time points after the onset of the experiments.

Time point 1: At the end of the first winter.
Time point 2: At the end of the first summer.
Time point 3: At the end of the second winter

applies also to two-dimensional examples. To support this assumption, we chose as our third test example a two-dimensional model experiment with masonry stone test pieces, which is described in detail below.

The masonry stone test pieces consist of lime silica brick; their dimensions are 49 x 11 x 7 cm^3. Their two largest surfaces (49 x 11 cm^2), which we call the front and the back, and one side (49 x 7 cm^2), were sealed to become water and vapour tight. Their initial water content corresponds to equilibrium moisture at 23 °C and 50% relative humidity. At the beginning of the experiment, we stood one of the end faces (11x7 cm^2) of the test piece into a container filled with about 1 cm of water, as shown schematically in 0. During the entire experimental period, the ambient conditions were held constant at 23 °C and 50% relative humidity. Due to evaporative cooling, the water in the container was about 20 °C. The total water content of the test pieces, which resulted from water uptake by the lower end face and simultaneous evaporation via the upper end face and one side, was determined by weighing the samples regularly. After 72 days, one test piece, hereafter called sample A, was divided with a saw into 50 equal parts by making 9 vertical cuts and 4 horizontal cuts, to determine the two-dimensional moisture distribution. The water content of the individual parts was determined by subsequent drying. A second test piece, hereafter called sample B, at first remained in the water container, standing on its end face for a total of 120 days. Then sample B was removed from the water, so that the water that was taken up could dry out again under equal ambient conditions.

To calculate the moisture transport processes during the model test, we needed not only the above-mentioned boundary and initial conditions, but also the surface transfer conditions and the material properties of the masonry stone pieces. The boundary conditions on the surfaces, which were in contact with the room air, are described by boundary conditions of the third kind.

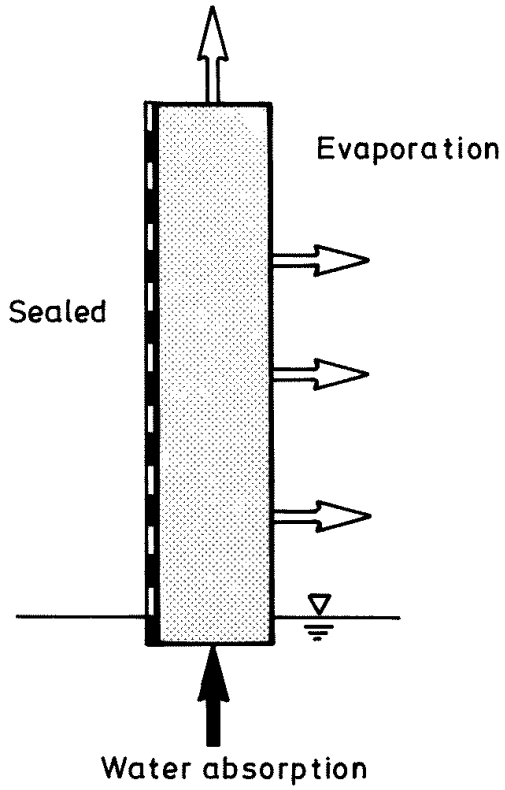

Fig. 40: Schematic diagram showing the diagram showing the masonry stone test piece during the suction process.

The test piece is 49 cm high, 11 cm wide and 7 cm thick. Its front and back as well as its left side are sealed. Water takeup is via the bottom end face, while there is simultaneous evaporation via the top end face and the right side. During subsequent drying, moisture is also released through the bottom end face.

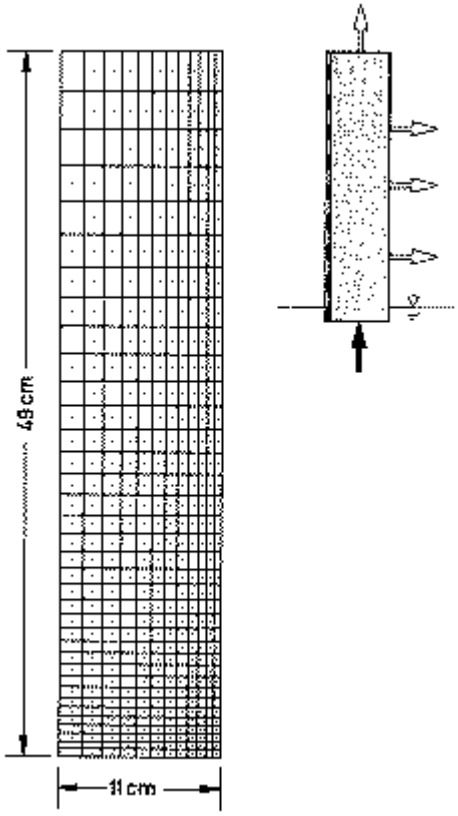

Fig. 41: Diagram showing the numerical grid for the two-dimensional calculation of the moisture process in the masonry stone test piece. The points in the middle of the grid elements represent the variable positions.

The regions where larger water content gradients occur (suction zone and right-hand evaporation zone) are marked by narrow mesh sizes of the numerical grid.

The surface transfer conditions correspond to the room conditions in Table 5. Contact with water constitutes boundary conditions of the first kind, i.e. the surface temperature is identical to the water temperature. The same applies to the vapour pressure, which corresponds to the saturation vapour pressure at the water temperature, and to the relative humidity, which equals "one" at the water contact surface. The standard material properties for the lime silica brick test pieces are listed in Table 8. The moisture storage function was already introduced in Fig. 10. The liquid transport coefficients for the suction process and redistribution or drying are shown in Fig. 15, bottom right ("lime silica brick B").

When producing the numerical grid, as explained below in section 3.5, the expected moisture gradients must be taken into account. In areas with steep gradients, as during the transient suction process in the zone of the bottom end face, or in the drying-out zone near the unsealed side, the mesh sizes of the grid should be as narrow as possible. However, to minimize the calculation effort, it is of advantage to work with greater mesh sizes in the areas of lower moisture gradients. In this example, such areas are expected in the zone of the sealed side (where directly on the surface the gradient is theoretically zero) and in the top part of the model piece. The numerical grid used here is shown in Fig. 41. With a mesh size of only 5 mm in the area of the water contact zone and the evaporation zone near the side, which continuously enlarges in the directions where the gradients become smaller, this

grid meets the above-named conditions. It consists of a total of 12 x 36 elements, whose central points constitute the positions of the variables. The time increments are chosen in a similar manner. That is why the length of the time increments varies between 10 minutes in the initial phase of the suction or drying-out process and 12 hours in the corresponding end phase.

Fig. 42 compares the experimental and calculative results for the development of water uptake and release of the model pieces. The differences in the water uptake of samples A and B are relatively small up to the time when sample A is cut for profile measurements. The comparison shows good agreement between measured and calculative results up to about 50 days after the experiment has begun. Then the calculative results flatten out in comparison with the measured results, up to a difference of about 25 kg/m^3 after 120 days. This difference, which amounts to about 15% of the total water content, could be attributable to the "after suction" effect described in [123]. This effect is based on the observation that capillary-active building materials in long-term contact with water take up more water than corresponds to their free water saturation. The "after suction" results from the slow solution of pore air in the water and from the fact that this pore air is then replaced by water. In the calculation model, this "after suction", which seldom occurs under practical conditions, was not taken into account, which explains the discrepancy between the measured and calculated values, which occurred after about 50 days, toward the end of the suction process. When the model piece is removed from the water container, the drying process starts, as the measured and calculated results show in Fig. 42. The difference that exists at the onset of drying between measured and calculated results is reduced within a few days. Later there is good agreement between both types of results until the end of the study period after 200 days. The quick adaptation of the measured and calculated results is attributable to the quick release of the water taken up by after suction, since this water is located close to the former suction surface area which has become a drying zone.

Fig. 43 shows the measured and calculated moisture distributions in the model piece after 72 days of water contact in the form of isolines. The agreement between the profile of the isolines can be regarded as good, considering that the steep decline of these lines in the evaporation zone, which shows the calculative distribution, can only be measured as a mean value over the thickness of the cut pieces, which is the equivalent of levelling the

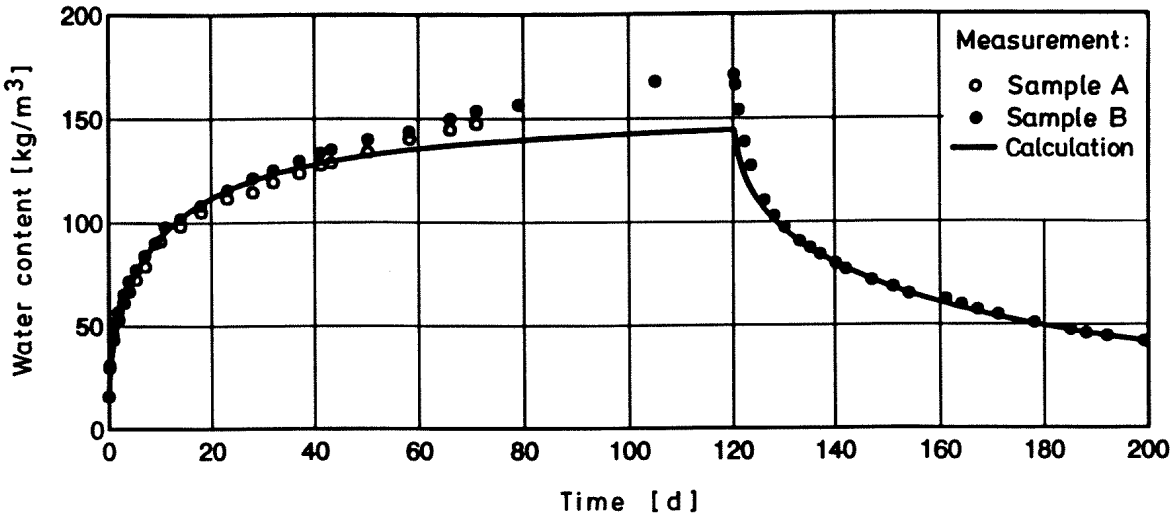

Fig. 42 Comparison between the measured and calculated mean water contents of the test piece during the suction process and during drying which begins after 120 days by removal of the water container. Sample A was cut into slices after 72 days of the experiment, to determine the moisture distribution.

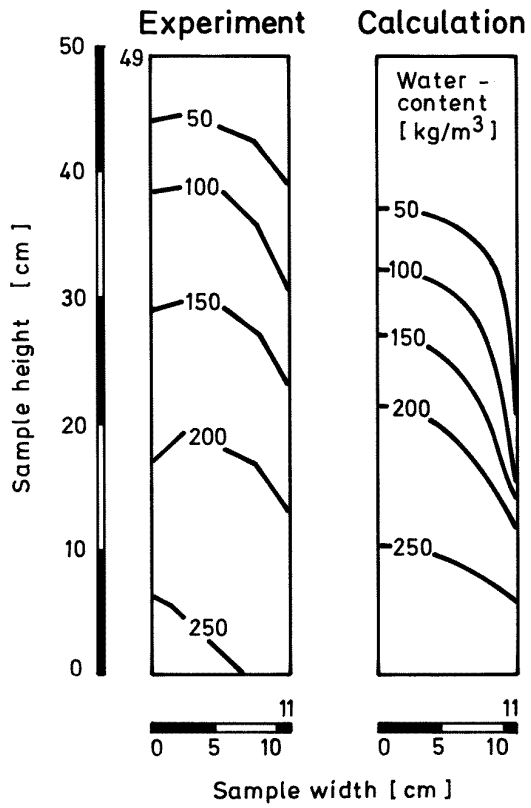

Fig. 43: Comparison between measured and calculated water content distribution in masonry stone piece after standing in a water container for 72 days, with isolines.

In comparison with the measured results, the calculated moisture distribution shows a somewhat steeper transition from the wet to the dry regions of the test piece.

gradients. However, the spreading of the moisture distribution, which is characterized by the distance between the isolines, is greater with measuring than with calculation. This could be attributable to a possible anisotropy in the capillary suction behaviour of the masonry stone, which leads to a greater liquid transport in vertical direction than in horizontal direction.

In spite of certain differences between the experimental and calculative results, this example shows the relatively good suitability of the WUFIZ (WUFI-2D) computer model, for two-dimensional moisture transport processes, especially when one considers that two-dimensional processes always react more sensitively to inaccuracies in the non-linear material parameters than one-dimensional processes.

5. Assessment of the calculation method

Below, we will first of all summarize and assess the new calculation techniques and functional characteristics of the newly developed calculation method, which in some respects clearly differs from previous models. Subsequently, some open questions will be discussed with regard to the moisture transport in building materials which are subject to change their properties as a function of time.

5.1 New calculation techniques and functional characteristics

The methods we have introduced here were developed for the calculation of the simultaneous one and two-dimensional transient heat and moisture transport in multi-layered building components. The method takes into account the new findings published in [59] and [67], regarding the hygric material properties of porous building materials. This means that as far as mineral building materials are concerned, we assume that the vapour diffusion resistance is not moisture-dependent, and that the transport phenomena observed in higher moisture regions, which increase vapour diffusion under isothermal conditions, are allocated to liquid transport.

When examining liquid transport, we also differentiate between two separate transport coefficients, to take into account the different capillary transport intensities during the suction process in contact with water and during redistribution after the interruption of the water supply. The moisture transport phenomena below the freezing point and during solution diffusion in organic polymers are contained in the computer model. The same applies to the hygric effect on heat storage and heat transport.

As driving potentials for the vapour and liquid transport we are using vapour pressure and relative humidity, both of which are material-independent. When the temperature and the relative humidity are known, the vapour pressure is clearly defined and

the independent variables in calculating the simultaneous heat and moisture transport are reduced to the temperature and the relative humidity as scalar quantities, which can be determined by solving two partial differential equations. Thanks to a novel problem-oriented discretization of the moisture transport equation and thanks to an efficient solution logarithm, a stable and oscillation-free numerical solution technique is ensured, which because of its high efficiency regarding spatial and temporal resolution allows detailed computations which do not require a great amount of time.

By using simple hygrothermal material parameters, most of which can be derived from standard material parameters, the effort required in determining building material-oriented input data is reduced in comparison with previous computation methods. Because temperature and relative humidity are well-known quantities, they allow a simple plausibility control of the calculative results and input data. They are also included in almost all sets of climatic data and form the major parameters to describe the indoor climate of buildings. With the additional consideration of rain and solar radiation, the effect of natural weather conditions on the heat and moisture behaviour of building materials can be calculated realistically.

This was confirmed by our first test example which we used to validate the calculative results, in which rain and solar radiation had a major effect on the moisture behaviour of the building component. Our second test example, the drying-out of a moist light-weight concrete roof, showed that even when approximated moisture transport and storage functions are used, good agreement can be achieved between experimental and calculative results. The calculation method supplies reliable results even for two-dimensional cartesian and axisymmetric applications, as comparative examinations (e.g. our third test example) have shown. This extends the application range of the calculation model to areas in which measuring involves a major technical effort if it is possible at all.

5.2 Further research required (open questions)

In spite of the positive assessment of the method based on the good agreement between calculative and measured results explained in section 4 and in other calculative studies not described here [e.g. [81]; [82]; [83]], the question remains how well the present calculation model describes the moisture behaviour of such building materials which show a distinctly time-dependent behaviour due to moisture-related changes in their pore structure. This time-dependent behaviour can be short-term and reversible in nature, as for example the swelling and shrinking of the cell walls in wood, which at an equal water content leads to difrferent liquid trans-port coefficients, depending on the initial state [44].

But it can also be a long-term irreversible process, such as the moisture-dependent carbonation of mortar or plaster, which also leads to a change in the hygric transport properties [75]. In the case of concrete, an important building material, reversible and irreversible moisture-related changes in pore structure seem to overlap. In analogy to mortar and plaster, the long-term conversion processes take place through carbonation or continuous hydraulic hardening, which results in a continuous change of the hygric transport coefficients [7]. The observation made in [118] and [121] that the water uptake of concrete in case of long-term suction deviates from the expected increase which is proportional to the square-root of time, may be attributed to reversible swelling processes, by which the size of the capillary-active pores is decreased. This is also indicated by the behaviour of concrete when it is penetrated by organic liquids. In the case of normal concrete, the uptake of non-polar liquids is proportional to the square-root of time [118]. However, if the concrete contains plastic components which swell in contact with organic liquids, a distinct deviation from this proportionality can be observed.

While long-term continuous changes in the thermal or hygric material properties can be adequately taken into account through the link-by-link calculation with appropriately modified coefficients,

this cannot be done in the case of short-term fluctuations of properties caused by swelling and shrinking processes in the pore space. For that reason, material parameters must be used in such cases which are independent of time and which represent the means of short-term property fluctuations adapted to the problem. How such a problem-oriented averaging can be done and what effect it would have on the calculative results must still be determined by future studies.

6. Practical conclusions

The characteristics of the new calculation method which in comparison with many previous models is marked especially by the use of simple, physically plausible quantities and material parameters and by repeated experimental validation, enable moisture transport calculations to become a cost-effective alternative or supplement to experimental studies and measuring methods. The calculation method also allows us to deal with objectives which cannot be achieved by measuring. It is not possible, for example, to determine experimentally the long-term hygrothermal behaviour of new building products. Such an extrapolation can only be done with calculative methods. Calculations are equally helpful in quantifying the effect of individual parameters by means of parameter studies, since often in experiments it is only possible to determine the interaction of many overlapping influences. In connection with advanced calculative models, for example the determination of hygrothermal stresses in a building component, the calculation of moisture can be of good service in the interpretation of damage-causing mechanism, as Möller [96] has shown in the case of natural-stone walls. Also easier to accomplish with calculations than with measuring techniques is the evaluation of cyclically recurring surface phenomena, such as efflorescence [3] or dew-water formation, since these processes affect only thin layers within the surfaces. In these examples, moisture calculations can be used for etiological research, and the variation range of the expected heat and moisture behaviour of building components can be estimated.

Since in practice, however, there are often uncertainties about the material parameters on which calculations are based and about the climatic boundary conditions, or since some parameters may be of importance which are not taken into account in the calculation (e.g. air flows in a building component), a validation of the calculative results by means of measuring techniques involving random sampling is required to ensure quantitatively reliable results.

Provided that it is successfully confirmed by experiments, the calculated hygrothermal behaviour of building components can be applied to other climatic conditions or extrapolated into the future, as long as the aging behaviour can be estimated. Conversion to other orders of magnitude is possible as well. Especially as a supplementary method to experimental studies, the calculation of simultaneous heat and moisture transport can be expected to have a large range of future applications, since the reliability of the calculative results can be confirmed through measuring techniques.

7. Summary

Object of this study was the development of a method for the one and two-dimensional calculation of the simultaneous heat and moisture transport in building components, using simple parameters. For this purpose, we first examined closely the moisture storage and transport mechanisms and their effect on heat transport. We disregarded moisture movements based on air flows, gravitation, hydraulic pressure differentials as well as osmotic or electro-kinetic effects.

Moisture storage in building components is divided into three regions. The first region is characterized by hygroscopic equilibrium water contents (sorption isotherms). In capillary-active materials, this is followed by the super-hygroscopic region with water contents up to free saturation. In this region, the equilibrium moisture depends on the capillary suction stress in the water-filled pores or the relative humidity over the pore water. This dependence,

which can be determined with measuring techniques, forms the basis for supplementing the sorption isotherms for high water contents. This results in a continuous storage function which can be defined throughout the entire moisture region of 0 - 100 % relative humidity. Water contents above free saturation are characterized by a third region, in which there are no more equilibrium states. The building material is supersaturated, i.e. the relative humidity, regardless of the water content, is always 100 %. Using results from the literature as well as our own findings, we analyze the significance of the temperature dependence and hysteresis of the moisture storage function for moisture storage calculations. For the determination of the moisture storage function, we provide a simple approximation which is sufficiently accurate in cases without liquid transport across layer boundaries.

By means of a critical analysis of the literature and by introducing new measuring results, we describe the physical principles of moisture transport mechanisms. The resulting calculation techniques describe vapour diffusion in porous building materials as a transport due to vapour pressure gradients with moisture-independent water vapour diffusion resistances. The often observed "increase" in vapour diffusion in the higher moisture region is attributed to liquid transport effects, also known as surface diffusion. Since its driving potential is not vapour pressure, but relative humidity, these effects are combined with capillary conduction in one calculative formula. This formula is derived from a flow model whose driving potential, the capillary suction stress can be converted into relative humidity. The transport coefficient is not only highly moisture-dependent, but it also varies with the boundary conditions. For that reason, two different coefficients are introduced, one for capillary suction in contact with water, the other for redistribution or drying after interruption of the water supply.

To determine these liquid transport coefficients, we describe a simple approximation method based on hygric standard material parameters. A more accurate determination is possible by means of transient moisture profile measurements. By choosing the relative humidity as the potential for liquid transport, the transport intensity in the supersaturated region must go to zero. Experimental studies prove that this is indeed the case in capillary-active building materials.

Not comparable with the transport in porous building materials is the solution diffusion in polymeric plastics. It is described by means of a formula which corresponds to that for vapour diffusion, but because of the peculiarities of the interaction between water and polymer molecules, the diffusion resistance can be moisture-dependent. One marginal region, which nevertheless can be of great importance in practice, is that of moisture transport below the freezing point. While generally, vapour diffusion is not much influenced by temperatures below 0°C, capillary suction comes to an end. In spite of this, a reduced moisture transport remains, due to unfrozen water in the micropores and on pore walls. It can be approximated through the introduction of a freezing limit potential, which characterizes the relative humidity above the unfrozen pore water.

In a similar manner we determined the effect of latent heat during the transition from water to ice on heat storage in moist building materials. In evaluating the hygric effect on heat conduction, we did not differentiate between the physical states of water because this was of minor significance. With the exception of pure insulation materials we can assume a linear relationship between the thermal conductivity of a building material and its water content. We clearly differentiated between the moisture-dependent increase in thermal conductivity and heat transport through vapour diffusion with phase change. This heat transport was considered separately because it does not take place in proportion to the temperature gradient. As shown by means of examples, its effect can be significant, while heat transport due to capillary water flows is negligibly small.

As climatic boundary conditions we used the temperature and the relative humidity of the surface or the surrounding area, in addition, we took solar

radiation and precipitation into account. The uptake of rain water was determined by using a boundary condition of the second kind, which was converted into a boundary condition of the first kind when the building component surface was completely wet. This guarantees that the building component can take up only as much rain water as impacts on its surface. Since on-site rain measurements, and especially the measurement of driving rain, can seldom be carried out over long periods of time if at all, we examined the possibility of deriving such information from meteorological sets of data.

Based on the above-described principles of simultaneous heat and moisture transport, we classified previous calculation methods according to transport potentials for vapour diffusion and liquid transport. We examined and evaluated the resulting transport formulas for their application range and choice of coefficients. This was supplemented by examining the calculation examples used to test the various models.

Together with the described considerations, our critical evaluation of the literature led to a derivation of new transport equations. Temperature, vapour pressure and relative humidity are the potentials best suited for heat and moisture transport. These potentials can be derived from the two independent variables, temperature and relative humidity, since the vapour pressure is dependent on the other two potentials. Thanks to two coupled partial differential equations for heat and moisture transport, these variables can be numerically solved for simultaneously.

For the discretization of these equations, we used an implicit finite volume method which, to avoid inaccuracies in calculating the vapour transport, was adapted by means of a novel formulation of the moisture calculation. The resulting matrix equation systems were solved by means of an alternating directly iterative algorithm. The functioning of the WUFI res. WUFIZ (WUFI-2D) computer program developed on this basis is explained through a flow chart. The appropriate choice of the numerical grid and the time increments, as well as the accuracy of the calculation and the required convergence criteria are discussed.

The results of the calculation method were evaluated by comparing the measured moisture development and moisture distributions by means of three test examples. The first two examples are one-dimensional applications. In these we examined the moisture behaviour of a natural stone wall section with western exposure during natural weathering, and the drying-out of a moist cellular concrete roof. As a two-dimensional test example we determined the water uptake and release behaviour of a masonry stone test piece.

The fact that the calculative and experimental results largely coincided and the fact that in comparison with many previous models, we used material parameters which are relatively easy to determine, led us to conclude that the calculation method can be used in practice. However, further research is necessary to determine the moisture behaviour of building materials whose hygric properties are subject to change as a function of times.

8. Literature

[1] Achtziger, J.: Kerndämmung von zweischaligem Mauerwerk; Einfluß des Wassergehalts und der Feuchtigkeitsverteilung auf die Wärmeleitfähigkeit der Dämmschicht.*(Core insulation of a two-layered masonry wall; Effect of the water content and moisture distribution on the thermal conductivity of the insulation layer.)* Bauphysik 7 (1985), H. 4, S. 121-124.

[2] Andersson, A.: Computer programs for two-dimensional heat, moisture, air flow. Division of Building Technology, Lund, Institute of Technology, Report TVBH-3005, Schweden 1981.

[3] Arnold, A.: Salze: Lästige weiße Ausblühungen oder Hauptschadensursache? *(Salt formation: annoying efflorescence or major cause of damage?)* Jahresbericht Steinzerfall - Steinkonservierung 1990, Verlag Ernst & Sohn, Berlin 1992.

[4] Auracher, H.: Wasserdampfdiffusion und Reifbildung in porösen Stoffen *(Water vapour diffusion and frost formation in porous materials).* VDI-Forschungsheft 566, Düssseldorf 1974.

[5] Bagda, E.: Berechnen instationärer Wärme- und Feuchteströme *(Calculating of unsteady-state heat and moisture flows)*. Expert Verlag, Böblingen 1991.

[6] Bagda, E.: Bestimmung der Absorptionszahl der Sonnenstrahlung *(Determining the absorptivity of solar radiation)*. Bauphysik 13 (1991), H. 6, S. 243-245.

[7] Balayssac, J.-P., Detriche, C.-H. und Grandet, J.: Interêt de l'essai d'absorption d'eau pour la caracterisation du beton d'enrobage. Materials and Structures 26 (1993), S. 226-230.

[8] Barrow, G.M.: Physikalische Chemie *(Physical chemistry)*. Bohmann-Verlag, Wien 1979.

[9] Bear, J.: Dynamics of fluids in porous media. Elsevier Verlag, New York 1972.

[10] Bird, R.B., Stewart, W.E. und Lightfoot, E.N.: Transport phenomena. John Wiley & Sons, New York 1960.

[11] Bjorck, A. und Dahlquist, G.: Numerische Methoden *(Numerical methods)*. Oldenbourg Verlag, München 1972.

[12] Blümel, K. et al.: Die Entwicklung von Testreferenzjahren (TRY) für Klimaregionen der Bundesrepublik Deutschland *(The development of test reference years (TRY) for climate regions in the Federal Republic of Germany)*. Bericht des Bundes-ministeriums für Forschung und Technologie BMFT-FB-T - 86-051, 1986.

[13] Bomberg, M.: Water flow through porous materials. Division of Building Technology, Lund, Institute of Technology, Report 21, Schweden 1972.

[14] Brunauer, S., Emmett, P.H. und Teller, E.: Adsorption of Gases in Multimolecular Layers. Journ. Amer. Chem. Soc. 60 (1938), H. 2, S. 309-319.

[15] Buchner, N.: Theorie der Gasdurchlässigkeit von Kunststoff-Folien *(Theory of gas permeability in plastic films)*. Kunststoffe 49 (1959), H. 8, S. 401-406.

[16] Cammerer, J. und Achtziger, J.: Einfluß des Feuchtegehaltes auf die Wärmeleitfähigkeit von Bau- und Dämmstoffen *(Effect of the moisture content on the thermal conductivity of building materials and insulation products)*. Kurzberichte aus der Bauforschung 1985, Bericht Nr. 115, S. 491-494.

[17] Carnaham, B. et al.: Applied numerical methods. Verlag John Wiley & Sons, New York 1969.

[18] Crank, J.: The mathematics of diffusion. Oxford University Press 1975.

[19] Crausse, P.: Etude fondamentale des transfers couples de chaleur et d'humidite en milieu poreux non sature. Dissertation Institut National Polytechnique de Toulouse 1983.

[20] Da Cunha Neto, J. und Daian, J.-F.: Experimental analysis of moisture transport in consolidate porous media under temperature gradient. International seminar on heat and mass transfer, Dubrovnik 1991.

[21] D'Ans, J. und Lax, E.: Taschenbuch für Chemiker und Physiker *(Handbook for chemists and physicists)*. Springer Verlag, Berlin 1970.

[22] Deutscher Wetterdienst: Aspirationspsychrometer-Tafeln *(German Weather Service: Aspiration psychrometer tables)*. 5. Auflage, Vieweg Verlag, Braunschweig 1976.

[23] DIN 4108: Wärmeschutz im Hochbau *(Insulation in building construction)*. August 1981.

[24] DIN 52615: Bestimmung der Wasserdampfdurchlässigkeit von Bau- und Dämmstoffen *(Determination of water vapour permeability in building materials and insulation products)*. November 1987.

[25] DIN 52617: Bestimmung des Wasseraufnahmekoeffizienten von Baustoffen *(Determination of the water uptake coefficient of building materials)*. Mai 1987.

[26] DIN 52620: Bestimmung des Bezugsfeuchtegehalts von Baustoffen*(Determination of the reference moisture content of building materials)*. April 1991.

[27] Eichler, K.: 2 von 3 Wohnungen sind sanierungsreif (*2 in 3 housing units need renovation)*. Bausubstanz 6 (1990), H. 8, S. 42-45.

[28] Eisner, M. und Winter, E.: Wärme- und Feuchtetransport in Hochlochziegeln *(Heat and moisture transport in vertically perforated bricks)*. Bauphysik 11 (1989), H. 5, S. 190-197.

[29] Erhorn, H. und Szerman, M.: Überprüfung der Wärme- und Feuchteübergangskoeffizienten in Außenwandecken von Wohnbauten *(Testing heat and moisture transfer coefficients in corners of outside walls of residential buildings)*. Gesundheitsingenieur 113 (1992), H. 4, S. 177-186.

[30] Fehlhaber, T. und Reinhardt, H.-W.:Beton beim Umgang mit wassergefährdenden Stoffen *(Concrete in contact with water polluting liquids)*. Teilbericht 2, Deutscher Ausschuß fur Stahlbeton, Beuth Verlag, Berlin 1991.

[31] Fischer, S. et al.: Ein Beitrag zur Behandlung von Temperatur und Feuchteproblemen mittels der Finite-Elemente-Methode *(Contribution on dealing with temperature and moisture problems with the finite elements method)*. Bauingenieur 66 (1991), S. 53-60, Springer-Verlag.

[32] Gagarin, V.G. und Mogutov, V.A.: Vapour barrier in three-layer concrete wall panels with efficient insulation. Bericht des

Forschungsinstituts für Bauphysik Gosstroy, Moskau.

[33] Garrecht, H.: Porenstrukturmodelle für den Feuchtehaushalt von Baustoffen mit und ohne Salzbefrachtung und rechnerische Anwendung auf Mauerwerk *(Pore structure models for the moisture household of building materials with and without salt loads, and the calculative application for masonry)*. Dissertation Universität Karlsruhe 1992.

[34] Gertis, K.: Hygrische Transportphänomene in Baustoffen *(Hygric transport phenomena in building materials)*. Schriftenreihe des Deutschen Ausschuß für Stahlbeton, H. 258, Verlag Ernst & Sohn, Berlin 1976.

[35] Gertis, K.: Verstärkter baulicher Wärmeschutz - ein Weg zur Vermeidung der bevorstehenden Klimaveränderung? *Increased insulation in buildings - a way to avoid the coming change in climate?)* Bauphysik 13 (1991), H. 5, S. 132-137.

[36] Gertis, K. und Erhorn, H.: Wasserdampfdiffusion in Auftenbauteilen unter nichtisothermen Bedingungen *(Water vapour diffusion in outdoor building components under non isothermal conditions)*. Bauphysik 3 (1981), H. 5, S. 169-173.

[37] Gertis, K. und Werner, H.: Die Problematik der Porenanalyse von Baustoffen. Kritische Ansätze zur Interpretation des Porengefüges *(Problems of pore analysis in building materials. Critical approaches to interpreting the pore structure)*. Schriftenreihe des Deutschen Ausschuß für Stahlbeton, H. 258, Verlag Wilhelm Ernst & Sohn, Berlin 1976.

[38] Glaser, H.: Vereinfachte Berechnung der Dampfdiffusion durch geschichtete Wände bei Ausscheidung von Wasser und Eis *(Simplified calculation of vapour diffusion through layered walls involving the formation of water and ice)*. Kältetechnik 10 (1958), H. 11, S. 358-364 und H. 12, S. 386-390.

[39] Gösele, K. und Schüle, W.: Schall, Wärme, Feuchte *(Sound, heat, moisture)*. 9. Auflage, Bauverlag, Wiesbaden 1989.

[40] Göttig, R.: Untersuchung von Feuchtetransportvorgängen (kapillares Saugen und Weiterverteilen nach Unterbrechung der Flüssigkeitszufuhr) in porösen Baustoffen mit Hilfe der kernmagnetischen Resonanz *(Study of moisture transport processes (capillary suction and redistribution after interruption of liquid supply) in porous building materials, by means of nuclear magnetic resonance)*. Diplomarbeit Fachhochschule München 1991.

[41] Greubel, D.: Vergleich von Rechen- und Meßergebnissen zum Feuchtehaushalt hölzerner Wandelemente unter instationären Klimarandbedingungen *(Comparison of calculative and measured results regarding the moisture behaviour of wooden wall elements under unsteady-state climatic boundary conditions)*. Bauphysik 8 (1986), H. 6, S. 183-188 & Bauphysik 9, H. 1, S. 21-25.

[42] Hansen, K.K.: Sorption isotherms catalogue. Technical report 162/86, Technical University of Denmark 1986.

[43] Häupl, P., Stopp, H. und Strangfeld, P.: Feuchteprofilbestimmung in Umfassungskonstruktionen mit dem Bürocomputer unter Berücksichtigung der kapillaren Leitfähigkeit *(Moisture profile determination in enclosure walls, with the office computer, taking into account the capillary conductivity)*. Bauzeitung 42 (1988), H. 3, S. 113-119.

[44] Heizmann, P.: Die Bewegung von flüssigem Wasser in kapillarporösen Körpern unter dem Einfluß kapillarer Zugkräfte sowie dem Einfluß von Zentrifugalkräften *(The movement of liquid water in capillary-porous bodies under the influence of capillary tractile forces and centrifugal forces)*. Diss. Technische Hochschule München, 1969.

[45] Hettmann, D.: Zur Beeinflussung des Feuchte- und Salzgehaltes in Mauerwerk *(Effect of the moisture and salt content in masonry)*. Bautenschutz + Bausanierung 16 (1993), H. 5, S. 72-75.

[46] Huebner, K.H.: The finite element method for engineers. John Wiley & Sons, New York 1975.

[47] Husseini, F.: Feuchteverteilung in porösen Baustoffen aufgrund instationärer Wasserdampfdiffusion *(Moisture distribution in porous building materials based on unsteady-state water vapour diffusion)*. Diss. Universität Dortmund, 1982.

[48] Illig, W.: Die Größe der Wasserdampfübergangszahl bei Diffusionsvorgängen in Wänden von Wohnungen, Stallungen und Kühlräumen *(The magnitude of the water vapour transfer value during diffusion processes in walls of housing units, stables and cold storage rooms)*. Gesundheits-Ingenieur 73 (1952), H. 7/8, S. 124-127.

[49] International Energy Agency: Guidelines & Practice. Report Vol. 2, IEA-Annex XIV, Leuven 1990.

[50] Isaacson, E. und Keller, H.: Analyse numerischer Verfahren *(Analysis of numerical methods).* Verlag Harri Deutsch, Zürich 1973.

[51] ISO 7345: Thermal insulation - Physical quantities and definitions. Second edition, 1987.

[52] ISO 9346: Thermal insulation - Mass transfer - Physical quantities and definitions. First edition, 1987,

[53] Kari, B., Perrin, B. und Foures, J.C.: Modelisation macroscopique des transferts de chaleur et d'humidité dans des materiaux du bailment. Manuskript zur Veröffentlichung in RILEM. Université de Toulouse 1992.

[54] Kast, W. und Jokisch, F.: Überlegungen zum Verlauf von Sorptionsisothermen und zur Sorptionskinetik an porösen Feststoffen *(Considerations regarding the development of sorption isotherms and the sorption kinetics in porous solids)*. Chemie-Ingenieur Technik 44 (1972), H. 8, S. 556-563.

[55] Keresteciogiu, A. und Gu, L: Theoretical and computational investigation of simultaneous heat and moisture transfer in buildings: "Evaporation and condensation" theory. ASHRAE Transactions, USA 1990.

[56] Kießl, K.: Bauphysikalische Einflüsse bei der Krustenbildung am Gestein alter Bauwerke *(Effects of factors in building-physics on the crust formation in the masonry of old buildings)*. Bauphysik 11 (1989), H. 1 , S. 44-49.

[57] Kießl, K.: Kapillarer und dampfförmiger Feuchtetransport in mehrschichtigen Bauteilen *(Capillary and vaporous moisture transport in multi-layered building components)*. Diss. Universität-Gesamthochschule Essen 1983.

[58] Kießl, K. und Gertis, K.: Feuchtetransport in Baustoffen *(Moisture transport in building materials)*. Forschungsberichte aus dem Fachbereich Bauwesen, H. 13, Universität-Gesamthochschule Essen 1980.

[59] Kießl, K., Krus, M. und Künzel, H.M.: Weiterentwickelte Meß- und Rechenansätze zur Feuchtebeurteilung von Bauteilen *(Advanced measurement and calculation techniques for the evaluation of moisture in building components)*. Bauphysik 15 (1993), H. 2, S. 61-67.

[60] Kießl, K. und Möller, U.: Zur Berechnung des Feuchteverhaltens von Bauteilen aus Holz und Holzwerkstoffen *(On the calculation of the moisture behaviour of building components made of wood and wood products)*. Holz als Roh- und Werkstoff 47 (1989), S. 317-322.

[61] Klopfer, H.: Wassertransport durch Diffusion in Feststoffen *(Water transport by diffusion in solids)*. Bauverlag, Wiesbaden 1974.

[62] Kohonen, R.: A method to analyze the transient hygrothermal behaviour of building materials and components. Dissertation Helsinki University of Technology 1984.

[63] Van der Kooi, J.: Moisture transport in cellular concrete roofs. Dissertation Technische Hochschule Delft 1971.

[64] Krischer, O. und Kast, W.: Die wissenschaftlichen Grundlagen der Trocknungstechnik *(The scientific principles of drying technology)*. Dritte Auflage, Springer-Verlag Berlin 1978.

[65] Krus, M.: Laufende Untersuchungen. Noch nicht veröffentlicht *(Current studies. Not yet published)*.

[66] Krus, M.: Bestimmung der Tiefenwirkung von Klimaeinflüssen in Natursteinmauern durch Feuchteprofilmessungen an ausgewählten Probekörpern *(Determining the in-depth effect of climatic influences in natural stone walls by means of measuring moisture profiles of selected test pieces)*. Unveröffentlichte Untersuchungen des BMFT-Verbundprojektes Steinzerfall, Holzkirchen 1992.

[67] Krus, M. und Kießl, K.: Ist der Diffusionswiderstand von Baustoffen wirklich feuchteabhängig? *(Is the diffusion resistance of building materials really moisture-dependent?)* IBP-Mitteilung 18 (1991), Nr. 208.

[68] Krus, M. und Kießl, K.: Kapillartransportkoeffizienten von Baustoffen aus NMR-Messungen *(Capillary transport coefficients of building materials from NMR measurements)*. IBP-Mitteilung 16 (1989), Nr. 175.

[69] Krus, M. und Kießl, K.: Vergleichende Messungen der Porenradienverteilung von Natursteinen mittels Saugspannung und Druckporosimetrie *(Comparative measurements of the pore radius distribution of natural stone by means of suction stress and Hg-porosimetry)*. IBP-Bericht FtB-11/1991.

[70] Krus, M. und Künzel, H.M.: Liquid water transport above capillary saturation. Beitrag zur Tagung des IEA-Projektes Annex 24, Eindhoven 1992.

[71] Krus, M., Künzel, H.M. und Klier, M.: Liquid transport over the boundary layer of two different hygroscopic capillary active materials. Beitrag zur Tagung des IEA-Projektes Annex 24, Holzkirchen 1993.

[72] Künzel, H.: Bestimmt der volumen- oder der massebezogene Feuchtegehalt die Wärmeleitfähigkeit von Baustoffen? *(Does the volume-related or the mass-related moisture content determine the thermal conductivity of building materials?)* Bauphysik 8 (1986), H. 2, S. 33-39.

[73] Künzel, H.: Der Regenschutz von Mauerwerk aus Natursteinen *(Rain protection of natural-stone masonry)*. Bauphysik 10 (1988), H. 1, S. 12-16.

[74] Künzel, H.: Feuchteeinfluß auf die Warmeleitfähigkeit bei hygroskopischen und nicht hygroskopischen Stoffen *(The moisture effect on the thermal conductivity of hygroscopic and non-hygroscopic materials)*. WKSB 36 (1991), H. 29, S. 15-18.

[75] Künzel, H.: Feuchtigkeitstechnische Untersuchungen an Außenputzen und verputzten Wänden *(Studies of moisture in outdoor stucco and rendered walls)*. Dissertation Technische Hochschule Stuttgart 1964.

[76] Künzel, H.: Gasbeton, Wärme- und Feuchteverhalten *Autoclaved Aerated Concrete, heat and moisture behaviour)*. Bauverlag GmbH., Wiesbaden 1971.

[77] Künzel, H.: Untersuchungen über Feuchtigkeitsverhältnisse in verschiedenen Flachdachkonstruktionen *(Studies regarding moisture conditions in various flat-roof con-*

structions). Berichte aus der Bauforschung, H. 48, Verlag Ernst & Sohn, Berlin 1966.

[78] Künzel, H.: Zusammenhang zwischen der Feuchtigkeit von Außenbauteilen in der Praxis und den Sorptionseigenschaften der Baustoffe *(Relationship between the moisture of outdoor building components in practice and the sorption characteristics of the building materials)*. Bauphysik 4 (1982), H. 3, S. 101-107.

[79] Künzel, H. und Schwarz, B.: Die Feuchtigkeitsaufnahme von Baustoffen bei Beregnung *(The moisture uptake of building materials under irrigation)*. Berichte aus der Bauforschung, H. 61, Berlin 1968.

[80] Künzel, H.M.: Connection between liquid water and vapour transport in porous media and its consequences for heat and moisture transfer models. Beitrag zur Tagung des EG-Projektes SCIENCE, London 1992.

[81] Künzel, H.M.: Untersuchung des Austrocknungsverhaltens von im CSO-Verfahren applizierten Wärmedämmschichten aus Isofloc *(Examining the drying-out behaviour of Isofloc insulation layers installed with the CSO process)*. IBP-Bericht FtB-18/1992.

[82] Künzel, H.M.: Heat and Moisture Transfer in Porous Media; a comparison of measurement and calculation and its consequences for the treatment of vapour diffusion. IEA-Annex 24 project, Report T1-D-92/01, 1992.

[83] Künzel, H.M.: Rechnerische Untersuchungen des Langzeit-Feuchteverhaltens von Wärmedämmschichten in Umkehrdächern mit Begrünung *(Calculative examinations o the long-term moisture behaviour of insulation layers in inverted roofs with greening)*. IBP-Bericht FtB-23/1993.

[84] Künzel, H.M.: Rainloads on building elements. Beitrag zur Tagung des IEA-Projekts Annex 24, Holzkirchen 1993.

[85] Künzel, H.M. und Kießl, K.: Bestimmung des Wasserdampfdiffusionswiderstandes von mineralischen Baustoffen aus Sorptionsversuchen *(Determining the water vapour diffusion resistance of mineral building materials through sorption experiments)*. Bauphysik 12 (1990), H. 5, S. 140-144.

[86] Kupke, C. und Pfrommer, P.: Ein Modell zur Beschreibung des instationären Wärme-, Wasserdampfdiffusions- und Kapillartransports in porösen Bauteilen *(Model to describe the unsteady-state heat, water vapour diffusion and capillary transport in porous building components)*. Gesundheits-Ingenieur 113 (1992), H. 4, S. 187-197.

[87] Lacy, R.E. und Shelland, H.C.: An index of driving rain. The Meteorological Magazine (1962), H. 91, S. 177-184.

[88] Le Sage de Fontenay, C. und Sellevold, E.J.: Ice Formation in Hardened Cement Paste. Durability of Building Materials and Components, ASTM STP 691 (1980), S. 425-438.

[89] Lindauer, E. und Snatzke, Ch.: Spektrale Messung des Absorptionsgrades *(Spectral measurements of the radiative absorptivity)*. Persönliche Mitteilung, Holzkirchen 1993.

[90] Luikov, A.V.: Systems of differential equations of heat and mass transfer in capillary-porous bodies. International Journal of Heat and Mass Transfer (1975), H. 18, S. 1-14.

[91] Lutz, P. et al.: Lehrbuch der Bauphysik *(Textbook of building physics)*. Teubner Verlag, Stuttgart 1985.

[92] Matsumoto, M. und Sato, M.: A harmonic analysis of periodic steady state solution of the internal condensation process. Proceedings CIB-W67-Sympos., Rotterdam 1990.

[93] McLean, R. Galbraith, G. und Sanders, C.: Moisture transmission testing of building materials and the presentation of vapour permeability values. Building research and practice, Journal of CIB 2 (1990), S. 82-91.

[94] Meng, B.: Charakterisierung der Porenstruktur im Hinblick auf die Interpretation von Feuchtetransportvorgangen *(Characterising the pore structure for the interpretation of moisture transport processes)*. Diss. RWTH Aachen 1993.

[95] Mizuhata, M. et al.: Moisture transfer in material. Proceedings CIB-W67-Symposium, Rotterdam 1990.

[96] Möller, U.: Thermo-hygrische Formänderungen und Eigenspannungen von natürlichen und künstlichen Mauersteinen *(Thermo-hygric changes in structure and internal stresses of natural and synthetic masonry stones)*. Diss. Universität Stuttgart 1992.

[97] Neiß, J.: Numerische Simulation des Wärme- und Feuchtetransports und der Eisbildung in Boden *(Numerical simulation of heat and moisture transport and ice formation in soils)*. VDI-Verlag, Düsseldorf 1982.

[98] Nicolas, P.; Modelisation mathematique et numerique des transfers d'humidité en milieu poreux. Dissertation Université Paris VI 1992.

[99] Nielsen, A.F.: Measurements of drying-out of cellular concrete. Meddelelse Nr. 26, Thermal Insulation Laboratory, Technical University Denmark 1973.

[100] Nonweiler, T.R.F.: Computational mathematics. Ellis Horwood Limited, Chichester 1984.

[101] Patankar, S.V.: Numerical heat transfer and fluid flow. McGraw-Hill, Washington 1980.

[102] Patankar, S.V. und Baliga, B.R.: A new finite-difference scheme for parabolic differential equations. Numerical Heat Transfer, vol. 1 (1978).

[103] Peaceman, D.W. und Rachford, H.H.: The numerical solution of parabolic and elliptic diff. equations. Journal of Industrial Applied Mathematics 1 (1955), H. 3, S. 28-41.

[104] Phillip, J.R. und de Vries, D.A.: Moisture movement in porous materials under temperature gradients. Transactions, American Geophys. Union 38 (1957), H. 2, S. 222-232.

[105] Potter, D.: Computational Physics. John Wiley & Sons, London 1972.

[106] Prazak, J. et al.: Bemerkungen zur Beschreibung des Flüssigtransports in porösen Baumaterialien *(Notes on the description of liquid transport in porous building materials)*. Gesundheits-Ingenieur 110 (1989), H. 6, S. 308-312.

[107] Pult, P.: Krankheiten durch Schimmelpilze *(Diseases caused by moulds)*. Beitrag zu den Aachener Bausachverständigentagen 1992, Bauverlag Wiesbaden 1992.

[108] Richards, L.A.: Methods of measuring soil moisture tensions. Soil Science (1949), H. 68, S. 95-112.

[109] Ricken, D.: Ein einfaches Berechnungsverfahren für die eindimensionale, instationäre Wasserdampfdiffusion in mehrschichtigen Bauteilen *(A simple calculative method for the one-dimensional unsteady-state water vapour diffusion in multi-layered building components)*. Diss. Univ. Dortmund 1989.

[110] Rode Pedersen, C.: Combined heat and moisture transfer in building constructions. Diss. Technical University of Denmark 1990.

[111] Rosenberg, D.U.: Methods for the numerical solution of partial differential equations. American Elsevier Publishing Company, New York 1969.

[112] Schaschek, H.: Bewegungsmechanismus von Wasserdampf in porösen blattförmigen Materialien *(Movement mechanism of water vapour in porous leaf-shaped materials)*. Chemie-Ingenieur Technik 28 (1956), H. 11, S. 698-702.

[113] Schaube, H. und Werner H.: Wärmeübergangskoeffizient unter natürlichen Klimabedingungen *(Heat transfer coefficient under natural climatic conditions)*. IBP-Mitteilung 13 (1986), Nr.109.

[114] Schwarz, B.: Die Wärme- und Stoffübertragung an Außenwandoberflächen *(Heat and material transfer in outdoor wall surfaces)*. Diss. Universität Stuttgart 1971.

[115] Schwarz, B.: Witterungsbeanspruchung von Hochhausfassaden *(Weathering loads of high-rise walls)*. Heizung, Lüftung, Haustechnik 24 (1973), H. 12, S. 376-384.

[116] Schwarz, B. und Künzel, H.: Der kritische Feuchtegehalt von Baustoffen *(The critical moisture content of building materials)*. Gesundheits-Ingenieur 95 (1974), H. 9, S. 241-246.

[117] Sommer, E.: Beitrag zur Frage der kapillaren Flüssigkeitsbewegung in porigen Stoffen bei Be- und Entfeuchtungsvorgängen *(Contribution to the question of capillary liquid movement in porous materials during humidification and dehumidification processes)*. Diss. Technische Hochschule Darmstadt 1971.

[118] Sosoro, M.: Modell zur Vorhersage des Eindringverhaltens von organischen Flüssigkeiten in Beton *(Model for predicting the penetration behaviour of organic liquids in concrete)*. Diss. Universität Stuttgart 1994.

[119] Tveit, A.: Measurements of moisture sorption and moisture permeability of porous materials. Norwegian Building Research Institute, Rapport 45, Oslo 1966.

[120] VDI 3789 Umweltmeteorologie, Blatt 2: Wechselwirkungen zwischen Atmosphäre und Oberflächen; Berechnungen der kurz- und der langwelligen Strahlung *(Environmental Meteorology, Sheet 2: Interaction between atmosphere and surfaces; calculation of short and long-wave radiation)*. Entwurf, Dezember 1992

[121] Volkwein, A.: Untersuchungen über das Eindringen von Wasser und Chlorid in Beton *(Examining the penetration of water and chloride in concrete)*. Bericht aus dem Baufoschungsinstitut Heft 1/1991, Tech. Universität München, 1991.

[122] Vos, B.H.: Kondensation in Dächern *(Condensation in roofs)*. Gesundheits-Ingenieur 90 (1969), H. 11, S. 334-342

[123] Wagner, A. und Niesel, K.: Kapillaritätskenngrößen von Mauerziegeln *(Capillary parameters of bricks)*. Materialprüfung 31 (1989), H. 4, S. 109-113

[124] Ziegler, et al.: Lehrbuch der Botanik *(Textbook of Botanies)*. 31. Auflage, Gustav Fischer Verlag 1978.